Lodz University of Technology

Interdisciplinary Doctoral School, Materials Engineering Discipline

Doctoral Thesis Title

Layer-by-layer deposition of PAMAM dendritic material onto polylactide nonwoven

Supervisor and co-supervisor:

Prof. Dawid Stawski, TUL, Poland

Dr. Somaye Akbari, AUT, Iran

Produced by:

Sima Shakoorjavan

ID No.: 801455

September 2024, Poland

Abstract

Multilayer self-assemblies build up through layer-by-layer (LBL) deposition of polyelectrolytes has been recognized as a straightforward, adaptable, and bottom-up surface modification approach which can be applied on various substrates, regardless of their shape, size, and surface chemistry, under mild conditions. The growth profile and structure of polyelectrolyte (PE) multilayer assemblies constructed through LBL technique on fully smooth, flat, and non-porous inorganic surfaces including quartz slides or silica wafers have extensively investigated in literature. However, there is a significant gap in the understanding of the fundamental mechanism governing the LBL deposition and PE multilayer assemblies on rough, uneven, and porous surfaces, particularly those found in textile materials, including nonwoven fabric. Therefore, the aim of this study is to monitor the construction of multilayer assemblies consisting of dendritic amine-terminated poly(amidoamine) (PAMAM) and poly(acrylic acid) (PAA) on pre-treated polylactide (PLA) nonwoven fabric using the layer-by-layer technique via the dipping method.

In order to functionalize PLA substrate with positively charged surface, aminolysis reaction at different time interval and two temperature was designed. According to characterization tests, optimum conditions to provide the highest amine content with acceptable mechanical properties were obtained.

After finding the optimum condition of pre-treatment, the experiments and characterization tests have been engineered to understanding the multilayer growth on the PLA nonwoven. Three key parameters including polyelectrolytes solution pH, their concentration ratio, and intermediate drying was consider in LBL deposition. Since PAMAM and PAA are both weak polyelectrolytes, can possess different surface charge and conformational structure based on the PE pH, which can directly influence PE complex formation. Therefore, the study was conduct in two phases: liquid-liquid phase to study polyelectrolytes complex formation and liquid-solid phase to monitor multilayer growth with hydrated and dry LBL (intermediate drying effect).

According to liquid-liquid phase, the optimal pH and concentration ratio of PAMAM: PAA complex to form stable and irreversible turbid colloidal PEC dispersion were determined through turbidimetry measurements. Acid-base titration and DLS analysis revealed that PAMAM: PAA at their partially charged state (PAMAM/pH=8 and PAA/pH=4) where both have compact and globular conformation (not fully compact), provide the stable higher concentration of aggregated PECs (highest turbidity~1668 NTU). UV-visible spectroscopy were employed to characterized PECs interaction and confirmed PAA penetration into PAMAM structure, along with electrostatic interaction of primary amines and carboxylate groups of PAA.

Three different concentration ratios of PAMAM: PAA, corresponding to the obtained highest turbidity at each series of titration in liquid-liquid phase, were selected to study the PEC multilayer growth on the substrate in liquid-solid phase. Based on the K/S value of the colored substrate, a concentration ratio of 7:7 (x 10^{-4} g/mL), at the obtained optimal pH, provided the highest PE multilayer growth on the substrate in liquid-solid phase. Ninhydrin assay was conducted to quantify amine density after each deposition step. It was revealed that PAMAM/PAA PE multilayer assemblies till the 7 layers have the converging profile growth, while applying one step intermediate drying between LBL caused the stability of the PAA layers and final divergent profile growth with more NH_2 density at the even top layer of the material. In addition, according to air permeability analysis, it was found that PE multilayered assembled on the substrate with dry LBL have less compact structure than those assembled hydrated LBL. In addition, based on the staining test as a function of layer number, it was revealed that highest NH_2 density on the top even layer did not always lead to higher accessible amine site to interact with another molecule. Indeed, the highest NH_2 density does not lead to higher dye adsorption; there is a thresholds and limitation of the substrate layering to achieve the desirable application such as dye adsorption or drug delivery.

In conclusion, knowledge of the PE multilayer growth profile and controlling their density to tailor surface properties with optimal accessible functional groups is crucial for designing nonwoven substrates with developed multilayer assemblies for applications like drug delivery where microbial contamination is crucial.

Streszczenie

W pracy opisano proces samorzutnego tworzenia układów wielowarstwowych w wyniku nakładania polielektrolitów metodą layer-by-layer. Jest to prosty, efektywny i prowadzony w łagodnych warunkach sposób modyfikacji powierzchni, który można stosować na różnych podłożach, niezależnie od ich kształtu, rozmiaru i struktury chemicznej warstwy wierzchniej. Profil wzrostu i struktura polielektrolitowych układów wielowarstwowych tworzonych tą metodą na całkowicie gładkich, płaskich i nieporowatych powierzchniach nieorganicznych, takich jak szkiełka kwarcowe czy wafle krzemowe, były szeroko badane w literaturze. Niemniej jednak istnieje istotna luka w poznaniu podstawowych mechanizmów rządzących procesem nakładania warstw techniką layer-by-layer i wytwarzanymi wówczas układów wielowarstwowych na nieregularnych, nierównych i porowatych powierzchniach, takich jak włókniny. Celem niniejszej pracy jest zbadanie struktury układów wielowarstwowych składających się z poliaminowych dendrymerów oraz poli(kwasu akrylowego) nałożonych na wstępnie modyfikowaną włókninę polilaktydową za pomocą techniki layer-by-layer.

W celu funkcjonalizacji podłoża włókninowego przeprowadzono reakcję aminolizy w różnych przedziałach czasowych oraz w dwóch temperaturach. Na podstawie pomiarów ilościowych określono optymalne warunki, które zapewniają najwyższą zawartość grup aminowych przy akceptowalnych poziomach właściwości mechanicznych.

Po określeniu optymalnych warunków wstępnej modyfikacji, zaplanowano dalsze etapy wprowadzania warstw polielektrolitów. Przy stosowaniu techniki layer-by-layer uwzględniono trzy kluczowe parametry: pH roztworu polielektrolitu, stosunek stechiometryczny poszczególnych składników oraz możliwość stosowania pośredniego suszenia. Ponieważ dendrymer PAMAM i poli(kwas akrylowy) są słabymi polielektrolitami, mogą posiadać różną ilość ładunków na powierzchni, a także różne struktury konformacyjne w zależności od pH roztworu, co może bezpośrednio wpływać na formowanie kompleksów polielektrolitowych. Dlatego przeprowadzono badania formowania kompleksów w dwóch fazach: ciecz - ciecz, oraz ciecz - ciało stałe.

W wyniku badania układu ciecz-ciecz, określono optymalne pH i stosunek stężenia poszczególnych składników układu prowadzące do formowania stabilnej i nieodwracalnej koloidalnej dyspersji kompleksu. Badania te przeprowadzono stosując analizę turbidymetryczną. Natomiast analiza miareczkowa i wyniki DLS wykazały, że dendrymer i poli(kwas akrylowy) w częściowo naładowanym stanie (pH=8 dla PAMAM i pH=4 dla poli(kwasu akrylowego)), mają zwartą i globularną konformację (kłębka) co zapewniaja stabilne, wysokie stężenie zagregowanych polikompleksów (najwyższa mętność ~1668 NTU). Spektroskopia UV-Vis została wykorzystana do badania wzajemnych interakcji składników polikompleksu i potwierdziła penetrację polikwasu w strukturze PAMAM, a także występowanie oddziaływań elektrostatycznych grup aminowych i karboksylowych.

Trzy różne stosunki stężeń dendrymeru i polikwasu, odpowiadające najwyższym poziomom mętności w każdej serii miareczkowania w fazie ciecz - ciecz, zostały wybrane do badania procesu tworzenia wielowarstwowego polikompleksu w fazie ciecz - ciało stałe. Na podstawie wartości K/S zabarwionego podłoża, określono stosunek stężeń 7:7 (x 10^{-4} g/mL), który przy optymalnym pH zapewnił najwyższy wzrost układu polielektrolitowego na podłożu w fazie ciecz - ciało stałe. Przeprowadzono test barwienia ninhydryną w celu ilościowego określenia ilości grup aminowych po każdym etapie modyfikacji. Stwierdzono, że układy wielowarstwowe dendrymer aminowy / polikwas mają profil wzrostu zbieżny aż do siódmej warstwy. Natomiast zastosowanie kroku pośredniego w postaci suszenia pomiędzy nanoszeniem kolejnych warstw daje większą stabilność warstw. Dodatkowo, na podstawie analizy przepuszczalności powietrza, stwierdzono, że wielowarstwowe układy polielektrolitowe z zastosowaniem etapu suszenia mają mniej zwartą strukturę niż wówczas, gdy próbek nie suszono. Ponadto, na podstawie wyników testów barwienia analizowanego w funkcji liczby warstw, stwierdzono, iż najwyższa ilość grup NH_2 na zewnętrznej warstwie nie zawsze prowadzi do większej interakcji grup aminowych z innymi cząsteczkami. W rzeczywistości, najwyższa gęstość grup NH_2 nie prowadzi do najwyższej adsorpcji barwnika. Istnieją także inne ograniczenia hamujące proces kompleksowania, które należy pokonać, aby móc zastosować otrzymane układy do zastosowań takich jak adsorpcja barwnika czy dostarczanie leków.

Podsumowując można stwierdzić, że znajomość profilu wzrostu kompleksu polielektrolitowego na włókninie oraz kontrolowanie ilości grup funkcyjnych w jej warstwie wierzchniej jest kluczowe dla projektowania materiałów włókninowych z rozwiniętymi układami wielowarstwowymi przeznaczonych do zastosowań takich jak dostarczanie leków.

Acknowledgment

I would like to express my sincere gratitude to my supervisor, Prof. Dawid Stawski, for his sincere support and excellent guidance throughout my research. It has been a privilege to conduct my work under his guidance. He was an exceptionally supportive and understanding supervisor who taught me the values of patience, sincerity, insight, collaboration, and creativity, all of which have been essential in my journey to becoming an independent researcher.

I would also like to express my gratitude to my second supervisor, Dr. Somaye Akbari, for her unwavering support, kindness, patience, and understanding. She offered valuable insights and assisted in troubleshooting technical challenges. Additionally, her generous sharing of laboratory equipment and resources significantly facilitated my work.

I would like to formally express my sincere gratitude to the officers of the Interdisciplinary Doctoral School (IDS) at TUL, particularly Miss Marta Romaniszyn and Ms. Katarzyna Margas. Their invaluable assistance with my documentation has been immensely helpful, and I truly appreciate their support.

My deepest thanks go to my family, including my parents, my dear sister, and my grandmother for their never-ending love and support. They have been praying for me throughout this journey and have provided unwavering support during my most challenging times, especially after the profound loss of my husband. I also extend my heartfelt thanks to my little girl, Sofia, whose love remains steadfast, even though I have been unable to spend as much time with her as I would like.

Table of Contents

Abbreviations

PLA-polylactide nonwoven

GSM-Gram per square meter (g/m^2)

PLA1-Polylactide nonwoven with 40 g/m^2

PLA1-Polylactid nonwoven with 120 g/m^2

LBL- Layer-by-Layer

Ln- layer number "n" deposited on polylactid nonwoven prepared with hydrated layer-by-layer

Ln-D- layer number "n" deposited on polylactide nonwoven prepared with dry layer-by-layer method

PE-Polyelectrolyte

PEC-Polyelectrolyte complex

PAA-Poly (acrylic acid)

PAMAM- Amine-terminated poly (amidoamine) dendrimer

PLA$_n$- Multilayered polylactide nonwoven with layer number of n, where add n (1, 3, 5, and 7) refers to **PAA** as the top layer and even n (2, 4, 6, and 8) refers to the PAMAM as the top layer

C$_{PAMAM}$ or C$_{PAA}$-Concentration of PAMAM solution or PAA solution

Wn- waste-dye solution after staining procedure of multilayer PLA nonwoven with n layer prepared with hydrated layer-by-layer method

List of Scheme

List of Tables

List of Figures

1. Introduction

1.1.   Objective

Layer-by-layer (LBL) deposition is a well-defined, versatile, and straightforward surface modification technique applicable to various substrates, irrespective of their shape, size, or surface chemistry, and can be conducted under mild conditions [1][2], [3]. The polyelectrolyte (PE) multilayers formed via LBL are easily tunable based on the selected polyelectrolytes and by controlling operational factors such as pH, concentration, ionic strength, and the application method. The LBL approach encompasses various techniques, including dipping, spray coating, spin coating, and brushing [4]. In this study, polylactide nonwoven fabrics, recognized for their biocompatibility and eco-friendliness, have been chosen for LBL modification. Poly (acrylic acid) (PAA), serving as a linear polyanion (-), and poly(amidoamine) (PAMAM), functioning as a dendritic polycation (+), have been chosen for the LBL technique, utilizing electrostatic attraction as the driving force. The amine-terminated PAMAM exhibits unique physicochemical properties, including numerous positive functional groups and an interior hydrophobic cavity, making it highly effective for host-guest applications such as drug delivery, wastewater treatment, and filtration [1], [5], [6]. Additionally, its abundance of positively charged terminal groups allows for electrostatic interactions with negatively charged molecules. Furthermore, the primary amines confer excellent antibacterial properties [7]. Therefore, the introduction of PAMAM into PLA nonwoven fabric through the LBL technique can enhance its functionality and broaden its application scope. Consequently, the primary objective of this study is to monitor the multilayer assemblies of PAA and PAMAM polyelectrolytes on pre-treated and functionalized PLA nonwoven fabric. One of the most important characteristics of the LBL technique is the activation of the substrate to facilitate the depiction of the first layer. As a result, the optimal conditions for PLA pre-treatment through aminolysis using the dendritic aminolysis agent PAMAM were systematically investigated, aimed at creating a higher density of amine anchors for the deposition of the first PAA layer. Following this, the study examines the effects of operational factors, such as the pH and concentration of the polyelectrolytes, on the formation of turbid

colloidal complexes in the liquid-liquid phase. Based on the established optimal conditions, multilayers were assembled on the pre-treated PLA. The investigation then transitions to the liquid-solid phase, focusing on the influence of polyelectrolyte concentration ratios and intermediate drying during the dipping approach of LBL on the growth profile, structure, and density of the polyelectrolyte multilayers.

1.2. Hypothesis

Weak polyelectrolytes exhibit varying degrees of ionization depending on the pH of the medium, which can lead to different conformations based on their ionization state. The repulsive forces between ionized groups may cause the polymer structure to expand or swell, subsequently influencing its complexation with oppositely charged molecules. Therefore, it was hypothesized that:

(1) Polyelectrolytes in the same conformational structure have a greater probability of forming irreversible complexes.

Conversely, an increase in the concentration of polyelectrolytes at a specific pH results in a higher charge density. Thus, it was hypothesized that:

(2) An increase in the concentration ratio of polyelectrolytes leads to greater formation of aggregated polyelectrolyte complexes (PEC) in the liquid-liquid phase, although there will be a point beyond which PEC formation decreases.

(3) The condition leading to maximum complex formation in the liquid-liquid phase may in turn resulted in the most significant growth of polyelectrolyte multilayers on the substrate in liquid-solid phase

Additionally, it was hypothesized that:

(4) The polyelectrolytes concentration ratio and intermediate air drying may influence the adsorption-desorption phenomenon in the LBL process.

(5) Intermediate air drying may affect the growth profile, which can be quantified using the ninhydrin assay.

(6) Intermediate air drying may impact the density of the assembled multilayers on the substrate, as well as their mechanical properties.

(7) The multilayered PLA may exhibit superior antibacterial properties compared to simple aminolyzed PLA.

2. Literature review

2.1.   Polymer modification methods

Most industrial polymers, due to the absence of functional end groups, exhibit hydrophobic surfaces and an inert nature. This characteristic significantly restricts their applicability across various fields and limits the potential for further modifications. The inherent hydrophobicity can hinder adhesion, compatibility, and interaction with other materials, which are critical factors in many applications, including coatings [8], adhesives [9], and biomedical devices [10]. As a result, polymer modifications aimed at enhancing and developing their properties are essential. [11], [12] [13]. Polymer modification methods, as illustrated in Scheme 1, can generally be classified into three primary categories: "blending," "grafting," and "curing." Each of these methods serves distinct purposes in enhancing the properties of polymers [14].
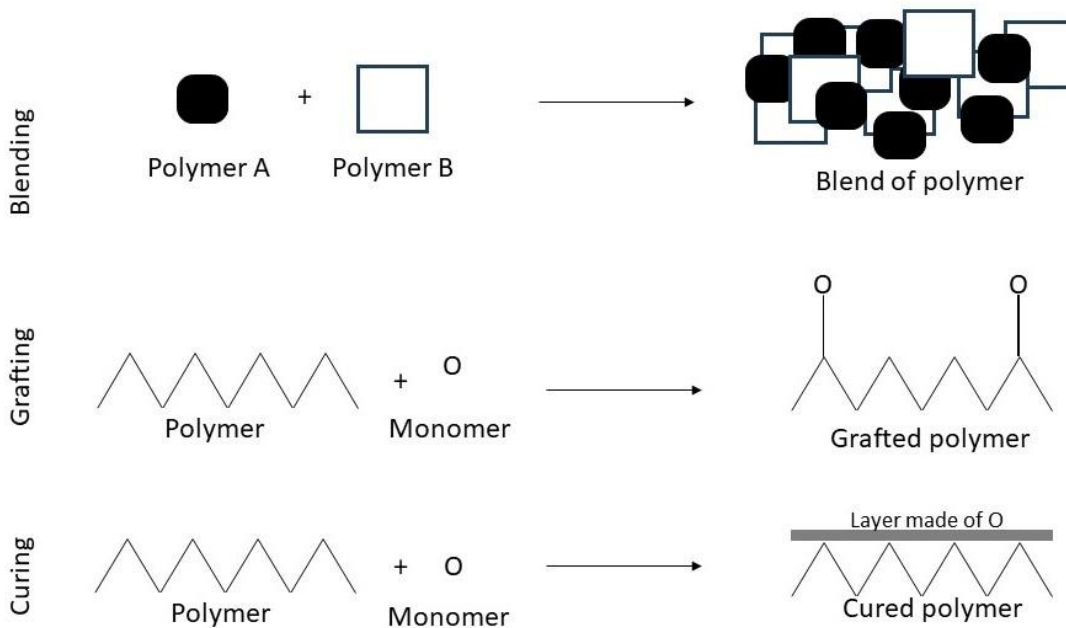
Scheme 1. Schematic representation of the methods of polymer modification [14].

Briefly, as illustrated in Scheme 1:

- *Blending* refers to the mechanical and physical mixing of at least two different polymers to create a composite material. This technique allows for the combination of advantageous properties from each polymer, resulting in a material that can exhibit improved performance characteristics such as increased toughness, flexibility, or thermal stability. The effectiveness of blending is influenced by factors such as the compatibility of the polymers involved, the specific ratios used, and the processing conditions applied during the mixing process [15]–[17].

- *Grafting* involves the covalent attachment of monomers or polymer chains to the main backbone of an existing polymer. This method allows for the introduction of specific functional groups or properties that may not be inherent in the original polymer. By modifying the polymer in this way, it is possible to enhance properties such as hydrophilicity, thermal resistance, or chemical reactivity, thereby broadening the potential applications of the modified material. Grafting can be accomplished through various chemical reactions, including radical polymerization, click chemistry, and other synthetic pathways [14], [18].

- *Curing* is a process in which a monomer or a mixture of monomers is used to create a coating on a polymer substrate, typically through physical forces or chemical reactions. This method often results in the polymerization of the applied monomers, leading to the formation of a cross-linked network that significantly enhances the mechanical and chemical properties of the underlying polymer. Curing can improve characteristics such as hardness, chemical resistance, and overall durability, making it suitable for applications in coatings, adhesives, and sealants. Curing methods can be categorized into two main types: radiation curing, which includes ultraviolet light, gamma rays, accelerated electron beams, and X-rays; and thermal curing, which encompasses radiation heating (such as infrared, laser, and microwave), convection and conduction heating (including flame and oven), as well as induction heating, ultrasonic heating, and resistance heating [19]–[21].

Notwithstanding the aforementioned classification of polymer modification methods, an alternative categorization may also be considered. From a different perspective, the properties of polymers can be tailored at two distinct levels: surface and bulk. Each level offers unique opportunities for modification, allowing for the enhancement of specific characteristics that are critical for various applications. Various chemical modification methods can be employed to achieve these modifications, enabling researchers and engineers to optimize polymer performance for specific needs [22].

(a) *Bulk Modifications* refer to techniques that alter the entire volume of the polymer material, affecting its overall properties. Key techniques at this level are blending [23], [24], solvent casting [25], [26], copolymerization [27], [28], and cross-linking [29], [30]. For example, Raj A. et al. [31] successfully enhanced the thermomechanical properties of poly (L-lactic acid) by blending it with 30 wt% of polyamide. This modification resulted in a final product exhibiting a maximum ductility of 225%, an impact toughness of 48 kJ/m², and thermal resistance up to 123ºC, highlighting the effectiveness of bulk modification techniques.

(b) *Surface Modifications* focus on altering the outer layer of the polymer material, which can significantly influence its interaction with the environment. These modifications enhance surface characteristics such as adhesion, surface charge, wettability, and biocompatibility [32], [33]. In the following section, we will provide a comprehensive explanation of this method.

In summary, both bulk and surface modifications play critical roles in tailoring polymer properties for specific applications. While bulk modifications focus on enhancing the overall material characteristics, surface modifications are essential for optimizing interactions with other materials and the environment. The details of these surface modification techniques will be discussed in greater depth in the subsequent section, highlighting their significance and applications in polylactide.

2.2.   Surface modification methods

Polymer properties can be determined not only based on its intrinsic nature but also as results of the polymer modification. Surface treatment and improvement of outermost surface properties such as hydrophilicity, hydrophobicity, biocompatibility, surface hardness, and introduction of new functionalities can obviate the polymer application problems [13]. Surface modification can combine the main properties of polymers with superficial properties which has been introduced to the polymer surface [22]. Polymer surface modification can be categorized based on two different aspects: (a) type of treatment process and (b) treatment methodology. In the former aspect, a wide range of process treatments are available to tailor the top layer of polymer properties. The most common method is the manipulation of surface energy by adding functional groups [34] and the introduction of micro- and nanoscale surface roughness by mechanical or chemical abrasion process [35]. In the latter, surface treatment (based on the treatment methodology), can be divided into four categories including physical, chemical, thermal, and optical methods [22]. For example, Kamalov A. et al. [36] improved the biocompatibility of polylactide films by employing plasma treatment as a physical surface modification to enhance human fibroblast proliferation activity. In another study, J. Q. Kim et. al [37], introduced a novel surface modification strategy designed to create a poly(ethylene terephthalate) (PET)-based membrane with a hydrophilic surface, resistance to organic fouling, enhanced nutrient ion permeability, and adequate mechanical strength. This is achieved through the use of anthracene (ANT)-attached polyethylene glycol (PEG) surface modification agent (SMA) in which the anthracene moieties of the SMAs penetrate and anchor to the surface of a commercially available PET woven fabric through physical interactions and mechanical locking. Meanwhile, the PEG chains extend over the surface in brush and arch configurations, forming a hydration layer on the fabric. The resultant surface properties and unique structure of the modified PET-based membrane lead to significantly improved nitrate ion permeability, enhanced resistance to organic fouling, and increased microalgae production compared to the unmodified membrane. In another study, alkaline hydrolysis as a chemical

surface modification was employed to functionalize PET fabric for further modification with poly (vinyl alcohol) (PVA) [38].

In the following sections, we focus on the surface modification methods implemented in this research.

2.2.1. Grafting

Grafting is a common surface modification technique categorized into two approaches: "grafting to" and "grafting from," as illustrated in Scheme 2. The "grafting to" approach, also known as "direct polymer coupling reaction," involves the direct attachment of a known polymer with specific molecular weight and composition onto a polymer surface that has reactive groups capable of bonding with the other polymer [13]. For instance, the grafting of poly (ethylene glycol) chain onto cellulose surface via esterification is an example of a direct polymer coupling reaction or "grafting to" approach [39]. Typically, achieving high grafting densities with this approach due to steric hindrance and diffusion restriction of the modifier is challenging [40]. To address these challenges, the "grafting from" approach, referred to as "graft polymerization of monomers," is employed. This method entails growing polymer chains directly from a surface through graft polymerization of a specific monomer, initiated by high-energy radiation or oxidizing agents [13]. The "grafting from" approach typically involves two main steps: (1) activating the inert surface and (2) reacting selected monomers at the newly created active sites on that surface [13]. The activation step for graft polymerization can be performed using several techniques, including (a) plasma discharge [41], [42], (b) irradiation by ozone [43], electron beam [44], gamma rays [45], [46], ultraviolet radiation (UV) [47], and (c) chemical method initiation through free-radical mechanism [14]. For example, in a study acrylic acid monomer was polymerized on an activated polypropylene nonwoven filter surface with induced oxygen plasma to introduce carboxylic acid groups onto the PP surface to prepare a cesium adsorbent filter [48].
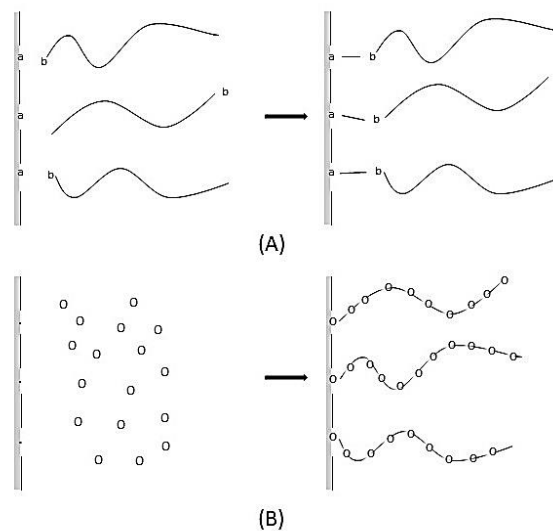
Scheme 2. Schematic of (a) grafting to and (b) grafting from approaches [13]

In our research team, we successfully functionalized the surfaces of poly (propylene) (PP) and polylactide (PLA) nonwovens with acrylic acid monomer using the "grafting from" approach. This process was accomplished through three distinct activation methods including (1) chemical reaction using ammonium peroxydisulfate an oxidizing agent, (2) photografting under UV light, and (3) plasma treatment using air and oxygen [49]. In the context of chemical reactions using ammonium peroxydisulfate, commonly known as ammonium persulfate, as an oxidizing agent, sulfate-free ion radicals can be generated by heat, leading to the production of hydroxyl radicals. This process, outlined in mechanism (I), initiates graft polymerization by abstracting hydrogen from the polymer chain, thereby creating free radicals on the polymer backbone [14], [50]. For photografting under UV light, using hydrogen peroxide as a photosensitizer, free radicals on the polymer chains are produced by hydroxyl radicals formed through the photolysis of H_2O_2 under UV light, as described in mechanism (II) [51]. In the case of plasma discharge, macromolecular radicals on the polymer chains, which facilitate graft polymerization, can be generated by accelerated electrons in the presence of oxidizing gases such as oxygen and air, as detailed in mechanism (III) [14], [52].

Mechanism (I):

$$S_2O_8^{2} + heat \rightarrow 2SO_4^{\bullet-}$$

$$SO_4^{\bullet-} + H_2O \rightarrow HSO_4^- + OH^{\bullet}$$

Mechanism (II):

$$H_2O_2 + h\upsilon \rightarrow 2OH^{\bullet}$$

Mechanism (III)

$$O_2 + e \rightarrow O_2^+ + e$$
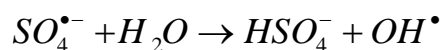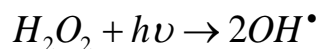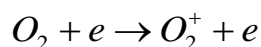
According to the obtained results, the ATR-FTIR analysis revealed the emergence of a new peak around 1727 and 1650 cm^{-1} corresponding to PP and PLA nonwoven, respectively, associated with the stretching of the carbonyl bond, confirming the successful grafting of acrylic acid (AA) onto PP and PLA nonwovens through three distinct methods. Quantitative assessment of the area under this new carbonyl peak indicated that photografting under UV light produced a significantly larger standardized peak area, suggesting enhanced AA grafting on both nonwovens, with values of approximately 42.7 for PLA and 22.7 for PP, in comparison to other grafting methods. Furthermore, UV-visible spectrophotometry corroborated these findings, demonstrating that photografting resulted in higher levels of AA grafting on both PP and PLA nonwovens, as reflected by increased dye adsorption percentages in the grafted samples compared to those processed by alternative methods. The findings help to find an appropriate method to create a functionalized surface of PP and PLA with the highest carboxylic groups for future applications [49].

2.2.1.1 Aminolysis

The reaction of amines with esters, known as aminolysis, has roots in organic chemistry that date back to the early 20th century. While it is difficult to pinpoint a single individual who first proposed this reaction, to the best of our knowledge, Hawkins and Tarbell [53] first suggested the mechanism of ester aminolysis in 1953. According to records, all ester-containing polymers including polyesters [54], polyurethane [55], and polycarbonate [56] are susceptible to aminolysis reactions when exposed to aminolysis agents. This

chemical process involves the reaction of these polymers with amines, leading to significant enhancements in the hydrophilicity and functionality of their surfaces [57], [58].

Aminolysis reaction, as described in Scheme 3, involves cleavage of hydrophobic ester bonds through nucleophilic attack of amines on the carbonyl carbon of an ester, resulting in the replacement of them with relative hydrophilic amid bonds and release of hydroxyl groups [59]. The molecules bearing one or more nucleophilic amine groups can be considered as aminolysis agents [57]. Utilizing diamine molecules with two amine groups ($-NH_2$) as an aminolysis agent would endow the polymer surface with amino ($-NH_2$) and hydroxyl (-OH) groups. Indeed, one amine participates in an aminolysis reaction and the second amine can be utilized for further modification such as layer-by-layer [56] deposition or can participate in different reactions leading to the polymer surface having other functional groups including –SH, -COOH, and –$CH=CH_2$ [57]. Furthermore, the formation of hydroxyl (–OH) groups on the polymer surface as a result of the aminolysis reaction can serve as a critical initiator for various chemical processes including atom transfer radical polymerization (ATRP), or other covalent bond or physical adsorption [57], [60]. The most common diamines serves as aminolysis agents are hydrazine, ethylenediamine, and 1,6-diaminohexane, 1,3-diaminopropane (1,3-DAP), 1,2-diaminopropane (1,2-DAP) [61], [62]. Besides diamines, some polyamines polymers can serve as aminolysis agents as well but are more complicated in stoichiometry than diamines in terms of both the reactants and the products [57]. G. Mallamaci et al. [63] employed three poly aminolysis agents including 1,6-hexamethylenediamine (HDA), polyallylamine hydrochloride (PHA), and tetraethylenepentamine (TEPA) to develop antifouling properties of 2D-matrices of polylactic acid (PLA) and polyhydroxybutyrate (PHB). It was revealed that PHB was more sensitive than PLA to aminolysis and the highest amino group density was obtained on the surface through aminolysis with PAH.
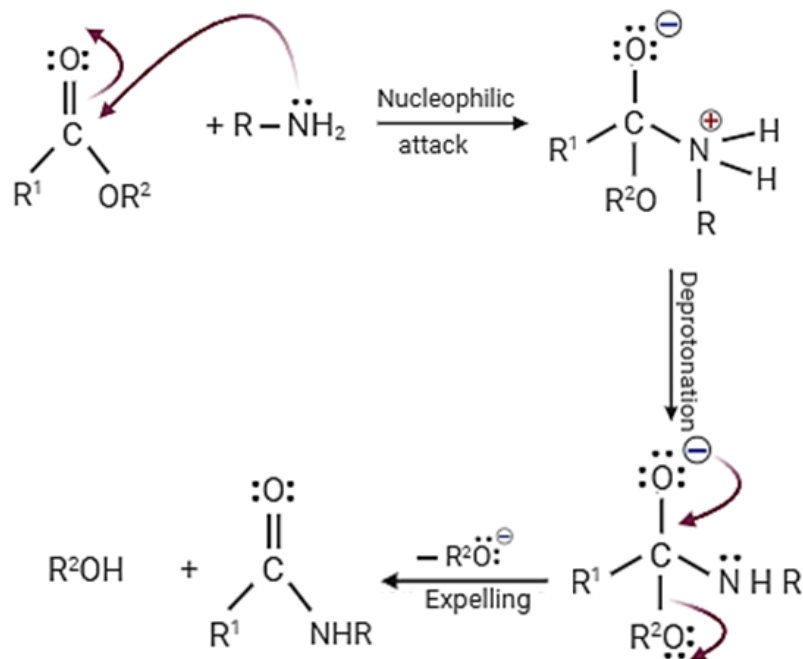
Scheme 3. minolysis reaction of an aminolysis agent with one amine groups [59]

Several factors can influence the aminolysis rate, including temperature, time, concentration of aminolysis agent, and the solvent [60]. For instance, M. Somani et al. [55] investigated the influence of reaction parameters including temperatures, time, and ethylene diamine (EDA) concentration as an aminolysis agent on the formation of free amino ($-NH_2$) groups and the physicochemical properties of the polyurethane film. The highest yield of aminolysis resulted in ~ 0.08 $\mu M/cm^2$ with 10% EDA for 15 minutes. In another study, the impact of the solvent on aminolysis was investigated. Bech et al. [64] (27) revealed that the rate of aminolysis reaction on poly(ethylene terephthalate) fibers with 1,2-ethane diamines was faster in methanol than water. Also, Z, Yang et al. [60] investigated the aminolysis rate of 1,6-hexanedimine with poly(Ɛ-caprolactone) (PCL) as a function of solvent. This sequential order was obtained for the aminolysis are water< isopropanol< ethanol< and methanol. This might be attributed to the solvent polarity. The reaction proceeded very slowly in water, the most polar solvent, primarily due to the inadequate wetting of the hydrophobic PCL membranes. This poor wetting created challenges for the diamine molecules to effectively approach the PCL chains. In contrast, the reaction rates were considerably higher in relatively

less polar alcohols, with methanol exhibiting the highest reaction rate among the solvents tested [60]. Another crucial factor that significantly affects the aminolysis reaction is the molar mass of the aminolysis agent. Research has shown that as the molar mass of the amine increases, the density of amine groups in PET fibers decrease, while other conditions remain constant. This decrease can be attributed to the fact that aminolysis occurs at the interface between the polyester and the amine solution, making the reaction highly dependent on the ability of diamine molecules to effectively contact the carbonyl carbons in the ester bonds. Higher molar mass amines may have reduced mobility, limiting their interaction with the polyester surface and consequently hindering the aminolysis process [64].

In addition to the commonly utilized linear aminolysis reagents, there exists a significant class of polymeric materials known as dendritic polymers, particularly those with amine-terminated structures, can serve as aminolysis agent [6], [65]. These dendritic structures possess a branched architecture, which provides unique properties and functionalities that can enhance the aminolysis process. The following section (2.3.1) will explore the potential applications and advantages of using dendritic polymers in aminolysis reactions, highlighting their ability to improve reaction efficiency and surface modifications. Aminolysis reaction creates functional groups that act as the activating layers in different surface modification methods like the layer-by-layer (LBL) assembly technique explained in the next section.

2.2.2. Layer-by-layer technique as surface modification method

The manipulation of surface functionality in polymers to control their chemical properties has been a focus of research for many years. This process often involves the direct introduction of discrete functional groups, such as alcohol or hydroxyl groups, which can then be transformed into a series of chemically distinct surfaces through well-controlled chemical reactions. However, a significant drawback of this method is its impracticality [66]–[68]. Conversely, practical methods like plasma treatment or graft polymerization, while widely used, often fail to produce chemically well-defined surfaces [68]. In this context, the layer-

by-layer (LBL) assembly technique presents a promising approach, enabling the design and preparation of surfaces with precisely defined chemical functionalities [67].

The deposition of multilayer nanoscale film on solid substrates through the layer-by-layer (LBL) technique is recognized as a straightforward, adaptable, and bottom-up surface modification approach. This method allows for the incorporation of desired properties into various substrates, regardless of their shape, size, and surface chemistry, under mild conditions [2]. LBL deposition was first modeled by Iler [69] in the 1960s and further developed by Decher et. al [70] in the 1990s, continuing to the present day. The Langmuir-Blodgett (LB) technique, which pioneered the creation of monolayers of organic molecules at the air/water interface and their subsequent transfer onto a solid substrate, served as the foundation for the layer-by-layer (LBL) technique. The LBL method aims to employ LB films to construct nanostructured films with polyelectrolytes for specific applications [71]. There are various driving forces for the multilayer assembly though the LBL technique including [72], [73]:

- *Biological affinity*; the growth of multilayer nanoscale film achieved by biological components, including enzyme (glycoenzymes) and non-catalytic protein (concanavalin A) through LBL to prepare electrochemical biosensor [74].
- *Charge-transfer interaction*; the growth of multilayer film achieved by nonionic molecules containing electron-acceptor and electron-donor groups, for example, poly[2-(9-carbazolyl)ethyl methacrylate] as electron-donor and poly[2-[(3,5-dinitrobenzoyl)oxy]ethyl as electron-accepter where assemble to prepared ultrathin film based on charge transfer interaction [75].
- *Hydrophobic interaction*; the growth of multilayer film achieved by uncharged molecules. For instance, stable ultrathin film can be obtained by repetitive physical adsorption of poly(vinyl alcohol) (PVA) onto gold substrate followed by drying process [72].
- *Hydrogen bonding*; the growth of multilayer film achieved by uncharged materials that can act as hydrogen bonding donors and hydrogen bonding acceptors. For instance, multilayers of poly(N-vinylpyrrolidone and poly(methacrylic acid) were prepared by hydrogen bonding attraction [76].

- *Covalent bonding*; the growth of multilayer film achieved by intermolecular interaction between complementary functional groups of two polymers which can covalently bond in situ leading to the formation of the most stable, robust and functional multilayer. For instance condensation reaction of nucleophiles (such as amines) and carbonyl derivatives (anhydride polymer) [77].

- *Electrostatic attraction*; the primary driving force for multilayer self-assembly relevant to our study, is explained in detail below.

The self-assembly electrostatic interaction is the most typical driving force behind the layer-by-layer (LBL) technique for forming multilayer thin films. This interaction occurs between the oppositely charged regions of at least two polyionic components. The primary objective of the LBL technique is to deposit thin organic layers containing functional groups of charged water-soluble materials on the surface [71]. As depicted in Scheme 4, the LBL principle involves the sequential immersion of an activated substrate into diluted solutions of oppositely charged polyelectrolytes (PEs) until the desired number of layers obtained. The rinsing between the LBL processes is crucial to remove any excess PEs and weakly adsorbed molecules, preventing cross-contamination with the PE complex assembled during the LBL deposition. These successive adsorptions of cationic and anionic polyelectrolytes lead to the creation of multilayered thin films [78], [79]. The features of LBL components, polyelectrolytes, and the factors governing multilayer formation are going to be discussed in the following section.
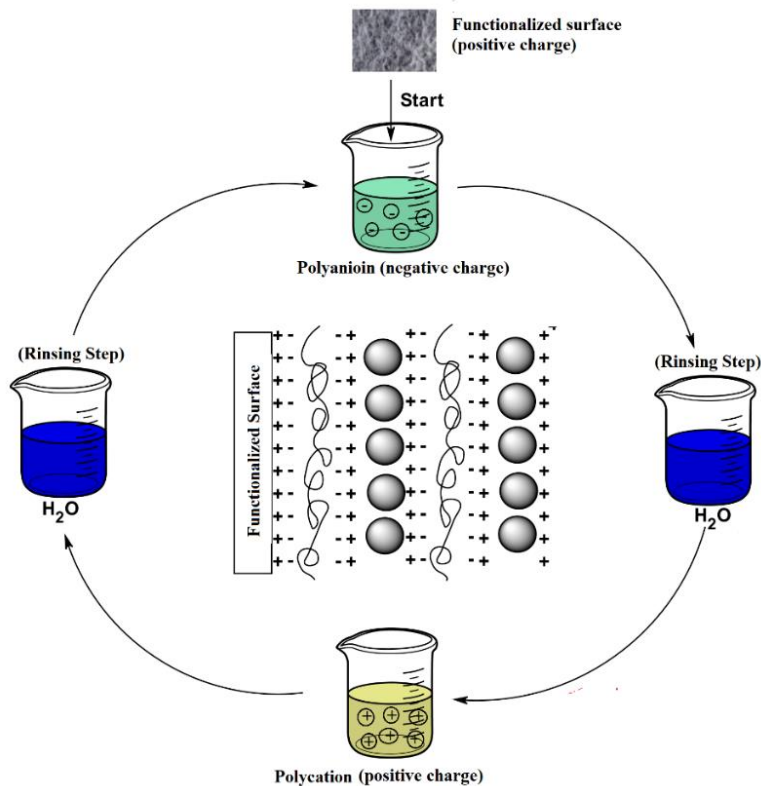
Scheme 4. Multilayer construction on functionalized substrate by layer-by-layer technique

2.4.1.2 *Polyelectrolytes: characterization and types*

Polyelectrolytes (PE) are macromolecules bearing functional groups able to get charged when they are dissolved in a polar solvent like water. PE can acquire charges by the adsorption of ions or by the dissociation of the surface functional groups; especially proton exchange equilibria including the protonation and deprotonation process [80]. Polyelectrolytes are the primary components of the layer-by-layer technique, with electrostatic interactions serving as the driving force. Below are some polyelectrolytes that have been utilized in LBL deposition: polyethyleneimine (PEI), poly(sodium-4-styrenesulfonate) (PSS), poly(diallyldimethylammonium chloride) (PDADMAC) [81], poly(allylamine hydrochloride) (PAH) and poly(acrylic acid) (PAA) [82], PSS and PDADMAC [83], Poly(amidoamine) dendrimer (PAMAM) and PSS [84], chitosan and PSS [85], poly(allylamine) (PAM) and PSS [86] carboxyl-terminated poly(amidoamine) dendrimer (PAMAM–COOH) and poly(methacrylic acid) (PMA) [87].

PEs can be classified based on different aspects including [88]:

(1) *Their origin*: natural (e.g., proteins), semi-synthetic (e.g., xanthan gum), and synthetic (e.g., poly (styrene sulfonic acid)

(2) *Their charge*: polycation (e.g., +), polyanion (-), and polyampholyte (+ and -)

(3) *Their charge density*: strong and pH-independent charge and weak and pH-dependent charge

(4) *Their shape*: rigid (e.g., poly(p-phenylene) and spherical (e.g., globular proteins)

(5) *Their position of ion sites*: linear including integral (ions present in the backbone of the polymer) and pendant (ions present inside-chain of the polymer), branched/cross-linked

(6) *Their composition:* homopolymer (one type of small ion) and copolymer (two different of two types of monomers)

The most typical classification is based on their charge density. PEs can be considered as either strong or weak, depending on their ability to dissociate in aqueous media. Strong PEs, such as poly (styrene sulfonic acid) (PSS), can be fully charged in aqueous environments. In contrast, weak PEs, like poly (acrylic acid)(PAA), have a dissociation constant range of $0 < pK < 14$ and undergo proton exchange depending on the pH of the experimental conditions which can affect their conformational structure [80]. PEs exhibit a propensity to form complexes with one or more oppositely charged ionic species, giving rise to polyelectrolyte complexes (PECs). The formation of a PEC is driven by the electrostatic interactions between polycation and polyanion upon mixing aqueous solutions of oppositely charged PEs [88], [89]. The formed PECs can be categorized as either nonstoichiometric water-soluble PECs, which are formed by a large difference in the mixing ratio of PEs, or stoichiometric insoluble PECs, which are formed by a 1:1 molar ratio of the strong ionic groups of the PEs. Therefore, the electrical charge, degree of ionization, charge distribution, ionic strength and pH of the media, concentration, mixing ratio, nature and molecular weight of PEs can influence their interaction to form PEC formation [88].

According to the findings reported by T. Swift et al., [90] the conformational structure of poly(acrylic acid) (PAA) is heavily dependent on its molecular weight, in addition to the pH and ionic strength of the system. Particularly for low molecular weight PAA (M_n < 16.5 kDa) pH-responsive conformational changes was not observed. Therefore, for the high molecular weight of PAA, the conformational structure would be changed by the ionic strength and pH of the media. Generally, weak polyelectrolytes can undergo conformational changes based on the degree of protonation in which the greater protonation and molecular charge result in more expanded and hydrated polymer conformation [91]. Concerning PAA, it undergoes a reversible conformational transition from coil-to-globule from high to low pH. At low pH, it has a compact, not fully collapsed, and globular conformation. As pH increases, ionization along the polymer chain may cause the polymer structure to swell and change to an open coil conformation. The PAA chain conformation as a function of ionic strength revealed that as ionic strength increases, the repulsive force between the negatively charged groups along the chain is reduced due to counter-ion screening, leading to conformational changes from the open coil to globular conformation [90], [92], [93].

Poly(amidoamine) dendritic polycation as another weak polyelectrolyte can undergo conformational changes based on the degree of protonation. It was suggested that the PAMAM charging mechanism involve two independent protonation steps of primary and tertiary amine groups [94]. At high pH and deprotonated state, PAMAM possesses "dense core" conformation with a maximum density at the dendrimer core and uniform void spacing between branches; however, at low pH and fully protonated state, PAMAM conformation changes to "dense shell" with maximum density at the dendrimer periphery and non-uniform void spacing between branches [95].

2.4.1.3 Operational factors in Layer-by-layer

The profile growth and overall thickness of the multilayer assemblies deposited on the substrate via the layer-by-layer (LBL) technique governed by several key factors including:

1- *Polyelectrolyte pH*

The pH of the polyelectrolyte solutions can influence their degree of ionization, affecting the charge density and conformation of the adsorbing species. D. Scheepers et al. [81] studied the effect of the pH on the deposition of polyelectrolyte layers of poly(ethylene amine) (PEI) as polycation and poly(sodium-4-styrene sulfonate) (PSS) on a silicon wafer via layer-by-layer technique to produce nanofiltration membrane. PEI, one of the most common weak PE, has primary, secondary, and tertiary amines. Therefore, the growth behavior on silicon wafers at three charge density PEI (pH= 4, 8, and 9) was studied using optical fixed angle reflectometry. The results showed that for all charge density, the adsorption increased as a function of layer's number. However, increasing the pH leading to the lower charge densities of PEI and consequently more PEI adsorption on the substrate. It was shown that at the higher charge densities or number of charged groups of PEs lower number of counterpart PEs is required to compensate for the overall charge density. Therefore, at high charge density lower number of the PEI molecules are deposited on the oppositely charged substrate [81].

2- *Ionic strength*

The ionic strength of the deposition media can modulate the electrostatic interactions between the oppositely charged polyelectrolytes, influencing their adsorption behavior. At the high ionic strength, the repulsive force between the ionized groups due to the counter-ion screening reduces and causes the polymer structure to change from straight to coil conformation, and affect interaction with the oppositely charged PEs counterpart. Generally, salt may reduce the interaction between PEs and consequently permit the rearrangement process [93], [88]. B. Y. Kim et al. [96] investigate the multilayer film formation of poly(amidoamine) and poly(acrylic acid) at the present (0.2 M NaCl) and the absence of the salt on the gold-coated silicon wafer as a substrate. They found that films prepared in the absence of the salt possess larger pores than those prepared at an ionic strength of 0.2 M NaCl. It was proposed that the observed changes in morphology are a consequence of introduction of a supporting electrolyte. The added salt is expected to screen the charges within the films, thereby producing a structure characterized by an increased number of loops and tails. Such a loopy structure may account for the smaller pores observed in films

deposited in a 0.2 M NaCl solution [96]. In another study, the polyelectrolyte multilayers assemblies of poly(amidoamine) and poly(styrenesulfonate) (PSS) on silicon at different salt concentration including no salt, 0.154, 0.5, and 1.0 M NaCl were analyzed. It was revealed that the quantity of PSS deposited per bilayer, following the dendrimer adsorption step, initially rises with an increase in salt concentration (0.5 M NaCl). However, at elevated salt concentrations (1 M NaCl), this amount begins to decrease. This phenomenon is likely attributed to two factors: (i) the enhanced screening of electrostatic interactions at high ionic strength, and (ii) the more coiled conformation of PSS at elevated salt concentrations, which occurs due to charge screening. This coiling results in a reduced number of contact points, and lower PSS deposition at very high ionic strength (1.0 M NaCl) [97].

3- *Polyelectrolyte concentration*

The polyelectrolyte solutions used in the LBL process can affect the amount of material deposited per layer. M. Yu et al. [83] reported the effect of polyelectrolyte concentration on the filtration membranes performance. Various concentrations of poly(sodium 4-styrene sulfonate) (PSS) polyelectrolyte (1, 2, 3, 4, and 5 g/L) were examined to construct multilayer assemblies of PSS and poly(diallyldimethylammonium chloride) (PDADMAC) on a porous support substrate. The results indicate that an increase in PSS concentration leads to enhanced rejection of sulfate ions (SO_4^{2-}) while simultaneously decreasing permeance. This phenomenon can be attributed to the higher negative charge density on the membrane surface, which arises from the increased PSS concentration, thereby improving the membrane's separation performance. Conversely, the elevated charge density of PSS intensifies the electrostatic attraction between PSS and the oppositely charged polyelectrolyte poly(diallyldimethylammonium chloride) (PDADMAC). This interaction results in smaller pore sizes and a more compact structure of the polyelectrolyte multilayer. Consequently, these factors contribute to an increase in the membrane's rejection performance while reducing its permeance [83].

4- *Intermediate drying:*

The inclusion of drying stages between deposition steps can alter the conformation and profile growth of the adsorbed polyelectrolytes, affecting the overall film structure and thermal behavior. A. Vidyasagar et al. [98] reported the effect of drying on polyelectrolyte multilayer of poly(diallyldimethylammonium chloride) (PDAC) and poly(styrene sulfonate sodium salt) (PSS) on Teflon and quartz substrate. It was revealed that hydrated LBL showed exponentially growing film while dried LBL exhibited linearly growth behavior. Also, dry LBL assemblies were glassy at room temperature and did not show glass transition temperature up to 250 °C, while hydrated LBL showed glass transition at 49-56 °C.

5- *Adsorption time*

The duration of polyelectrolyte adsorption during each deposition step can influence the thickness and morphology of the individual layers [3].

6- *Intermediate rinsing*

The rinsing steps between polyelectrolyte depositions are crucial for removing weakly bound species and preventing cross-contamination between layers [3].

When carefully controlled, all these mentioned parameters govern the growth profile and ultimate thickness of the multilayered polyelectrolyte films fabricated via the LBL technique. Optimizing these factors is essential for tailoring the properties and performance of the resulting functional thin film assemblies [86], [97], [99], [100]. However, another phenomenon, adsorption-desorption, dominates the growth of polyelectrolyte multilayer assemblies, which is discussed in the next section.

2.4.2.3 Adsorption-desorption phenomenon

In addition to the factors mentioned above influence the growth, structure, and properties of polyelectrolytes multilayer growth, another interesting phenomenon that governs multilayer assemblies constructed via the LBL technique is the adsorption-desorption phenomenon. This dynamic process involves partial desorption and removal of the previously adsorbed layer upon exposure to the oppositely charged PE solution to deposit the next layer [85], [87]. However, this trend is not commonly observed in multilayer films composed of linear polyanion/polycation polyelectrolytes [86]. Such behavior has been more significantly reported when one of the constituent species possesses a low molecular weight like dye [101] or in dendrimer/polyanion systems [97]. For example, A. J. Khopade et al. [84] investigated the adsorption-desorption behavior during the construction of multilayers composed of poly(styrenesulfonate) (PSS) and poly(amidoamine) dendrimers on planar supports. Results from quartz crystal microbalance measurements indicated consistent layer growth, while UV-Vis spectroscopy of the film demonstrated partial removal of PSS upon the deposition of PAMAM. Notably, the absorption peak at 227 nm, associated with the phenyl groups of PSS, was observed to decrease following the deposition of PAMAM.

The investigation of the adsorption-desorption phenomenon has primarily focused on multilayer film formation on smooth and uniform substrates, such as quartz slides and silicon wafers. Techniques like quartz crystal microbalance measurements and UV-Vis spectrophotometry of the layered substrate have been extensively employed to elucidate this dynamic behavior [84], [97]; however, there is a gap in understanding of the adsorption-desorption behavior of multilayered dendrimer-based assemblies on prose and rough substrates like textiles materials including nonwoven.

The occurrence of adsorption-desorption during the LBL assembly process can have profound implications for the growth kinetics and ultimate structure of the multilayer films, particularly in systems involving polyelectrolytes of varying molecular weights or dendrimer-based architectures. Developing a

comprehensive understanding of this phenomenon is crucial for the rational design and optimization of multilayer thin film systems with tailored properties and performance.

2.3 Dendritic Polymer

In the field of polymer science, a distinct class of synthetic polymers known as dendritic polymers has emerged, exhibiting unique and specialized physicochemical properties that attract considerable attention in both academic and industrial realms. Dendritic polymer can be divided into four groups, hyperbranched polymers, dendrigrafts, dendrons, and dendrimers [102]. Among dendritic polymers, hyperbranched polymers and dendrimers, attracted more attention since they possess unique structural characteristics, including three-dimensional highly branched topologies, functionalized structures, and relatively nonpolar interior cavities between their branches [103], [104].

Generally, hyperbranched and dendrimer polymers, as depicted in Scheme 5, possess three fundamental components: a central core, repetitive units, and surface functional groups. The core, which can have varying degrees of multiplicity, is situated at the center of the dendrimer, and the construction of the dendrimer either initiates or terminates from this core. The repetitive units or branches are covalently bonded to the central core and are organized in a series of radially concentric layers referred to as 'generations' (G) [6]. Dendrimers can be synthesized by two distinct approaches including divergent and convergent as ascribed in Scheme 6. Briefly, the divergent method involves the outward growth of the dendrimer from a multifunctional core molecule, progressing generation by generation. In contrast, the convergent synthetic approach is characterized by a stepwise construction that begins with the periphery groups and progresses inward to attach to the multifunctional core molecule [104]. Hyperbranched polymer synthesis involving single-step synthesis is a transition between liner polymers and highly branched dendrimers while providing many of the dendrimer's properties being a good alternative for the dendrimers [5], [104]. These distinctive features endow dendritic polymers with the potential to be utilized in a wide range of applications, such as biomedical and drug delivery systems [105], [106], energy-harvesting devices [107], [108], bio- and chemical sensors, wastewater treatment processes [102], [109], [110], and surface

modification [58], [111]–[113]. For instance, poly(amidoamine) dendritic polymer has been utilized as a poly(ether-b-amid) modifier to prepare dense membranes with CO_2/CH_4 gas separation properties [114].

Scheme 5. Dendritic polymer architecture [6]

(a) Divergent approach   (b) Convergent approach

Scheme 6. Diagram of dendrimer's synthesis route

2.3.1 Amine-terminated dendrimer as an aminolysis agent

The surface functionality of the dendrimer and hyperbranched polymer can be tailored, for example, adapting different terminal groups to make them more or less hydrophilic which can change their solubility properties, surface charge and functionalities, and applications [6], [102]. Among dendrimers and hyperbranched polymers, those with NH_2 terminated groups, namely amine-terminated dendritic polymers, are very promising and interesting dendritic polymers in textiles area. The most common amine-terminated dendritic polymers, are poly(propylene imine) (PPI), poly(ethylene amine) (PEI), and especially poly(amidoamine) (PAMAM) families [5].

Aminolysis through amine-terminated dendritic materials containing a large number of amine groups in their structure is an almost new approach to modifying and functionalizing polymers, even more efficient than previously used common aminolysis agent described in section (2.2.1.1) [65], [115]. Burnett et al. [65] investigated the aminolysis rate as a function of the number of amine groups. The aminolysis reaction of ρ-nitrophenyl acetate was conducted using ethylenediamine (EDA), which has 2 amine groups, and generations G1 to G5 of PAMAM dendrimers, containing 4, 8, 16, 32, and 64 terminal amines, respectively. The yield of the aminolysis reaction was monitored via UV absorbance measurements at 410 nm, corresponding to the yellow color produced by the leaving group during the aminolysis reaction. The results indicated that the initial aminolysis rate increased approximately 28-fold from EDA to generation 4. However, a decrease in the aminolysis rate was observed for G5, which has 65 terminal amines, compared to G4, although it remained 21 times greater than that of EDA with two amine groups. This increase in aminolysis rate from EDA to G4 was attributed to two factors. (1) The dendrimer acted as static covalent micelles, solubilizing p-nitrophenyl acetate within its hydrophobic interior cavities, thus increasing the effective molarity of the reagents and enhancing the aminolysis rate; (2) the internal amide groups of PAMAM stabilized the intermediate reaction product, lowering the activation energy and resulting in a faster aminolysis rate. However, the reduction in aminolysis rate for G5 relative to G4 was attributed to the highly crowded surface of dendrimer, which hindered substrate access to the hydrophobic environment

within the dendrimer [65]. In Table 1, the application of amine-terminated dendritic polymer as an aminolysis agent on the polyester polymer is summarized. In Table 2, examples of the chemical structures of common and dendritic aminolysis agents are presented.

Table 1. Examples of surface modification using dendritic polymer

Aminolysis agent	Substrates	Aims
Poly(amidoamine) (PAMAM)	Polylactide nonwoven	Hydrophilicity improvement and create an active site for further layer-by-layer deposition [58]
	Polycaprolactone nanofiber	Increasing the hydrophilicity, introduction of drug loading and anticancer properties [116]
Poly(propylene imine) (PPI)	Poly(l-lactic acid) electrospun fibers and films	Enhancement of wettability, antibacterial, host-guest properties [111], and promoted cell adhesion and viability [112]
Poly(ethylene imine) (PEI)	Poly(l-lactic acid) electrospun nanofibers	Controlled drug release and antibacterial properties [117]
	Polycarbonate film	Functionalized PPC surface for further layer-by-layer deposition to improve cytocompatibility [56]

Table 2. Example of aminolysis agents

Typical Aminolysis Agents [61], [62], [63]	Ethylenediamine Polyallylamine hydrochloride 1,6-diaminohexane
Dendritic Aminolysis Agents [5]	Poly(propylene imine) (PPI)-G2 Poly(ethylene imine) (PEI)-G2 Poly(amidoamine)(PAMAM)-G2
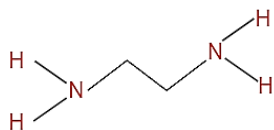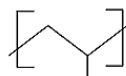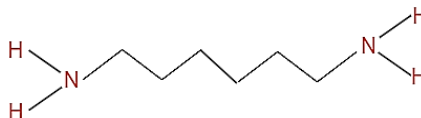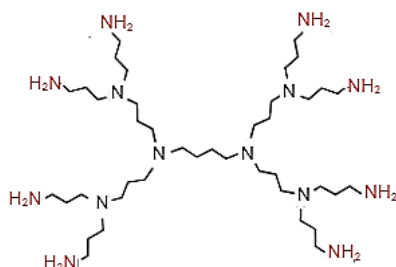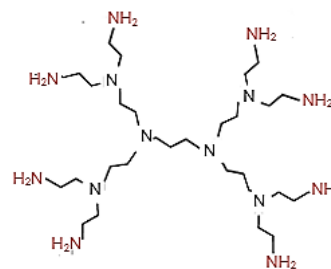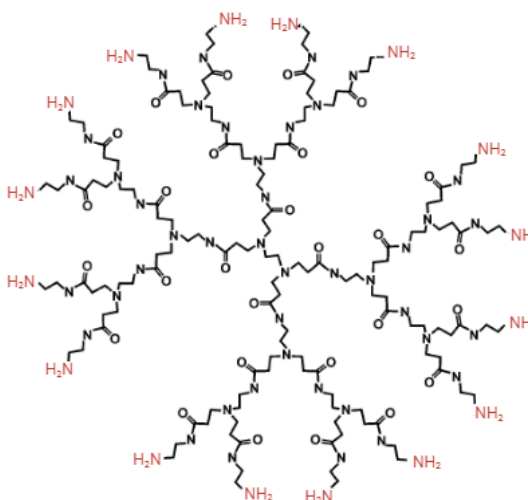
2.3.2   Amine-terminated dendritic polymer as Antimicrobial Agents

Numerous studies have shown that primary amino groups on the surface of the cationic dendritic polymer (PPAMAM, PPI, and PEI) contribute to their positive surface charge which can act as an antibacterial agent in drug delivery systems and biomedical applications [1], [118] as well as polyelectrolyte in the self-assembly system [119]. The antibacterial activity of positively charged polymers can be attributed to their interaction with negatively charged cell membranes. This interaction results in the formation of nanopores in the bacteria cell membrane, causing damage, leakage of cellular contents, and ultimately leading to cell death [7], [120]. For instance, in a study, functionalized electrospun poly(L-lactic acid) (PLLA) nanofibers were created by blending PLLA with polyethylene imine (PEI) at various weight ratios and mixing times to enhance the drug-loading capacity and antibacterial properties of the matrix. The findings demonstrated that the functionalized PLLA nanofibers exhibited 99.99% antibacterial activity, attributed to amine groups in PEI. The optimal mixing time and polymer ratio were also identified as critical factors in achieving suitable nanofiber characteristics and improving spin-ability for subsequent biomedical applications [117]. The application of the amine-terminated dendrimer in a self-assembly system using the layer-by-layer technique is discussed in the next section.

2.3.3   Dendritic polymer application in self-assembly application

Dendritic polymers, regarded as promising synthetic materials due to their distinctive physicochemical properties, can engage in layer-by-layer self-assembly processes through various mechanisms, including electrostatic interactions, hydrogen bonding, and covalent bonding, contingent upon their functional terminal groups. Multilayer assemblies can be formed using positively charged dendrimers paired with polyanion, negatively charged dendrimers combined with polycation, and oppositely charged dendrimers. In this context, the primary driving force is electrostatic attraction [119]. Regarding hydrogen bonding as a driving force in LBL assembly, dendrimers with terminal carboxylic acid groups can function as both hydrogen bond donors and acceptors. For instance, S. Tomita et al. [87] developed a multilayer thin film using carboxyl-terminated poly(amidoamine) and poly(methacrylic acid) (PMA) at pH 4 through LBL

assembly. At this pH, hydrogen bonding between the carboxyl groups of COOH-PAMAM and PMA served as the driving force. However, at a higher pH of approximately 7, the polymers became charged, leading to electrostatic repulsion between the negatively charged carboxylate groups, which resulted in the decomposition of the multilayer film. It has also been reported that amine-terminated dendritic polymers, such as PAMAM and PPI, can be covalently bonded to anhydride copolymers like poly(maleic anhydride)-co-poly(methyl vinyl ether) to facilitate multilayer self-assembly. This occurs through the reaction of primary amines with anhydride groups, resulting in the formation of amide and imide linkages. Furthermore, carboxyl-terminated PAMAM and diazo resin have demonstrated the ability to create multilayer film assemblies through photochemical reactions [119]. Consequently, dendritic polymers, such as PAMAM, can be effectively utilized to construct multilayer assemblies for a wide range of applications including biosensing to monitor the biological and biochemical process, bio-imaging, and gene therapy, drug/therapeutics delivery [119], [121]. Some notable applications of dendrimer-containing LBL multilayer assemblies include:

(1) *Filtration application*; D. Scheepres et al.[81] prepared an asymmetric membrane at three different pH (4, 8, and 9) with a combination of poly (diallyldim-ethylammonium chloride) (PDADMAC) and poly (sodium-4-styrene sulfonate) (PSS) base layer terminated with layers of highly branched poly (ethylenediamine) (PPI)/PSS. The results showed that independent of the pH, the asymmetric membrane showed >90% salt retention. In addition, the membrane prepared at pH=4 formed an open base layer and defect-free layer resulting in much higher permeability.

(2) *Waste-water treatment*; M. Xu et al. [122] developed a novel multilayered membrane that serves dual functions: it excels in catalytic degradation and oil separation while exhibiting high permeability and recovery performance for treating oily wastewater containing water-soluble dyes. The commercial PVDF membrane was modified using a one-step self-assembly method, driven by electrostatic attraction. The environmentally friendly polyelectrolyte complex was created through the sequential deposition of tetra (4-carboxyphenyl) porphyrin (TCPP), poly(amidoamine)

hyperbranched (PAMAM), and phytic acid (PA). The modified membrane showed >99% oil rejection, 93% and 96% degradation efficiency of rhodamine B and methylene blue.

(3) *Encapsulation and Controlled Release*; It has been reported that dendrimer-containing self-assemblies can effectively adsorb and release dye molecules at specific pH levels, functioning as both nanodevices and nanoreservoirs. A. J. Khopade et al. [84] fabricated ultrathin polyelectrolyte multilayers with 10 layers by sequentially dipping planar support into negatively charged poly (styrenesulfonate) (PSS) and a positively charged fourth-generation poly(amidoamine) dendrimer driven by electrostatic attraction. This approach demonstrated the potential for encapsulating 4,5-Carboxyfluorescein (CF) as a model acidic substance within the dendrimer-based shell, achieving an 80-90% release of CF after 4 hours. UV-visible spectroscopy measurements indicated no loss of PSS following CF release, which suggests the stability of the prepared film. In another study, hydrogen-bonding multilayers of carboxyl-terminated PAMAM (PAMAM-COOH) and poly (methacrylic acid) (PMA) were constructed on quartz slides. The results demonstrated that the film was capable of adsorbing Rose Bengal and 5,10,15,20-tetraphenyl-21H, 23H-porphine tetra sulfonate, which served as two model dyes. These dyes could be released in a controlled manner upon changes in pH. Consequently, it was proposed that PAMAM-COOH-containing layer-by-layer (LBL) films have the potential to function as effective nanodevice for pH-sensitive delivery systems [87].

(4) *Controlled drug release*; dendrimer-containing LBL can be effectively engineered for drug delivery systems, offering enhanced control release over multilayer due to well-defined dendrimer and hyperbranched architecture in comparison to conventional polymer-based LBL system [121]. In one study, mesoporous silica nanoparticles were functionalized using the LBL assembly method to deposit multilayers of biocompatible PAMAM and chondroitin sulfate (CS), a natural polysaccharide found in bone. The resulting multilayered nanocarriers exhibited self-fluorescent properties and demonstrated pH-dependent drug release behavior, along with enhanced targeted delivery performance [123].

2.3.   Polylactide Material

Polylactide (PLA) is a biocompatible and biodegradable thermoplastic aliphatic polyester derived from renewable resources such as biomass and agricultural waste. It has attracted significant attention as an eco-friendly, greener plastic alternative. PLA is one of the promising industrial polymers that can replace common petrochemical polymers, including polypropylene [124]–[127]. The PLA synthesis process begins with LA (Lactic Acid) production, which then leads to the formation of lactide as an intermediate step. The process concludes with the polymerization of the lactide to produce PLA. There are several polymerization processes to convert LA to PLA, as depicted in Scheme 7 [124].
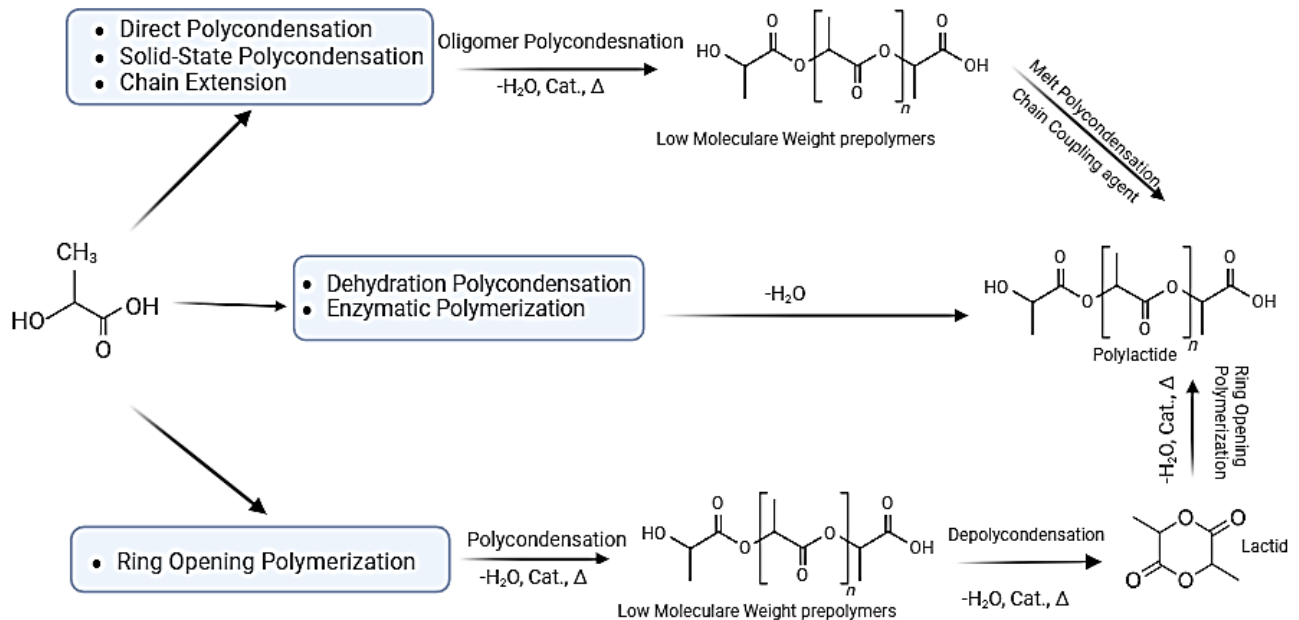
Scheme 7. Synthesis route of PLA [124]

2.3.1 Polylactide Surface Modifications Method

Polylactide (PLA) as an biodegradable and biocompatible polymer due to its physicochemical advantages such as good mechanical strength, non-toxicity, biocompatibility, and process-ability may be applied in a wide range of applications including drug transport and smart clothing in three-dimensional printing technology [128], [129] and in many other fields like drug delivery systems, biomedical, and tissue engineering [126], [130], [131], food packaging [132], [133], agriculture and automotive [126], [134]. However, PLA suffers from some drawbacks such as low thermal stability, a relatively slow degradation rate, and poor hydrophilicity limiting its range of application. Therefore, PLA modification is crucial [135], [136]. For instance, a recent study investigated modifying PLA film surface properties to enhance cellular compatibility. The researchers reported that improving the hydrophilicity of the PLA film surface led to a significant increase in the viability of fibroblast cells cultured on the modified PLA substrate. To achieve this, the PLA film was, first, subjected to the argon plasma, and then acrylic acid plasma grafting was followed [137]. The most well-established permanent surface modification techniques for PLA can be broadly categorized into two main approaches (1) chemical conjunction using alkaline hydrolysis and aminolysis and (2) photografting including liquid phase photografting and vapor phase photografting [54], [136], [138]. Table 3 provides a summary of selected publications that have addressed the surface modification of PLA materials.

Table 3. Summary of PLA Surface Modification Methods

Modification approaches	Materials	Aim
Chemical conjunction — Alkaline hydrolysis	NaOH and gelatin	Enhancement of the surface hydrophilicity [139] and surface compatibility with living medium after following post-treatment of gelatin grafting [140]
Aminolysis	The second generation of poly(propylene imine) dendrimer	Improvement of cell viability and hydrophilicity of the nanofibers to provide host-guest properties [111], [112]
photografting — Liquid phase	A radio frequency of 10.5 MHz discharge in air plasma as pre-treatment followed by photografting by acrylic acid and acrylamide as monomers, and benzophenone as an initiator	Bioactive surface with faster degradation [141]
Vapor phase	*N*-vinylpyrrolidone as a monomer, and benzophenone as an initiator	Improve wettability and adhesion of cell culture [142]

2.4.   Nonwoven Technology

Nonwoven fabrics are made of individual fibers that are tangled, bonded, or felted together. These are filament yarn or short (staple) fibers, which are bonded together by different methods to form the nonwoven roll. The binding of the web, layers of loosely networked, can followed by various methods including:

(1) Heat low melt fibers used and heat melts the fibers together

(2) Chemical fibers are chemically bonded to each other

(3) Mechanical treatment fiber entanglement.

Indeed, this binding corresponds to waving or knitting the yarn in traditional textile production [143], [144]. There is a three major areas in nonwoven technology [145].

(1) Drylaid nonwoven; carded or aerodynamically formed fibers bounded various methods including needle-punching, thermo-bonding, chemical bonding, hydro-entanglement, etc.

(2) Wetlaid materials in papermaking

(3) Spunlaid nonwoven in polymer extrusion and plastic.

Synthetic thermoplastic polymers, such as polylactide, can be utilized to produce spunlaid nonwovens. The spunlaid nonwoven is directly produced by the collection of extruded filaments onto a conveyor, forming a randomly oriented web, which is subsequently bonded through thermal, mechanical, and chemical methods to create the final nonwoven fabric [145]. The spunlaid technique involves two main processes, spunbond and meltblown, as operated often in sequence in the production line. Both spunbonding and meltblowing share a fundamental principle, yet the technologies employed in each process are markedly different. In both methods, the molten thermoplastic polymer is extruded through a spinneret, subsequently cooled, and then collected on a rotating drum or a moving belt. In the spunbonding process, from the extruded filaments, a continuous web is created; and then bonded together. Conversely, in the meltblowing process, molten filaments are thinned and entangled, achieving self-bonding as they are deposited onto a collector [146].

Textile materials, especially nonwovens have great applications in different areas ranging from hygiene, medical, and healthcare to electronics, automotive, and packaging. The common industrial polymers to produce nonwovens are polypropylene (PP), polyethylene (PE), polyester (PET), and nylon (PA6 and PAA66) which all are petroleum-based. Polylactide as an eco-friendly and natural-based polymer has been attracting the most attention in nonwoven technology [145], [143]. Therefore, the Spunlaid polylactide nonwoven had been selected as substrates for polyelectrolyte multilayer assembly.

3. Aim and area of dissertation

The growth profile and structure of polyelectrolyte (PE) multilayer assemblies constructed through layer-by-layer technique on fully smooth, flat, and non-porous inorganic surfaces including quartz slides or silica wafers have been extensively investigated in the literature. However, there is a significant gap in the understanding of the fundamental mechanism governing the layer-by-layer deposition and PE multilayer assemblies on rough, uneven, and porous surfaces, particularly those found in textile materials, including nonwoven fabric. Therefore, this study aims to monitor the construction of multilayer assemblies consisting of dendritic amine-terminated poly(amidoamine) (PAMAM) and poly(acrylic acid) (PAA) on pre-treated polylactide (PLA) nonwoven fabric using the layer-by-layer technique via the dipping method. This comprehensive study is structured into three phases:
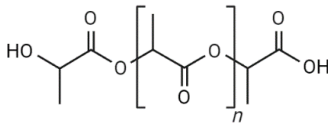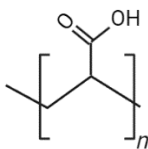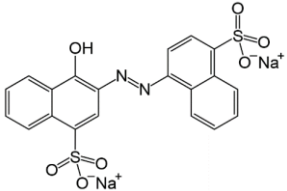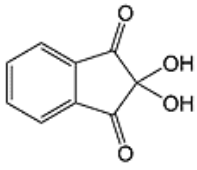
(1) Optimization of PLA Functionalization: This phase focuses on aminolysis to prepare the functionalized PLA for subsequent LBL deposition.

(2) Liquid-Liquid Phase Study: This phase encompasses the characterization of PAMAM and PAA polyelectrolytes, as well as the optimization of polyelectrolyte complex (PEC) formation based on the pH and concentration ratio of the polyelectrolytes.

(3) Liquid-Solid Phase: This phase involves monitoring the construction of PE multilayers (eight layers) on functionalized PLA nonwoven fabrics via the layer-by-layer technique.

(4) Confirmation of the structure and analysis of the properties: In this stage, the methodology of the modified surface analysis is included, as well as the selected properties of the material are investigated.

4. Experimental Part

4.1.　　　Materials

Polylactide polymer with M_n=167 700 g/mol (6202D) was produced by Nature Works. Polylactide (PLA) nonwoven with a gram per square meter (GSM) of 40 (PLA1) and 120 g/m^2 (PLA2) were prepared in Łukasiewicz – Institute of Biopolymers and Chemical Fibers. Ethanol with 99.6% purity, poly(acrylic acid) (PAA, M_w= 450 kDa), hydrochloride acid (HCl, 37% w:w), sodium hydroxide pallet (NaOH), and ninhydrin reagent were purchased from Merk & Co., Inc. Acid red 1 as an anionic model dye was obtained from Ciba, Inc. Amine-terminated poly(amidoamine) dendritic polymer (PAMAM, generation 2, M_w=3256 Da) was donated by Delta-Dolsk, Poznań, Poland. Distilled water was used for the pre-treatment modification and deionized water was used for all modifications.

Table 4. Chemical structures of Acrylic acid as first layer and dyes model

Chemical structure of the used materials

Polylactide (PLA)		**Poly (acrylic acid) (PAA**	
Acid red 1 (AR)		**Ninhydrin**	

Poly (amidoamine) (PAMAM)
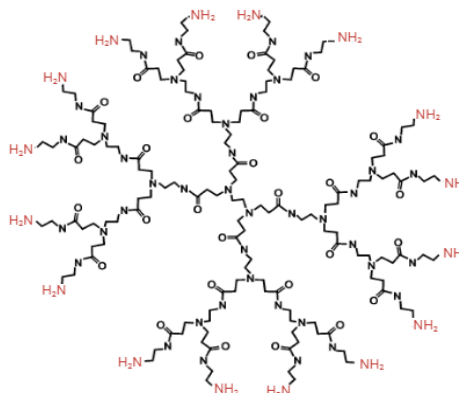
4.2.   Methods

4.2.1. Pre-treatments of PLA nonwoven via aminolysis reaction using amine-terminated dendritic poly (amidoamine) (PAMAM) polymer

PLA inert surface was amine-functionalized through aminolysis reaction using amine-terminated groups of dendritic poly (amidoamine) (PAMAM) [58]. PLAs nonwovens were immersed into 1% (w: v) PAMAM solution in ethanol at 2 different temperatures and 4 times intervals as summarized in Table 5 to find out the maximum PAMAM grafting conditions of aminolysis for the further layer-by-layer modification. Through aminolysis of PLA ester chains, amino groups and hydroxyl would be created that can facilitate the polyelectrolyte deposition.

Table 5. Aminolysis condition as pre-treatment `method of PLA nonwovens

	Temperature of aminolysis reaction (°C)							
	28±2				58±2			
Time of the aminolysis reaction (hour)	1	2	3	4	0.5	1	1.5	2
Rinsing process	Two time quick rinsing, followed by 1 hour immersing into distilled water, finalized by one quick rinsing							

4.2.2. Preparation of Polyelectrolyte Multilayer Assemblies via Layer-by-Layer Deposition on Functionalized PLA Nonwoven

To prepare multilayer assemblies of poly (acrylic acid) (PAA) and poly (amidoamine) (PAMAM) polyelectrolytes (PEs) on functionalized PLA nonwoven substrates, we first focused on the liquid-liquid phase interaction of PAA and PAMAM. This step aimed to identify the optimal pH and concentration ratio necessary to form aggregated polyelectrolyte complexes (PECs). Following this, the multilayer growth on the substrate was investigated.

4.2.2.1 Liquid-Liquid Phase Study

The polyelectrolyte's optimal pH and concentration ratio to form a turbid colloidal complex was first studied in a liquid-liquid phase based on polyelectrolyte titration. To determine the optimal pH for complex formation, 7×10^{-4} g/mL PAMAM polyelectrolyte at different pH values of 10, 8, 6, and 3 was titrated against 7×10^{-4} g/mL PAA polyelectrolyte at pH levels of 10 and 4 (8 titration experiments). After identifying the optimal pH, various concentrations of PAMAM and PAA polyelectrolytes were tested, ranging from 1×10^{-4}, 4×10^{-4}, 7×10^{-4} and 10×10^{-4} g/mL, resulting in a total of 16 titration experiments conducted.

4.2.2.2 Liquid-Solid Phase Study

The layer-by-layer (LBL) technique has been employed to assemble polyelectrolyte complex multilayers of PAA and PAMAM on functionalized PLA nonwoven substrates. Based on the results obtained from liquid-liquid phase studies, the LBL technique was performed as described in Table 6. Initially, the positively charged PLA nonwoven, achieved through aminolysis, was immersed into PAA PE solution at a specific concentration and pH for 10 minutes. After that to remove weakly adsorbed PAA molecules, the substrate was then immersed in deionized water for 1 minute. Subsequently, the negatively charged substrate was dipped into PAMAM polyelectrolyte solution at a defined concentration and pH for another 10 minutes. This cycle was repeated until a total of 8 layers was obtained, with PAMAM as the top layer.

To investigate the impact of intermediate drying on multilayer growth, a series of samples was prepared with intermediate drying at 40 °C following the rinsing process, prior to the deposition of the next layer.

Table 6. LBL conditions to assemble PAA/PAMAM multilayers on Functionalized PLA nonwoven

Polyelectrolyte	Concentration (10⁻⁴×g/mL)			pH	Dipping time (minutes)	Interval rinsing time (minutes)
	a	b	C			
PAA	7	10	10	4		
					10	1
PAMAM	7	7	4	8		

4.3 Characterization tests

4.3.1 Characterization tests of aminolyzed and layered PLA nonwovens

4.3.1.1 Weight changes

To analyze the weight reduction of PLA nonwovens resulting from surface erosion caused by aminolysis, the weights of the samples were measured both before and after the aminolysis process. Functionalized PLA is anticipated to exhibit increased hydrophilicity due to the presence of amino and hydroxyl groups. Therefore, to ensure that the observed weight changes were attributable solely to bond cleavage through aminolysis reaction and not to moisture adsorption, all samples were maintained in a desiccator for 24 hours before weighing. The experiments were repeated five times and the average with standard error was reported.

4.3.1.2 ATR-FTIR analysis

ATR-FTIR spectroscopy was employed to investigate the chemical changes in modified PLA nonwovens, utilizing a Thermo-Nicolet Nexus 870 system over a range of 500–4000 cm^{-1} with a resolution of 4 cm^{-1}. All spectra were normalized using the intensity of the CH_3 band at 1455 cm^{-1} as the internal standard for PLA [147].

4.3.1.3 Color depth (K/S value)

All samples, including neat and aminolyzed PLA nonwovens were stained with Acid Red 1 (AR) as an anionic model dyes as detailed in Table 7. The color strength of the samples (K/S value) was measured using a MiniScan EZ 4500L portable spectrophotometer with a 45°/0° geometry. Samples were one fold; and a white background were considered to minimize the error of the reflected light.

Table 7. Condition of staining procedure of the neat and aminolyzed PLA nonwovens

| Samples | Model dyes | The wavelength of maximum absorbance(nm) | Conditions | | | |
			pH	Temperature (°C)	Time (min)	L: G (cc:g)
PAMAM-grafted PLAs	C. I. Acid Red 1, 10 ppm	505	3	40	45	1:300

The color strength of the substrates after PE multilayer deposition through LBL up to the eighth layer was evaluated in terms of the host-guest properties of the PEC multilayer assemblies. Neat, aminolyzed, and layered PLA nonwovens were stained with a 40 ppm solution of Acid Red 1 at 70 ± 2 °C for 30 minutes. The K/S value of the stained samples was calculated using the Kubelka-Munk equation [148], as outlined in Equation I. Reflectance data for the stained substrates were measured from 400 to 700 nm at 10 nm intervals using a GretagMacbeth Color-Eye 7000A spectrophotometer. Furthermore, to assess the stability of the PEC multilayers, the adsorption of the dye solution after the staining procedure was recorded using a UV-visible spectrophotometer (HACH Company, DR 6000, Germany) at 505 nm.

$$\frac{K}{S} = \frac{(1-R)^2}{2R} \qquad \text{(Eq. I)}$$

Where R is the recorded reflectance data by spectrophotometer.

4.3.1.4 Ninhydrin assay as NH₂ content analysis

The ninhydrin assay was conducted to quantify the available amines following the aminolysis reaction and each layer deposition of PAMAM and PAA polyelectrolytes on PLA nonwoven substrates, as well as to investigate the growth profile of the multilayers. Samples were cut into 1×1 cm² pieces and immersed in a 1 wt% ninhydrin solution in ethanol, then heated at 85 °C for 10 minutes to achieve approximately 90% evaporation. Upon completion of the reaction between ninhydrin and the available amine groups on the substrate, the nonwoven surface developed a purple coloration. Subsequently, dichloromethane was introduced as a solvent for PLA, along with ethanol as a color stabilizer, maintaining a ratio of ethanol to dichloromethane of 1:1.6 (v/v). The absorbance of the resulting mixture was recorded over a range of 500–600 nm using a UV-visible spectrophotometer. The amine content was quantified using Equation (II).

$$NH_2 density(mol/g) = \frac{A \times V(L)}{\varepsilon(mol^{-1}cm^{-1}L)} / w(g) \qquad \text{(Eq.II)}$$

Where the "A" is recorded absorbance, "V" is the volume of solution, "ε" is the absorptivity coefficient measured from the calibration curve (ε=14161.39 mol⁻¹.cm⁻¹.L), and "w" is the weight of the substrate (1*1 cm²).

A calibration curve was established for the PAMAM solution in ethanol at a concentration of 2×10^{-3} g/mL. A total of eight diluted PAMAM solutions were prepared by diluting 16–20 μL of the stock PAMAM solution to 500 μL in ethanol. Then, 1 mL of 0.1 wt% ninhydrin solution in ethanol was added to each diluted PAMAM solution. The mixtures were then heated at 85 °C for 10 minutes. After cooling to room temperature, each sample was diluted to 5 mL with the ethanol-dichloromethane mixture (1:1.6 v/v). The absorbance of each solution was recorded at 575 nm.

4.3.1.5 Water Contact Angle

To investigate the changes in hydrophilicity of the samples after aminolysis using PAMAM dendritic polymer, water contact angles were measured in accordance with the ASTM D 724-99 test method. Each sample was tested ten times, and the average contact angle along with the standard deviation was reported.

4.3.1.6 Air Permeability

To examine the density and structure of the PEC multilayers assembled on the functionalized PLA nonwoven, airflow velocity at a pressure drop of 25 pascals was measured using the SDL-ATLAS Air Permeability Tester ($cm^3 \cdot cm^{-2} \cdot s^{-1}$) in accordance with the ASTM D 737 standard [149].

4.3.1.7 SEM images

The surface morphology of neat, aminolyzed PLA nonwovens, and layered-PLA nonwoven was investigated using scanning electron microscopy (SEM) (30XL, Philips, Netherlands) following gold coating.

4.3.1.8 Mechanical test

The mechanical properties of neat and aminolyzed PLA and layered nonwovens were measured using an INSTRON system (USA). Five samples of each type were cut into rectangular dimensions of 1×10 cm², and the average results along with the standard error of the mean were reported.

4.3.1.9 Antibacterial Properties

The antibacterial activity of neat, aminolyzed, and layered- PLA with PAMAM and PAA top layer was tested against gram-positive Staphylococcus aureus and gram-negative Escherichia coli using the colony-forming unit (CFU) method, as described by the ATCC 100 standard test method.

4.3.2   Characterization tests of polyelectrolytes and polyelectrolytes complex

4.3.2.1 Acid-base titration

To determine the pKa and pKb of the PAA and PAMAM PE, respectively, acid/base titrations were conducted using 5 mL of 10^{-3} g/mL PAMAM and PAA aqueous solutions, with 0.1 M HCl and NaOH as titrants, respectively. The initial pH of the solutions was adjusted to 12 and 2 using diluted NaOH and HCl of the same molarity. Data collection was performed using a pH 691 Microprocessor pH meter (Metrohm, Switzerland). The degree of ionization (DoI) at the equivalence point was calculated according to Equation III.

$$DoI\% = \frac{N_c}{N_m} \times 100 \qquad\qquad \text{(Eq. III)}$$

Where, N_c is mole of the ionized groups at the equivalence point, and the N_m is total mole of ionizable groups in sample.

4.3.2.2 Dynamic Light scattering measurement

The conformational changes of polyelectrolytes as a function of solution pH was analyzed by dynamic light scattering (DLS) test. The hydrodynamic radii of PAA and PAMAM PE solutions at concentrations of 2 mg/L and 1 mg/L, respectively, were measured using a dynamic light scattering device (DynaPro III, WYATT Technology) at various pH levels.

4.3.2.3 Turbidimetric measurements

To find the optimal pH conditions and concentration ratio of PAA and PAMAM PE necessary for forming stable and irreversible complexes in liquid-liquid phase solution, reliable and well-established turbidimetric measurements were carried out. Additionally, to monitor the desorption of the adsorbed species into the PE solution during subsequent layer deposition (LB), the turbidity of the waste polyelectrolyte after each layer deposition was recorded. Turbidity measurements were taken using a turbidity meter (HACH Company,

2100N TURBIDIMETER, Germany). The turbidity values were reported in Nephelometric Turbidity Units (NTU).

4.3.2.4 UV-Visible Spectroscopy

The UV-visible spectra of the pure polyelectrolytes and the PAA/PAMAM complex solution under optimal conditions were analyzed using a UV-visible spectrophotometer (HACH Company, DR 6000, Germany) within the wavelength range of 200 nm to 500 nm.

5 Results and discussion

Nonwoven fabrics, particularly those composed of polylactide, have gained significant attention due to their biodegradable properties and versatility. These materials find extensive applications across various fields, including medical textiles, hygiene products, and filtration. However, polylactide is characterized by its inert nature and limited functionality, which can impede its broader applications. The layer-by-layer (LBL) technique, recognized for its simplicity, versatility, and widespread use in surface modification, can be applied to various substrates including nonwoven, irrespective of their shape and size, to engineer surfaces with precise chemical functionalities. The driving forces in LBL deposition include electrostatic, covalent, and hydrogen bonding interactions. In the context of electrostatic interactions as a driving force in LBL, it is essential to charge the substrate to facilitate the deposition of the initial and subsequent layers. Therefore, pre-treatment of PLA to create functional groups and a charged surface is necessary. In this regard, the first attempt was to functionalized and charge PLA nonwoven surface to facilitate LBL deposition.

5.1 Pre-treatment of the PLA nonwoven with 2 different GSM using PAMAM dendritic Polymers as an aminolysis agent

Layer-by-layer (LBL) deposition of weak polyelectrolytes entails the sequential immersion of a functionalized and charged substrate into solutions of polyelectrolytes with opposing charges. The driving force behind this process is the electrostatic attraction between the charged species. Therefore, to enable effective LBL deposition, it is essential to functionalize the PLA nonwoven to increase the availability of functional charged groups. In this context, an aminolysis reaction was employed as a one-step treatment to introduce positively charged amine groups onto the PLA surface. This modification enhances the substrate's capacity to interact with negatively charged polyelectrolytes, thereby facilitating the LBL deposition process.

The optimal conditions for the aminolysis reaction to functionalize the PLA nonwoven surface with varying surface weights were investigated in this part. The following characterization tests were

conducted to determine the optimized aminolysis reaction conditions: weight changes, color strength (K/S value), water contact angle (WCA), ATR-FTIR analysis, scanning electron microscopy (SEM), mechanical tests, and a ninhydrin assay to quantify amine density.

5.1.1 Weight Reduction

As an aliphatic polyester, PLA can undergo aminolysis reaction, a nucleophilic addition reaction that cleaves ester bonds and replaces them with N-H bonds. This cleavage results in shorter polymer chain lengths and a slight decrease in weight as a surface erosion mechanism. Therefore, the weight reduction serve as an initial indicator of the aminolysis reaction's progress [57]. PLA nonwovens with two different grams per square meter (GSM) (PLA1/40 g/m^2 and PLA2/120 g/m^2) were subjected to aminolysis under varying conditions of time and temperature, with the percentage of weight loss per cm² illustrated in Figure 1.
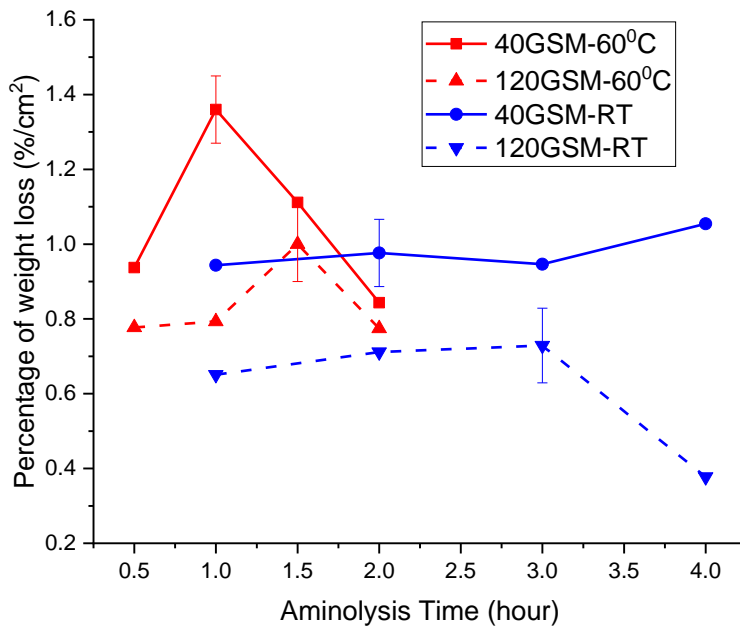
Figure 1. Percentage of weight loss per cm^2 of PLAs nonwovens through aminolysis at different conditions

According to Figure 1, PLA1 nonwoven, with the lower GSM, exhibited its maximum weight reduction after 1 and 1.5 hours at 60 °C and room temperature (RT), respectively; and PLA2 nonwoven, with the

higher GSM, showed maximum weight loss after 2 and 3 hours at 60 ℃ and room temperature (RT), respectively. This initial peak in weight loss suggests that maximum aminolysis and PAMAM grafting occur at these specific time intervals. As dendritic polymers reveal abundant amino functional groups, the aminolysis reaction first happened by reducing weight and followed by diminishing weight loss by re-crosslinking of residual cleaved PLA molecular chains with the PAMAM grafted onto the PLA surface.

To investigate the impact of nonwoven surface weight (measured in grams per square meter, GSM) on the kinetics of the aminolysis reaction, it was found that the rate of aminolysis for PLA1, which has a lower surface weight, is consistently higher than that of PLA2, which has a higher GSM, regardless of the reaction temperature. This is evidenced by the greater weight loss observed in PLA1 compared to PLA2, as indicated by the weight loss curves where PLA1 is positioned above PLA2. Specifically, PLA1 experienced a weight reduction ranging from 0.93% to 1.36%, ultimately reaching its maximum loss, while PLA2 exhibited a weight reduction between 0.78% and 0.79% over a reaction time of 30 to 60 minutes. To explain this, PLA1 and PLA2 demonstrated air permeability of approximately 165 ± 47 cm³·cm⁻²·s⁻¹ and 15.5 ± 0.87 cm³·cm⁻²·s⁻¹, respectively. The more open structure of PLA1 results in a greater available surface area for amine molecules to interact with, leading to an increased rate of aminolysis [60].

To investigate the impact of the temperature on the aminolysis rate, the percentage of weight reduction per cm² at 60 ℃ was consistently higher than that at room temperature. Elevated temperatures typically increase the rate of reactions by providing more energy to the reacting molecules, leading to more frequent and effective collisions [60]. Therefore, the higher temperature at 60 ℃ enhanced the reaction rate, resulting in a greater percentage of weight reduction per cm² compared to room temperature. For example, PLA1 experienced a weight reduction of 1.38% after 1 hour of aminolysis at 60 ℃, compared to a 0.94% reduction at room temperature.

To investigate the impact of reaction time on aminolysis rate, regardless of the reaction temperature, extending the aminolysis duration beyond the point of maximum weight loss led to a surprising decrease in weight reduction. This phenomenon may indicate the reformation of cross-links between the hydroxyl

group presented in detached and cleaved polymer chains and the amines of grafted PAMAM in the PLA backbone. Similar findings have been reported in other studies [112]. For further analysis of the effect of the reaction time on the aminolysis reaction of PLA nonwoven, the aminolysis reaction for PLA1 was extended to 4 hours at room temperature after observing a slight decrease in weight loss following 3 hours of treatment. After 4 hours, a second increase in weight loss was noted, likely due to increased interaction between PAMAM and PLA molecular chains. This interaction would enhance aminolysis, leading to additional cleavage of ester bonds, resulting in shorter polymer chains and further weight reduction. Thus, the initial peak in weight loss can be interpreted as a potential indicator of the grafting yield of PAMAM.

5.1.2   Surface density of amine groups

To evaluate the positive charge density of aminolyzed PLA nonwoven fabrics as a function of temperature, reaction time, and substrate GSM, a staining procedure utilizing the anionic model dye Acid Red 1 was conducted. The results of the color depth analysis are illustrated in Figure 2. Acid red 1 contains two sulfonic acid groups bearing negative charge as sulfonate (SO_3^-) groups in aqueous media [150]. The aminolyzed PLA, characterized by the presence of surface NH_2 groups, can exhibit positive charge due to the protonation of these amine groups (NH_3^+) in aqueous media, with a higher density of positive charge observed under acidic condition. Consequently, during the staining process conducted in acidic conditions, the driving force for dye adsorption is the electrostatic attraction between the negatively charged sulfonate groups SO_3^- of the dye molecules and the positively charged NH_3^+ groups present on the polymer surface. Thus, the color strength of the stained substrate serves as an effective indicator of the aminolysis reaction.
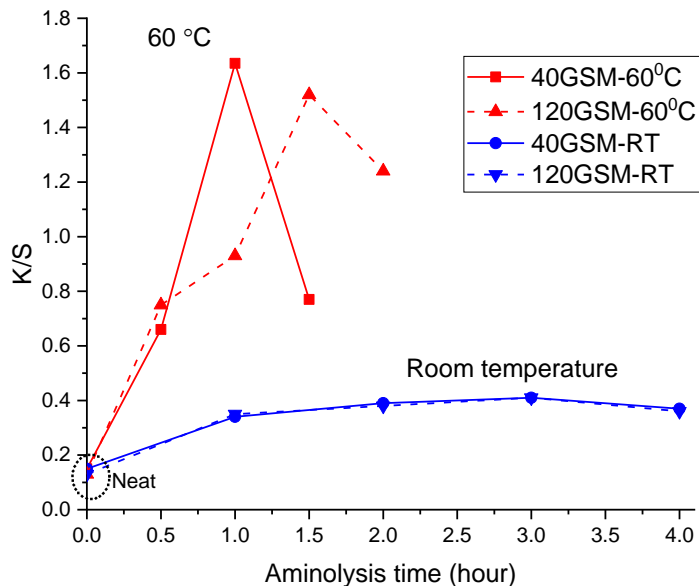
Figure 2. K/S value of stained neat and aminolyzed PLA nonwoven

As depicted in Figure 2, the color depth of the samples aminolyzed at 60 ℃ was significantly higher than that of those aminolyzed at room temperature, with the highest color depths achieved after 1 and 1.5 hours for PLA1 and PLA2, respectively. These findings align with the grafting yield results obtained from the weight change data presented in section 5.1.1. The increase in amino group density on the PLA surface during aminolysis initially enhances the availability of reactive sites. However, this density subsequently decreases, likely due to the re-crosslinking of residual cleaved PLA molecular chains with the PAMAM grafted onto the PLA surface as was identified by a decrease in the weight loss. This re-crosslinking reduces the number of available NH_2 groups, leading to a lower positive charge density and diminished electrostatic attraction for the negatively charged dye molecules. Therefore, aminolysis conducted at the elevated temperature of 60 ℃ resulted in an accelerated reaction, which facilitated greater PAMAM grafting. This, in turn, led to significantly higher dye adsorption and increased color depth (K/S) compared to samples aminolyzed at room temperature.

To assess the effect of GSM, the analysis at 60 ℃ demonstrates a pronounced difference in amine density. Samples with a more open structure provide a greater available surface area, resulting in higher K/S values. This increase is attributed to the elevated amine density, which enhances electrostatic attraction between the positively charged amine groups and the negatively charged dye molecules. Conversely, at room temperature, the aminolysis reaction appears to be limited. The amine molecules and ester bonds do not possess sufficient kinetic energy to facilitate effective collisions, thereby impeding the reaction process. In this scenario, the structural characteristics of the substrate become less significant, as the primary factor influencing the reaction—temperature—remains insufficient to promote the required interactions for successful aminolysis. Thus, the effectiveness of the reaction is largely contingent upon the temperature, highlighting its critical role in driving the aminolysis process.

Furthermore, a ninhydrin assay was performed to quantitatively assess the amine density on modified PLA nonwovens as a function of reaction temperature and substrate GSM. The ninhydrin assay is a widely recognized analytical method used to detect primary amine groups in materials. When ninhydrin reacts with primary amines, as depicted in Figure 3, it produces a purple color complex known as Ruhemann's purple, which can be measured at a wavelength of 570 nm [151], [152]. The average amine density per gram of aminolyzed PLA nonwovens, as a function of reaction temperature, is illustrated in Figure 4. As shown in Figure 4, the amine density of PLA with higher GSM is lower than that of PLA1 at both temperatures, attributed to the more compact structure and reduced surface area available for reaction in PLA2. Considering the reaction time, the amine density at room temperature experienced a reduction of approximately 67.0% for PLA1 and 67.8% for PLA2, compared to elevated reaction temperatures. As explained earlier, higher temperatures can facilitate the reaction by enabling molecules to overcome the activation energy required for the process. This ultimately leads to an increased amine content [60].

Pure ninhydrin
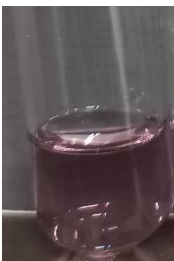
Aminolyzed

samples at

60C/1h
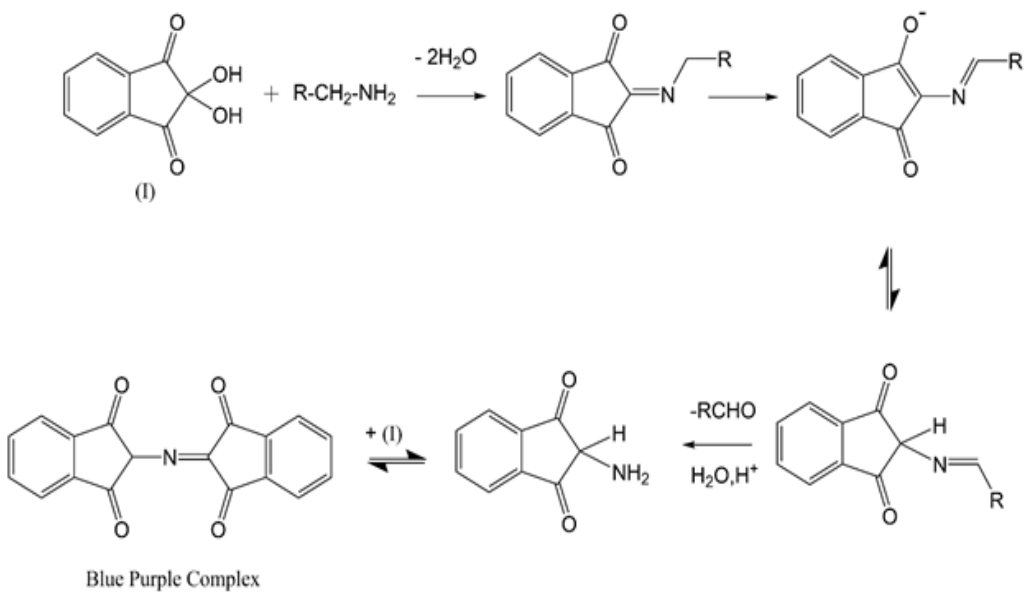
Figure 3. The mechanism of ninhydrin reaction with primary amine [153]
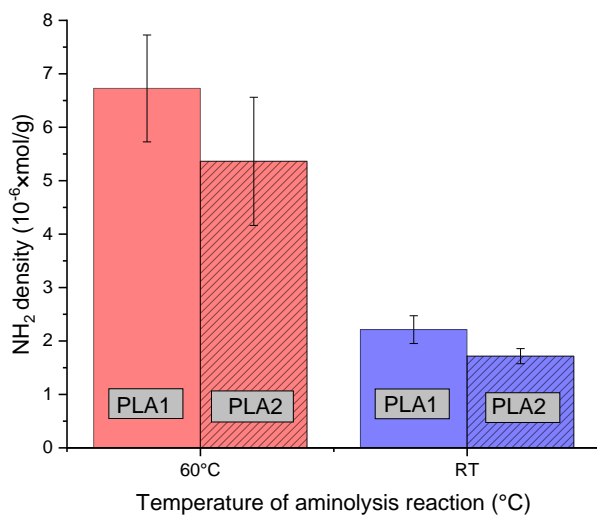
Figure 4. Amine density of aminolyzed PLA with different GSM as a function of temperature

5.1.3 Water contact angle (WCA)

To investigate the effect of grafting on the surface hydrophilicity of aminolyzed-PLA nonwovens, water contact angle (WCA) of neat and aminolyzed-PLA, at the maximum grafting condition obtained from weight change and amine density analysis, was measured; and the results presented in Figure 5. The neat PLA nonwoven exhibited a WCA of approximately 114.7º ± 1.5º. In contrast, the aminolyzed PLAs demonstrated lower WCAs, indicating an increase in surface hydrophilicity. Specifically, for aminolyzed-PLA1 at 60 ºC for 1 hour, the WCA decreased by approximately 22.7%, reaching 88.7º ± 6.6º. Similarly, for aminolyzed-PLA2 at 60 ºC for 1.5 hours, the WCA decreased by about 23.3%, resulting in a value of 88º ± 9º. These findings suggest that the functionalization process significantly enhances the hydrophilic properties of the PLA nonwovens due to the present of the amine and hydroxyl groups upon the aminolysis reaction.
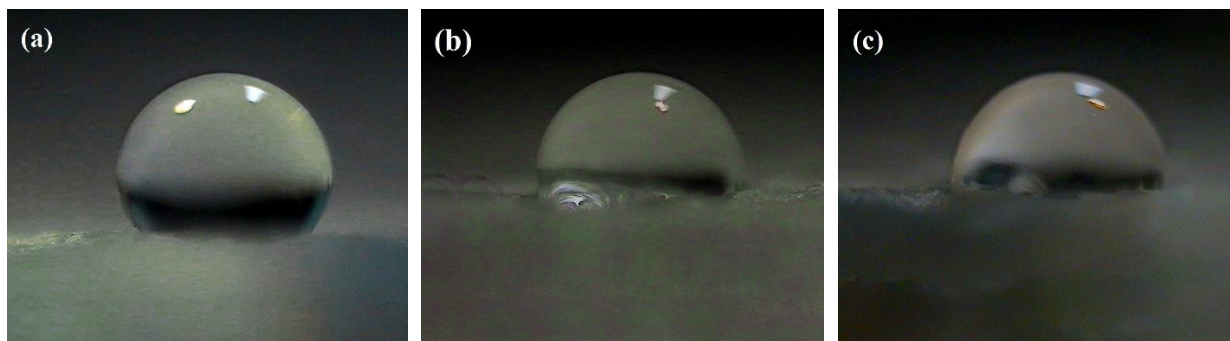
Figure 5. Water droplet images on (a) neat PLA nonwoven, (b) aminolyzed-PLA1 at 60°C for 1h, and (c) aminolyzed-PLA2 at 60°C for 1.5 h

5.1.4 ATR-FTIR analysis

To examine the chemical alterations on the surface of aminolyzed PLA nonwovens, Attenuated Total Reflectance Fourier Transform Infrared Spectroscopy (ATR-FTIR) analysis was conducted. The normalized ATR-FTIR spectra results are presented in Figure 6 (a and b), while the calculated peak heights (intensities) and peak areas are detailed in Table 8. Figures 6a and 6b correspond to PLA1 (40 g/m²) and PLA2 (120 g/m²), respectively. Notably, a new peak appears around 1650 cm⁻¹ for PLA1 and at 1645 cm⁻¹ for PLA2 attributed to the N-H bending vibration. Additionally, a distinct double peak in the range of 3100-

3650 cm^{-1} is associated with the stretching vibrations of the –NH amide groups, indicating the absorption of amide carbonyl groups from PAMAM [112].

According to the literature [61], the cleavage of the ester bond is a critical step in the aminolysis reaction, necessitating a corresponding decrease in the intensity of the carbonyl bond of the PLA molecular chain. As illustrated in the curves and detailed in Table 8, for PLA1, there was a reduction in carbonyl intensity of approximately 31.0% at 60 ℃ and 41.4% at room temperature. In the case of PLA2, the reductions in carbonyl intensity were around 65.5% at 60 ℃ and 24.1% at room temperature. Additionally, the peak areas associated with N-H bending and stretching vibrations (as shown in Table 8) for substrates aminolyzed at 60 °C were greater than those treated at room temperature. This suggests a higher degree of PAMAM grafting on the PLA surface at 60 °C compared to room temperature, which aligns with the results observed in the weight changes and amine density results.

(b)
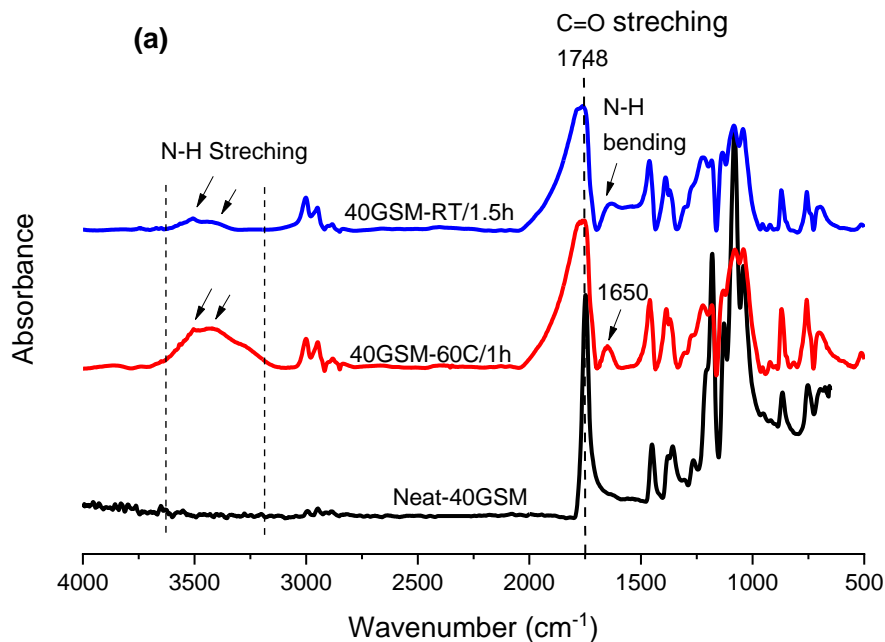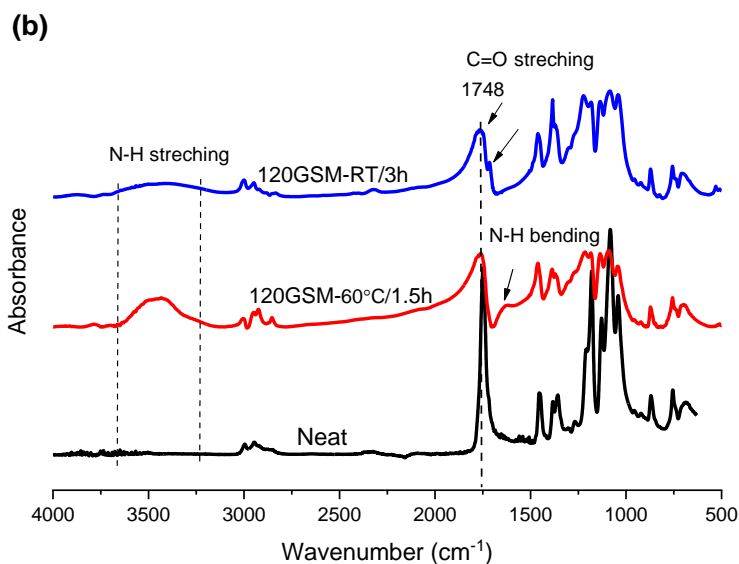
Figure 6. ATR-FTIR spectra of neat and aminolyzed (a) PLA1 and (b) PLA2 at the maximum PAMAM grafting reaction time

Table 8. Peak intensity of ester carbonyl bond of PLA and peak area of emerging new N-H bending and stretching associated with PAMAM

Substrate	Peak intensity	Peak area	
	C=O of PLA at 1766 cm^{-1}	N-H bending at 1590-1730 cm^{-1}	N-H stretching at 3100-3650 cm^{-1}
Neat	2.9	---	---
PLA1-60°C/1h	2.0	31.6	220.3
PLA1/RT/2h	1.7	25.1	48.3
PLA2-60°C/1.5h	1.0	26.2	125.2
PLA2-RT/3h	2.2	13.9	97.1

5.1.5 Scanning electron microscopy (SEM)

To examine changes in surface morphology, scanning electron microscopy (SEM) analysis was conducted. The SEM images presented in Figure 7 reveal that the initially smooth and homogeneous surface of PLA becomes noticeably rougher following the grafting of PAMAM under optimal conditions. Furthermore,

energy-dispersive X-ray spectroscopy (EDX) results confirm the successful grafting of PAMAM, as evidenced by the presence of nitrogen atoms in the analysis. This indicates a successful modification of the PLA surface, highlighting the effectiveness of the grafting process. Creating a rough surface may facilitate further modification as well.

N/C ratio for aminolyzed-PLA1 at 60°C for 1h and aminolyzed-PLA2 at 60°C for 1.5h are 0.24 and 0.16, respectively. Similarly, the O/C ratio for aminolyzed-PLA1 at 60°C for 1h and aminolyzed-PLA2 at 60°C for 1.5h are 2 and 1.755, respectively. More aminolysis reaction create more amide groups, more nitrogen and oxygen content present. Both N/C and O/C ratio confirm other results mention more functional groups for lower GSM samples.
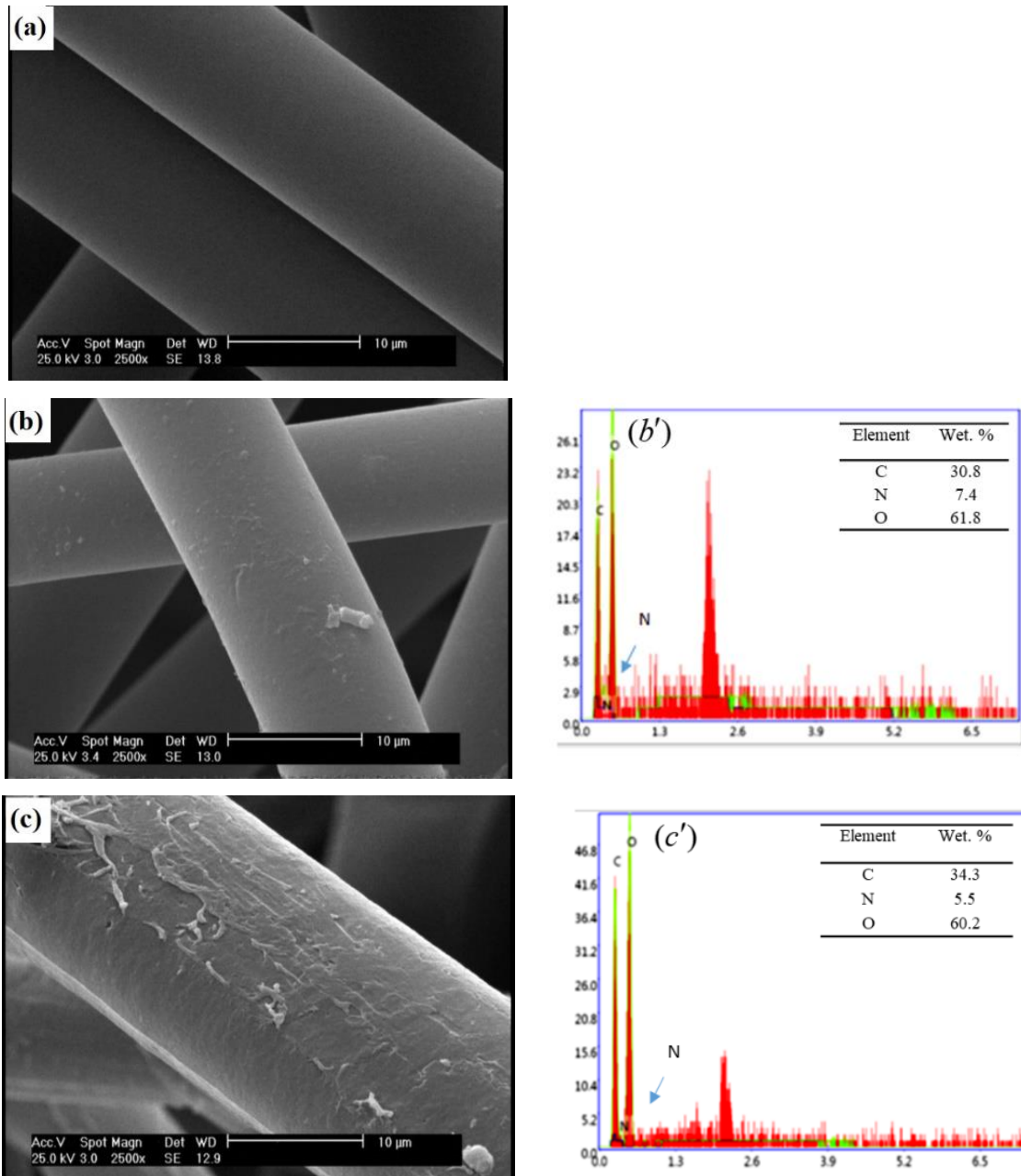
Figure 7. SEM images and EDX of (a) neat PLA; (b)/ (b') aminolyzed-PLA1 at 60°C for 1h and (c)/ (c') aminolyzed-PLA2 at 60°C for 1.5h

5.1.6   Mechanical tests

The mechanical properties of aminolyzed PLA nonwovens as a function of reaction temperature (60°C and room temperature) with two different GSM values were evaluated using static tensile tests. The stress-strain curve and the average of results are reported in Figure 8 (a and b) and Table 9, respectively.

Figure 8 showed neat PLAs exhibited the highest stiffness and tensile strength. In contrast, aminolyzed PLAs demonstrated a notable reduction in these properties, with more significant reduction for elevated aminolysis temperature (60°C). For PLA1 with a GSM of 40 g/m², aminolysis resulted in lower than 1% reductions and approximately 87.84% in Young's modulus corresponding to aminolysis at room temperature and 60°C, respectively. Concerning tensile strength, there was a reduction about 4.39% and 85.0% corresponding to aminolysis at room temperature and at 60°C, respectively. In contrast, PLA2 with a GSM of 120 g/m² showed reductions of about 15.60% and 65.72% in Young's modulus related to aminolysis at room temperature and 60°C; and about 9.18% and 73.96% in tensile strength under the same conditions. Furthermore, neat PLAs displayed elongation at break (EB) values of approximately $29.16 \pm 3.54\%$ for PLA1 and $10.83 \pm 2.58\%$ for PLA2. Aminolysis resulted in a marked decline in EB%, with more profound reduction for aminolysis at 60°C. Aminolyzed PLA1 showed an EB of about $7.29 \pm 2.8\%$, while PLA2 exhibited no elongation at break following aminolysis at 60°C. Indeed, the slippage of fibers in nonwovens plays a significant role. Neat PLA1, which has a lower GSM and surface density, exhibited higher elongation at break, facilitating easier fiber slippage compared to neat PLA2, which has a higher GSM and denser surface, resulting in lower EB%.

When comparing the mechanical properties of PLA as a function of reaction temperature, the decrease was particularly significant at 60°C compared to those treated at room temperature. These changes can be attributed to the aminolysis reaction and the cleavage of ester bonds, as confirmed by ATR-FTIR analysis, which resulted in a reduction in molecular chain length. This shortening of the molecular chains adversely affects the mechanical properties of the aminolyzed PLAs [154]. Aminolysis leads to a reduction in both ductility and tensile strength of the substrates, with the decrease being more pronounced at higher temperatures since elevated reaction temperatures accelerate the rate of aminolysis [60].

In conclusion, the aminolysis process and the incorporation of PAMAM into the molecular chains of PLA resulted in a brittle structure, particularly at higher temperatures (60°C) and for substrates with lower GSM. Despite the observed reductions in ductility and tensile strength, the modified substrates still possess

adequate mechanical integrity to withstand the subsequent processing steps involved in LBL assembly. This capability ensures that the functionalized surfaces can effectively interact with polyelectrolytes, facilitating successful deposition while maintaining the structural stability necessary for practical applications.
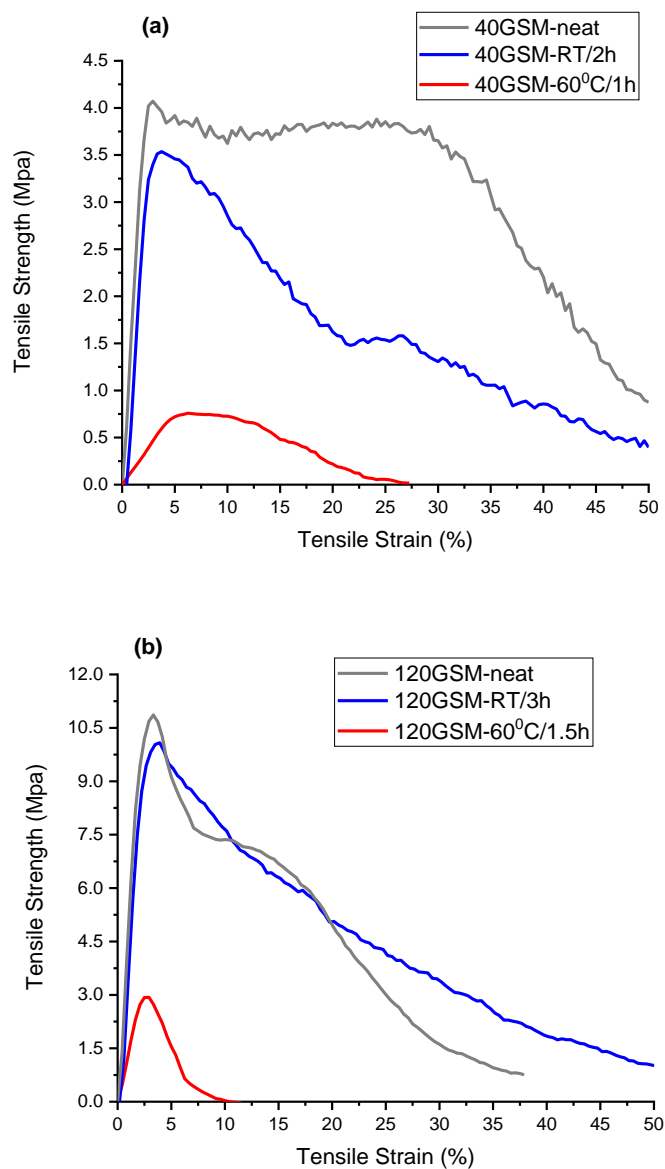
Figure 8. Stress-strain curve of neat and aminolyzed (a) PLA1-40GSM and (b)PLA2-120GSM

Table 9. Young's modulus (E_t), tensile strength (σ_m), and elongation at break of neat and aminolyzed PLA nonwoven

Samples	E_t (MPa)	σ_m (MPa)	Elongation
40GSM-neat	1.48±0.15	3.87±0.20	29.16±3.54
40GSM-RT/3h	1.47±0.02	3.70±0.24	13.60±2.3
40GSM-60C/1.5h	0.18±0.03	0.85±0.08	7.29±2.80
120GSM-neat	4.23±0.61	11.33±0.27	10.83±2.58
120GSM-RT/3h	3.57±0.12	10.29±0.27	---
120GSM-60C/1.5h	1.45±0.05	2.95±0.07	---

5.2 Preparation of multilayer assemblies on functionalized PLA nonwovens

In this section, efforts were made to design PLA nonwoven with polyelectrolyte (PE) multilayer assemblies on the pre-treatment PLA nonwoven with optimized conditions obtained previously. Three key factors including PE's pH, PE's concentration ratio, and intermediate air-drying were considered as prominent factors influencing multilayer growth on the substrate. Poly(amidoamine) (PAMAM), a dendritic polycation, and poly(acrylic acid) (PAA), a linear polyanion, were selected as weak polyelectrolytes for multilayer deposition. PAMAM, with its unique dendritic structure and amine-terminated groups, offers potential applications in biomedical systems, particularly in drug delivery, while also providing antibacterial properties.

This chapter is divided into two sections: liquid-liquid phase study and liquid-solid phase study. The first section focuses on the analysis of polyelectrolyte complex (PEC) formation in the liquid phase, investigating the effects of pH and concentration ratio on the formation of stable and irreversible turbid colloidal complexes. Techniques such as acid-base titration, turbidimetric analysis, UV-visible spectroscopy, and dynamic light scattering (DLS) were employed to study PEC formation. The second section is dedicated to applying the optimal pH and concentration ratio to the solid phase (functionalized PLA nonwoven) to examine the growth profile of multilayers. It also investigates the effect of intermediate

air-drying on multilayer growth profile, the density of amine groups after each layer deposition, and the multilayers' loading capacity and PE multilayer density and structure. The analytical tool to characterize the PE multilayers were ninhydrin assays, UV-visible spectroscopy, color depth measurements of stained substrates, air permeability tests, static mechanical tests, scanning electron microscopy, and assessments of antibacterial properties.

5.2.1 Liquid-liquid phase

5.2.1.1 Polyelectrolyte Characterization Based on Acid-Base Titration

The interaction between polyelectrolytes plays a vital role in deepening our understanding of their complexation behavior, particularly with respect to their charge density and structural conformation. This understanding is essential for elucidating the mechanisms underlying polyelectrolyte interactions, which can significantly influence their physical and chemical properties [89], [155]. To investigate these interactions, we conducted acid-base titrations of poly(amidoamine) (PAMAM) and poly (acrylic acid)(PAA) polyelectrolytes. This method allows us to estimate their dissociation constants and degrees of ionization, providing insight into how these polyelectrolytes behave in solution at different acidities. Additionally, we performed hydrodynamic radius analysis to assess conformational changes in response to varying solution pH levels. The results of these analyses are presented in Figure 9 and Table 10.

Amine-terminated poly (amidoamine) (PAMAM) dendrimers, classified as polyprotic bases, are anticipated to display two distinct endpoints in their titration curve. These endpoints correspond to the protonation of the peripheral primary amines and the interior tertiary amines of the dendrimer structure [156]. Studies have indicated that the pKb range for the terminal primary amines in amine-terminated PAMAM dendrimers is between 7 and 9. This range suggests that these amines exhibit basicity, allowing them to interact with protons under alkaline conditions. In contrast, the pKb range for the interior tertiary amines is reported to be between 3 and 6, indicating that they are more readily protonated in acidic environments [103], [157]. Here, the pK_b of the primary amines was calculated to be approximately 8.93 where 55.37% of all amines (DoI= 55.37%) are ionized. The pK_b of tertiary amines, where 92.6% of all amines were ionized

(DoI=92.66%), occurred at 3.19 which fell within the reported range. There values of pka and degree of ionization were in good agreement with those reported before where DOI of PAMAM-G2 around 3.50 and 8.50 was approximately 95% and 40% at ionic strength of 0.1 M, respectively; and the pKa ranged 7-9 and 3-6 for primary and tertiary amines, respectively [103], [157], [94].

To investigate the conformational structure of PAMAM at the equivalence pH, dynamic light scattering (DLS) analysis was performed, as presented in Table 10 (Figures are reported in supplementary data section). The results indicate that the PAMAM dendritic polymer can adopt either a compact or an open structural conformation, depending on the pH of the solution. At high pH levels, the PAMAM tends to maintain a more compact conformation, while at low pH levels, it exhibits a more open and extended structure. This observed behavior could be attributed to the repulsive electrostatic interactions among the protonated amine groups within the PAMAM structure. As the pH decreases and more amine groups become protonated, these repulsive forces increase, leading to a more open and extended conformation of the PAMAM [91], [95], [158]. As reported in Table 10, at a pH of 8, the hydrodynamic radius of PAMAM dendrimers is measured to be 66.57±4.73 nm. However, when the pH is decreased to 4, the structure undergoes an expansion, resulting in a hydrodynamic radius of 86.47±7.32 nm.
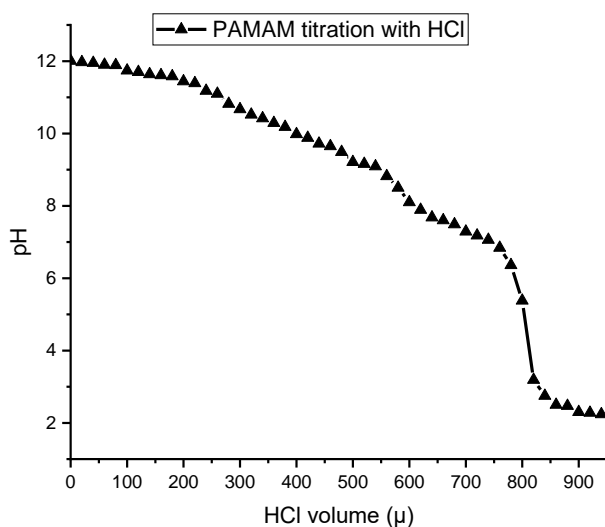
Figure 9. Titration curve of poly (amidoamine) with HCl

Poly (acrylic acid) (PAA), as a monoprotic acid, is capable of donating only a single proton, which corresponds to its carboxylic acid groups (–COOH). Studies have demonstrated that the titration curve of PAA exhibits a single endpoint, reflecting its behavior as a monoprotic acid. The pKa value of PAA can vary depending on factors such as its molar mass and the ionic strength of the solution, with reported values ranging between 4.52 and 4.55 [90] and 5.5 to 6.36 [92], [159]. However, as illustrated in Figure 10, the titration curve of PAA unexpectedly revealed two distinct endpoints: one at a pH of 4.27, corresponding to a degree of ionization (DoI) of 50.44%, and another at a pH of 9.73, with a DoI of 87.91%. The first equivalence point aligns well with the previously reported pKa range for PAA, suggesting a consistent behavior in its acid-base properties [90]. The slope of the titration curve in this region was observed to be quite gradual. This slow slope can be attributed to the increasing molecular weight of PAA, which makes the ionization of the polymer chains more challenging. As the molecular weight rises, the total electrostatic potential on each monomer unit increases, resulting in greater resistance to ionization. Consequently, this phenomenon reflects the complex interplay between molecular weight and the ionization behavior of PAA [92]. Consequently, this phenomenon contributes to the observed gradual slope in the titration curve, which corresponds to the initial equivalence point. It is hypothesized that at low pH, the polymer adopts a compact globular (collapsed) conformation, transitioning to an open coil (swelled) conformation as the pH increases. This transition is driven by the repulsive forces generated by ionized groups, leading to a globular-to-coil transformation. For PAA with a high molecular weight, the strong hydrogen bonding between non-adjacent monomers may result in a more collapsed structure. As a result, a polymer chain with a greater number of monomer-monomer interactions is less likely to fully swell, as these intermolecular interactions restrict the chain's ability to expand. Thus, the pH-induced conformational transition observed in PAA is dependent on its molecular weight, highlighting the intricate relationship between polymer structure and environmental conditions [90].

To elucidate the second sharp slope in the titration curve of poly (acrylic acid) (PAA), which occurs between pH 6 and 11, the following hypothesis can be proposed: this phenomenon is likely due to the sudden swelling of the polymer chains, resulting in a larger accessible surface area and the exposure of previously entrapped carboxyl groups to the alkaline media. This hypothesis is supported by dynamic light scattering (DLS) analysis, as shown in Table 10. At pH 4, the hydrodynamic radius of PAA is approximately 94.43 ±5.44 nm, indicating that the structure is not fully compact or collapsed. However, upon increasing the pH to 10, the hydrodynamic radius expands to 129.56±5.44 nm, reflecting a swelled and open coil conformation of the PAA. In conclusion, the unique and intriguing conformational behavior observed in PAA can be attributed to its relatively high molecular weight of 450 kDa, which influences its swelling dynamics and overall structural characteristics in response to changes in pH.

Layer-by-layer assembly of thin films is primarily governed by the electrostatic interactions between oppositely charged polyelectrolytes [71]. Therefore, it is essential to understand the optimal pH conditions and the conformational states of the polyelectrolytes, as these factors influence the formation of complexes between the two species. In the subsequent investigation, the PAMAM polyelectrolyte was titrated against the PAA polyelectrolyte at various pH levels around the obtained pKa values. This approach aims to elucidate the specific conditions under which the complex between PAMAM and PAA is formed.
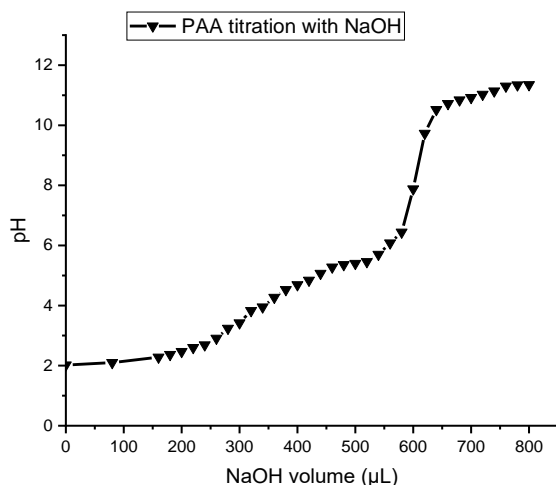
Figure10. Titration curve of poly (acrylic acid) with standardized sodium hydroxide

Table 10. Hydrodynamic radii (R_h) of PAMAM and PAA PE soulion at different pH

	PAMAM		PAA	
pH	4	8	4	10
R_h (nm)	86.47±7.32	66.57±4.73	94.43±5.44	129.56±25.26

5.2.1.2 The Effect of Polyelectrolyte's pH on Complex Formation between PAMAM/PAA

Based on the determined pKa and pKb values for PAA and PAMAM PEs, an investigation was conducted to identify the optimal pH conditions for complex formation. Solutions of PAMAM PE at a concentration of 7×10^{-4} g/mL were titrated against PAA solutions, also at 7×10^{-4} g/mL, across four distinct pH levels: 10, 8, 6, and 3. The PAA solution pH was adjusted to 10 and 4, performed under gentle stirring at room temperature. The turbidity of the resulting mixed solutions was measured as an indicator of complex formation, with increased turbidity correlating to a higher concentration of the formed polymeric electrolyte complex (PEC) [88]. The results are illustrated in Figure 11. At the partially charged state of PAA at pH 4 (Figure 11a), a decrease in pH from 8 to 3, which corresponds to an increase in the charge density of PAMAM from approximately 55.37% to over 92.66% as derived from the titration curve, resulted in a significant reduction in complex formation. The highest degree of complex formation, measured at 1668 NTU, was observed at the partially charged state of PAMAM at pH 8. Under these conditions, both polyelectrolytes, PAMAM and PAA, exhibit partial charge characteristics and adopt a nearly compact and globular conformation, respectively.

In contrast, as shown in Figure 11b, where PAA is nearly fully ionized at pH 10 and adopts an open coil conformation, the maximum complex formation was observed at a turbidity of approximately 50 NTU when PAMAM was at pH 6. However, this level of complex formation is not comparable to the significantly higher turbidity of around 1668 NTU recorded under conditions where PAMAM was at pH 8. Based on this information, it can be concluded that the optimal formation of the PAMAM/PAA complex occurs under conditions where both PAMAM and PAA are partially charged, rather than fully charged, and exhibit nearly compact and globular conformations (though not completely compact). In contrast, when both

polyelectrolytes are fully charged—specifically, PAMAM at pH 3 and PAA at pH 10 (as illustrated in Figure 11b)—the extent of complex formation is significantly reduced, resulting in turbidity values of less than 30 NTU. This is markedly lower than the turbidity exceeding 1000 NTU observed when both polyelectrolytes are in their partially charged states. As reported by D. Scheepers et al. [81], at higher charge densities or increased numbers of charged groups in polyelectrolytes (PEs), a smaller quantity of the counterpart PEs with oppositely charged densities is needed to balance the overall charge density of the polymeric electrolyte complexes. Consequently, at elevated charge densities, fewer PE molecules participate in complex formation, which results in a reduced formation of turbid colloidal PECs and, therefore, lower turbidity values. This observation led to the selection of pH 8 for PAMAM and pH 4 for PAA as the optimal pH conditions. Subsequently, the effect of polyelectrolyte concentration ratio on complex formation under these optimal pH conditions was also investigated.
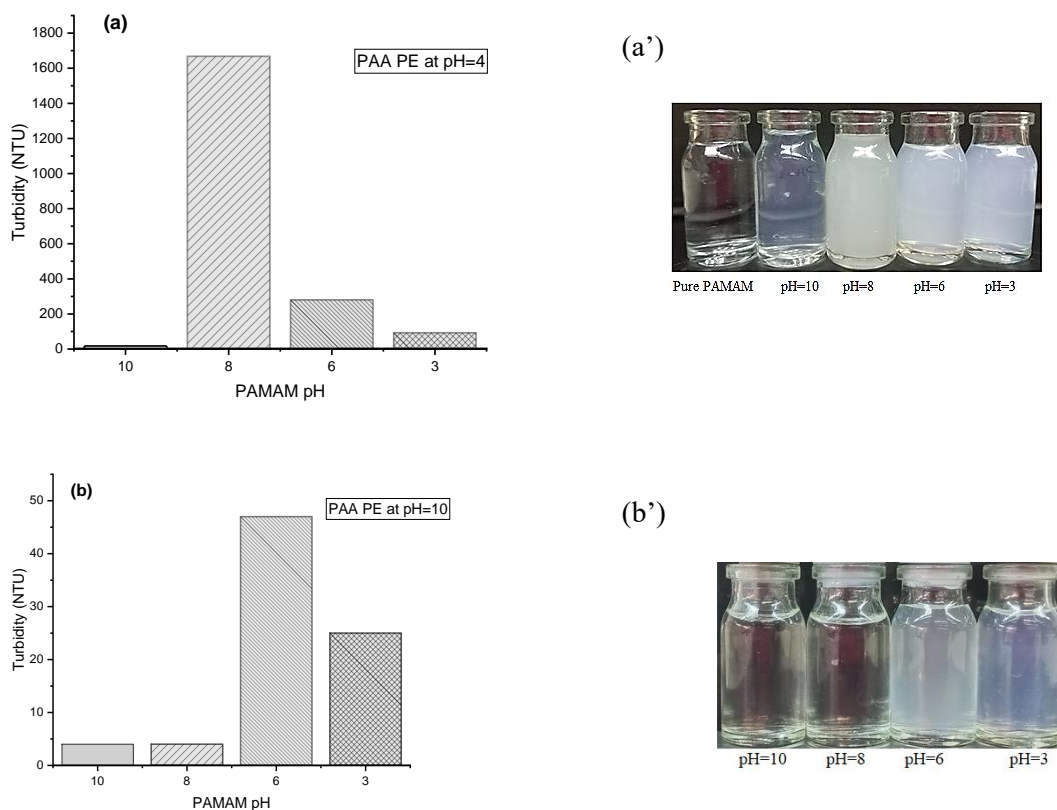
Figure 11. Turbidity of mixed solution at different pH of titration 0(a) PAMAM titrated with PAA at pH=4, and (b) PAMAM titrated with PAA at pH=10; (a') and (b') is presented for better visualization; PAMAM and PAA concentration was 7×10^{-4} g/mL

5.2.1.3 The Effect of Polyelectrolyte's Concentration Ratio on Complex Formation between

PAMAM/PAA

In addition to the pH of the weak polyelectrolytes, the concentration ratio is another critical factor influencing polyelectrolyte complex (PEC) formation. The turbidimetric method [40] was utilized to examine the effect of the concentration ratio of polyelectrolytes on the formation of the PAA/PAMAM complex. Solutions of PAMAM at varying concentrations (C_{PAMAM}) were titrated with PAA solutions across four different concentrations (C_{PAA}) under the obtained optimal pH conditions. The concentrations investigated ranged from 1×10^{-4} to 10×10^{-4} g/mL, encompassing a total of 16 titration experiments. The maximum turbidity of the mixed solutions as a function of the concentration ratio is illustrated in Figure 12.

Polyelectrolyte complexes can be classified into two categories: stoichiometric water-insoluble PECs, which have a molar ratio of 1:1, and nonstoichiometric water-soluble PECs. Stoichiometric PECs are electrically neutral and precipitate out of the solution. In contrast, nonstoichiometric PECs carry a net charge that depends on their molar ratio, and the turbidity of the solution serves as an indicator of their concentration within the solution [89]. Nonstoichiometric PECs, which are of particular interest, can be further divided into two types: (a) those that are soluble in a macroscopically homogeneous system, where their formation is reversible, and (b) those that are soluble but form irreversible turbid colloidal PECs, which are in a transition range leading to phase separation [160], [161]. Additionally, it is important to note that the interaction between polyelectrolytes is primarily influenced by two key factors: (1) the ionic strength of the solution and (2) the linear and colloidal surface charge density of the polymers [155]. Indeed, the quantity of dissociated groups must exceed a critical value to facilitate effective complex formation. This threshold is essential for achieving the necessary electrostatic interactions between the polyelectrolytes [88].

As shown in Figure 12, at a PAMAM concentration (C_{PAMAM}) of 1×10^{-4} g/mL and varying PAA concentrations no changes in turbidity were observed. This leads to two possible hypotheses: (1) the formed

complexes were unstable, similar to PEC type (a), where the PECs are uniformly dispersed in water, and their formation is reversible, resulting in a macroscopically homogeneous system; or (2) no complexes were formed, as at this low C_{PAMAM} concentration (1×10^{-4} g/mL); indeed, the quantity of charged and ionized amines available to interact with the ionized carboxyl groups of PAA electrostatically is insufficient to create any complex. Two approaches were examined to generate stable turbid colloidal PECs. In the first approach, the charge density of the PAMAM solution was increased by lowering the pH to 3. According to section 1.1, the obtained pK_b for the tertiary amines was approximately 3, resulting in about 92.6% of the amines being protonated and ionized. Under these conditions, a turbid colloidal PEC system was formed and precipitated at a C_{PAA} of 7×10^{-4} g/mL (supplementary data). Indeed, the aggregated PECs appeared to be electrically neutral (n+ /n-), leading to a loss of colloidal stability and subsequent precipitation from the solution [161]. In the second approach, to compensate for the charge density of the PAMAM PE solution, the concentration was increased to 4×10^{-4} g/mL at pH 8. As shown in Figure 13, stable PECs between PAMAM and PAA began to form, indicated by the creation of stable and irreversible turbid colloidal PECs. Therefore, the concentration required for incipient complex formation was considered to be $C_{PAMAM} \geq 4 \times 10^{-4}$ g/mL. This condition reflects a scenario where one polyelectrolyte's charge cannot neutralize the highly charged counterpart, resulting in excess charge and leading to the formation of stable soluble turbid colloidal PECs [160].

In the following, by increasing the C_{PAMAM} at a certain C_{PAA}, it was observed that turbidity increased, which can indicate the presence of larger PEC suspensions. This increase in turbidity is likely a result of PEC agglomeration at higher PAMAM PE concentrations, leading to the formation of bigger aggregates within the solution [88], [161]. Additionally, within a specific range of C_{PAMAM}, at certain PAMAM: PAA concentration ratios (10^{-4} g/mL)—including 4:10 (418 NTU), 7:7 (1668 NTU), and 10:10 (1810 NTU)— the highest concentrations of turbid colloidal PECs were formed. This observation highlights the importance of achieving an optimal charge density ratio of the polycation to the polyanion (n+/n-) and their

molar ratio. Maintaining these values is crucial to ensure the formation of irreversible and stable colloidal turbid complexes, thereby preventing the precipitation of PECs from the solution.
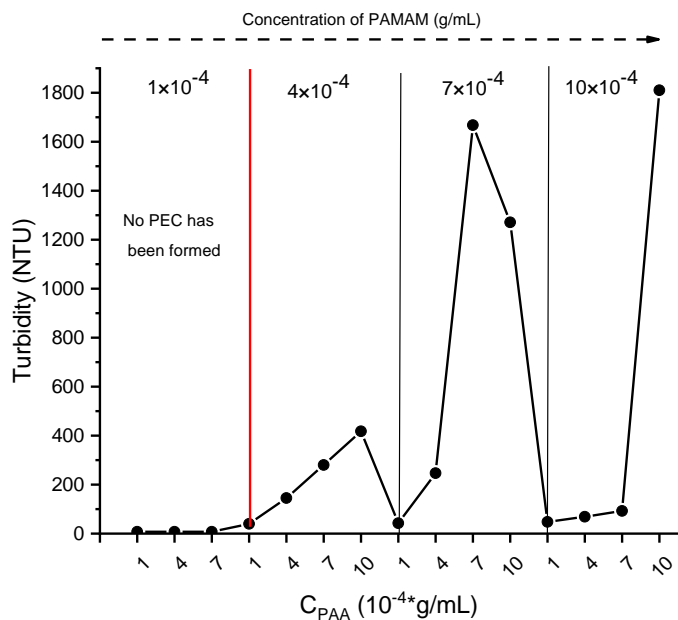
Figure 12. Turbidity of the PAMAM/PAA mixed solutions at different concentration ratios

5.2.1.4 UV-Visible Spectroscopy analysis of PAA/PAMAM complex

UV-Visible spectroscopy was conducted to study the interaction and mechanism of PAMAM and PAA complex formation. The conditions (pH and concentration ratio) under formation of the maximum turbid colloidal complex were considered. The PAA/PAMAM complex was obtained through titration at a concentration ratio of 7:7 (10^{-4} g/mL) and then examined using UV-Visible spectroscopy. The results are summarized in Table 11, and the spectra are depicted in Figure 13. As noted, the UV-Vis absorbance of PAMAM is expected to occur around 285 nm, corresponding to the interior tertiary amines [162], in accordance with our dendritic PAMAM maximum absorbance wavelength at 298 nm. As shown in Figure 13, the absorbance curve of the PAA/PAMAM complex exhibited two notable changes: (1) it was shifted to a higher position than that of the pure polyelectrolyte, and (2) the peak area at 298 nm (within the range of 270-320 nm) decreased by about 42%. The vertical shift in the absorbance curve may be attributed to the increase in solution concentration due to the addition of the second polyelectrolyte, leading to the

creation of a turbid colloidal system. This results from complex aggregation, which causes more light scattering and, consequently, a higher absorbance than the actual value. The reduction in peak area within the 270 to 320 nm range confirms the engagement of the tertiary amines in the complex formation. It appears that the PAA chain can penetrate the PAMAM structure, facilitating the interaction between the two components, and highlighting the host-guest behavior of complex formation between dendritic PAMAM polymer [163]. As reported by Welch et al. [163], computer-based Monte Carlo simulations were employed to study the molecular nature of dendrimer-linear polyelectrolyte complexes. The observations from this study revealed the formation of a unique complex between the polymer and dendrimer when a very small dendrimer was complexed with a large polymer chain, which aligns with our focus. In this specific case, it was noted that small segments of the polymer chain were able to penetrate into the dendrimer structure; however, a significant portion of the polymer chain density remained outside the dendrimer. This finding from the simulation study corresponds with our UV-Visible absorbance results obtained for the PAA/PAMAM complex system. The experimental data support the existence of this unique polymer-dendrimer complex structure, indicating that the dendrimer did not completely shield the self-repulsion of the polymer chain.

Table 11. Absorbance and turbidity of pure PEs and PAA/PAMAM complex

	Con. (g/l)	pH	λ_{max} (nm)	Maximum Absorbance	Peak area (270-320nm)	Turbidity (NTU)
PAMAM	0.7	8	298	0.25	3.33	7.45
PAA	0.7	4	230	0.30		4.16
PMAMA/PAA	---	---	298	2.05	1.94	1668
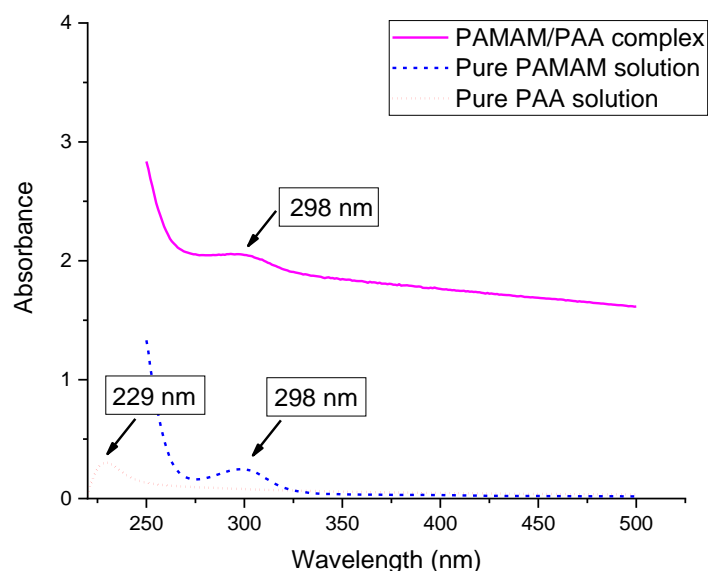
Figure 13. UV-visible spectra of pure PEs and PAMAM/PAA complex

5.2.1.5 The Effect of Mixing Order on Turbid Colloidal Complex Formation

To better understand the desorption behavior in the solid-liquid phase, the partial removal of previously adsorbed layers into the polyelectrolyte (PE) solution during the deposition of subsequent layers as well as the formation of turbid colloids as a function of mixing order in the liquid-liquid phase were investigated. PAMAM PE addition into PAA PE in the liquid-liquid phase (PAMAMàPAA) corresponds to the desorption of PAMAM upon deposition of the PAA layer in the liquid-solid phase, and PAA PE addition into PAMAM PE solution in the liquid-liquid phase (PAAàPAMAM) corresponds to the PAA removal upon the deposition of PAMAM layer in liquid-solid-phase. To simulate the desorption process of the solid-liquid phase within a liquid-liquid framework, the mixing process began with 15 mL of a polyelectrolyte solution composed of PAMAM and PAA, identical to that used in LBL assembly. The PEs concentration and pH were also identical to the LBL process; a concentration of 7×10^{-4} g/mL for both PEs, pH=8 and 4 for PAMAM and PAA, respectively. The oppositely charged polyelectrolyte was added incrementally in a dropwise manner, ranging from 0.1 mL to 4.0 mL; and turbidity measurements were recorded following each addition. The turbidity as a function of mole of the added PE is depicted in Figure 14. These curves

can be further employed as calibration curves to quantify layer removal during LBL deposition. As shown in Figure 14, the system exhibited distinct behavior depending on the mixing order, while in both cases; the data were well-fitted using a cubic polynomial model, resulting in an R^2 value exceeding 0.99. It is worth to mentioning that the moles of added polyelectrolyte were designed to align with the range of turbidity values obtained from the adsorption-desorption turbidity data presented in Section 5.2.2.5.

(a)	
Equation	y = Intercept + B1*x^1 + B2*x^2 + B3*x^3
Plot	Turbidity
Weight	No Weighting
Intercept	4.29 ± --
B1	2.03332E9 ± 2.61806
B2	-2.70086E15 ± 9.0117
B3	1.4946E21 ± 7.31558
Residual Sum of	4623.48944
R-Square (COD	0.99631
Adj. R-Square	0.99354

(b)	
Equation	y = Intercept + B1*x^1 + B2*x^2 + B3*x^3
Plot	Turbidity
Weight	No Weighting
Intercept	7.45 ± --
B1	3.27859E10 ± 2.62578E9
B2	-8.36786E18 ± 1.24781E
B3	7.44319E26 ± 1.39807E2
Residual Sum of S	17.82831
R-Square (COD)	0.99857
Adj. R-Square	0.99714

Figure 14. Turbidity of the turbid colloidal complex as a function of added PE; (a) PAMAM was added in to PAA PE solution, (b) the PAA PE was added into PAMAM solution

5.2.2 Liquid-solid phase

According to the results obtained from the liquid-liquid phase study, the optimal pH conditions for the two weak polyelectrolytes, which provide a sufficien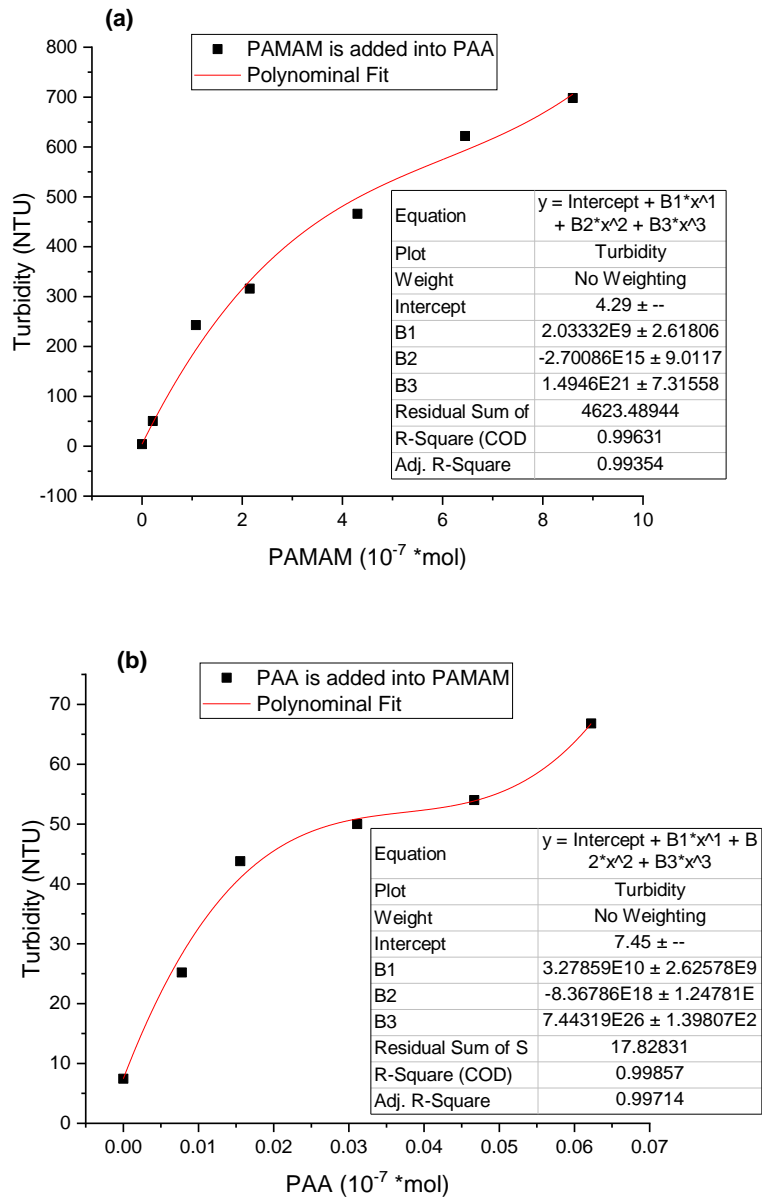t charge density ratio (n+/n-) to form a turbid colloidal complex, were pH 8 for PAMAM and pH 4 for PAA, both of which are partially charged. Furthermore, the concentration ratio of the polyelectrolytes indicated that the charge density also depended on the PE concentration; to form a stable PECs; the concentration of the polyelectrolyte needed to exceed a critical threshold at the specific pH. At specific PAMAM PE concentrations ranging from 1×10^{-4} g/mL to 10×10^{-4} g/mL, and varying PAA PE concentrations, maximum turbidity was achieved at the ratios of 7:7, 7:10, and 4:10 (PAMAM: PAA). Consequently, further investigations were conducted under these optimal pH and concentration ratios.

5.2.2.1 *The effect of PE concentration ratio on multilayer growth on Functionalized PLA nonwoven*

According to the results obtained from the liquid-liquid phase study, the growth of multilayers of the PAA/PAMAM complex on a functionalized PLA nonwoven substrate via the layer-by-layer (LBL) technique was studied. The LBL assembly was conducted up to the fourth layer, with PAMAM as the top layer (Functionalized PLA-PAMAM/PAA/PAMAM/PAMAM = PAMAM4), as summarized in Table 6 (in experimental section 4.2.2.2). The neat, aminolyzed, and layered PLA samples were then stained with an anionic model dye, Acid Red 1, to study the growth of the multilayer film. Negatively charged dye molecules are expected to electrostatically interact with the accessible positively charged amines introduced onto the PLA substrate by the LBL assembly. The color depth (K/S) and the absorbance of the waste dye (after the staining procedure) are presented in Figures 15 and 16, respectively.

To investigate the effect of PE concentration ratio on multilayer growth and their stability in different acidic media, a staining procedure was conducted at three distinct pH levels: 2, 3, and 5. As shown in Figure 15, higher acidity of the media resulted in greater K/S value, following the logical order of pH: 2 > 3 > 5. This can be attributed to the fact that in an acidic environment, both the dye molecules and the amines of layered

PLA are charged, ensuring electrostatic attraction between the negatively charged dye molecules and the positively charged amines of the layered PLA. To further investigate this condition, the absorbance of the dye solution after the staining procedure (waste-dye solution) at 505 nm was recorded. As illustrated in Figure 16, the absorbance of the waste dye at pH 5 was higher than at pH 2 and 3, which corresponded to the lowest K/S value. This information suggests that the staining condition at pH 5 did not facilitate the critical charge conversion necessary to ensure effective electrostatic attraction between the dye molecules and the amines.

To study the impact of the PE concentration ratio (C_{PAMAM}: C_{PAA}) on the multilayer growth on functionalized PLA nonwoven at pH=2 of the staining procedure, the logical order of K/S value was 7:7>7:10>4:10. This indicated the lowest and highest color depth at 4:10 and 7:7 ($10^{-4} \times$g/mL) concentration ratio, respectively. To evaluate the stability of the deposited PE multilayers on the substrate, the absorbance of dye solution after the staining procedure (waste-dye solution) corresponding to 7:7 and 7:10 samples measured and reported in Figure 16. As it can be seen from Figure 16, the adsorbance of the waste-dye solution of 7:7 and 7:10 samples was very close, while their K/S value was significantly different. This suggested that the partial removal of the adsorbed layer (containing turbid complex) into the dye solution contributed to a reduction in absorbance, which approached levels comparable to those of the 7:7 sample. A similar trend was noted at pH 3, where the K/S value for the 7:7 sample exceeded that of the 7:10 sample, resulting in lower dye content in the solution for the 7:7 sample. Conversely, the waste dye absorbance for the 7:10 sample was lower, indicating partial layer removal into the dye solution bath.

Concerning the substrate multilayers assembled at the concentration ratio of 4:10, the color depth was the lowest, and the absorbance of the waste dye was the highest at both pH 2 and 3. This implied that, although the multilayers were stable at this C_{PAMAM}: C_{PAA} ratio, the growth of the polyelectrolyte complexes on the substrate was constrained, leading to diminished dye absorbance; and consequently color depth.

In conclusion, it can be proposed that the highest turbidity observed in the solution-based study correlates with the most significant multilayer growth on the substrate. The subsequent investigation focused on the

multilayer film assembled on the PLA nonwoven substrate at the PE concentration ratio (10^{-4} g/mL) of C_{PAMAM}: C_{PAA} of 7:7.
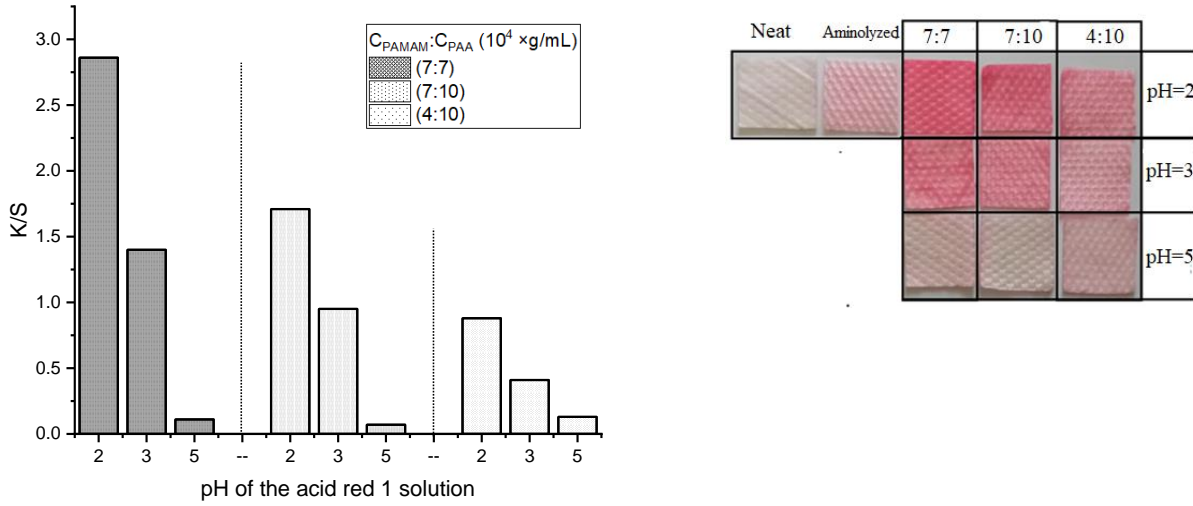

Figure 15. color strength of modified PLA via LBL at different PE concentration ratios as a function of dye solution pH (left side), to better visualization (right side)
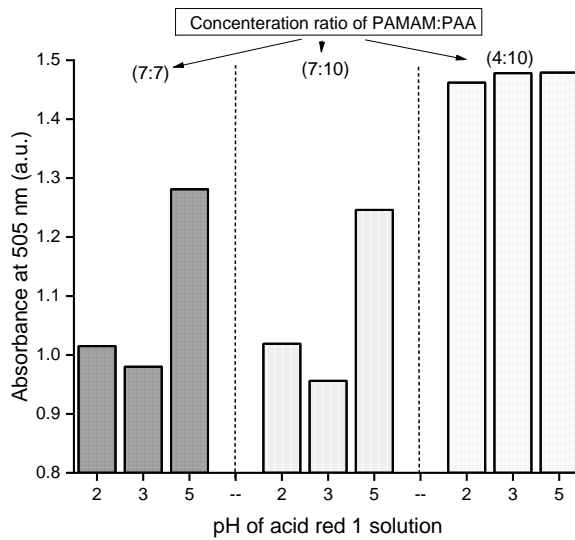

Figure 16. The absorbance of the acid red 1 at 505 nm after the staining procedure of layered-PLA nonwoven with different PE concentration ratio

The ATR-FTIR analysis was conducted to investigate the chemical changes in modified PLA nonwoven following pre-treatment and the deposition of the first PAA layer. The results, including the normalized ATR-FTIR spectra and the calculated peak areas, are presented in Figure 17 and Table 12, respectively. For the aminolyzed PLA, a new peak was observed around 1630 cm^{-1}, which is associated with N-H bending vibrations. Additionally, a distinct double-peak between 3300-3600 cm^{-1}, corresponding to the stretching vibrations of –NH amide groups, indicates the successful grafting of PAMAM amines, leading to the formation of amide carbonyl groups [112] Cleaving the ester bond is essential for the aminolysis reaction [54]; therefore, a decrease in the intensity of the carbonyl bond of PLA is necessary. As indicated in Table 12, the peak area for both aminolyzed-PLA decreased approximately 50%.

Following the successful introduction of amines into the PLA matrix, the deposition of the first layer of PAA as a polyanion onto the positively charged aminolyzed PLAs (NH$_3^+$ groups from PAMAM) was carried out using the layer-by-layer technique. As previously noted by Stawski et al. [164], non-ionic PAA exhibits a prominent peak around 1710 cm^{-1}, which is associated with the carbonyl bond (C=O) of its non-ionic carboxyl groups (COOH). In contrast, the ionized –COO$^-$ groups demonstrate symmetric and asymmetric vibrational bonds around 1590 cm^{-1} and 1408 cm^{-1}, respectively. As illustrated in Figure 17, the emergence of a new broad peak around 1535 cm^{-1} may be attributed to the symmetric vibration of ionized –COO$^-$ groups, while its asymmetric vibration may be overlapped or masked by the strong signals originating from the PLA substrate in that frequency range. Additionally, a reduction in the N-H bending vibration around 1630 cm^{-1} may indicate the masking of PAMAM by the molecular chains of PAA. Furthermore, there is a possibility of overlapping between the stretching vibrations of N-H and the hydroxyl (OH) groups of PAA, leading to a shift from the original range of 3300-3600 cm^{-1} to approximately 3500-3900 cm^{-1}. These findings collectively support the initial grafting of PAMAM onto the surface of neat PLA and suggest a masking of PAMAM due to the deposition of the first PAA layer on aminolyzed PLA.

Table 12. Peak area under specific ranges corresponding to the respective bonds.

Samples	C=O stretching (PLA) 1700-1800 (cm^{-1})	C=O stretching (PAA) 1480-1580 (cm^{-1})	N-H bending 1600-1700 (cm^{-1})	N-H stretching 3300-3600 (cm^{-1})
Neat PLA	108	---	---	---
Aminolyzed-PLA	54	---	7.8	21
Layered-PAA$_1$	---	19.1	1.0	---
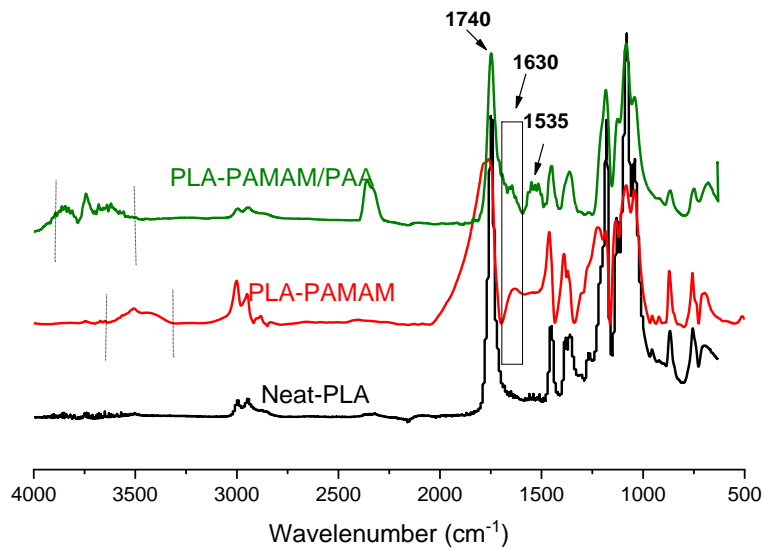
Figure 17. Normalized ATR-FTIR spectra of neat, aminolyzed (-PAMAM), and layered aminolyzed-PLA with PAA (-PAMAM/PAA)

5.2.2.3 Growth profile of multilayer assemblies on Functionalized PLA nonwoven

PAA/PAMAM multilayers were assembled on aminolyzed PLA by repeatedly immersing the amine-functionalized substrate in solutions of oppositely charged polyelectrolytes, as outlined in condition (a) in Table 6 (section 4.2.2.2). To investigate the growth profile of the multilayer assemblies, a ninhydrin assay colorimetric was performed to qualitatively assess the density of NH$_2$ groups present on the substrate following the deposition of each PAA and PAMAM layer via the layer-by-layer technique.

The ninhydrin assay is a well-established analytical method for detecting primary amine groups in materials, producing a purple color complex known as Ruhemann's purple (at 570 nm) upon reaction with primary amines [151], [152]. The reaction mechanism of ninhydrin with primary amines is illustrated in Figure 3 (section 5.1.2). The density of primary amine groups (moles of primary amines per gram of substrate) on the substrate was calculated according to Equation (II) in Section 4.3.1.4, and the results are presented in Figure 18.

A. J. Khopade et al. [97] was studied film growth of PSS and PAMAM-G4 on quartz slides. The reduction in PSS absorption following PAMAM deposition was occurred and interpreted as the removal of PSS. Additionally, a converging-diverging behavior was observed, which can be explained by the adsorption-desorption phenomenon. The partial removal of the adsorbed layer during subsequent deposition steps led to the complexation of PSS-PAMAM within the polyelectrolyte solutions, resulting in changes to the charge density and conformation of the deposited molecules. Consequently, this behavior produced a converging or diverging profile for the PSS-PAMAM system during the film growth of PSS and PAMAM-G4 on the quartz slide.

As illustrated in Figure 18a, the NH_2 density of functionalized PLA (aminolyzed-PLA) was initially measured at approximately 6.07×10^{-6} mol/g. After the deposition of the first layer of PAA, this density decreased to 5.6×10^{-6} mol/g, representing a reduction of about 7.7%. As the layering process continued up to the eighth layer, fluctuations in the amine density were observed. This decrease can be attributed to two primary factors: (1) the successful deposition of the PAA layer onto the aminolyzed-PLA surface, which effectively interacts with the NH_2 groups leading to the reduction in available amines, and (2) the partial removal of PAMAM during the layering process.

Furthermore, it was observed that the solid line connecting the data points before and after PAMAM adsorption converged as the number of layers increased. This indicates that the growth profile of the PAA/PAMAM multilayer assemblies on functionalized PLA nonwoven is converging. The explanation for this behavior is that the previously adsorbed PAA is partially removed into the PAMAM polyelectrolyte

solution during the deposition of next layer. This leads to the formation of PAA-PAMAM complexes in PE bath, which alters the dynamics of subsequent layer deposition. As a result, the adsorption of individual PAMAM molecules competes with the existing PAMAM-PAA complexes. This competition results in a diminished increase in NH_2 density upon the deposition of even layer, as the layering process progresses. Indeed, there exists a potential for the adsorption of complexed PAMAM, wherein a portion of the amine groups is occupied by PAA. Consequently, this results in a reduced availability of amine groups within the specific layer, leading to diminished deposition of PAA. This phenomenon becomes increasingly pronounced as the multilayer assemblies develop. The multilayers formed in this manner exhibit a converging behavior, as noted in reference [97]. It is important to highlight that this growth profile behavior was observed in layers one through seven; while the notable increase in amine density at the eighth layer may be attributed to PAMAM agglomeration.

The same experiments were conducted for the PLA2 with higher GSM, to study the impact of the substrate's structural impact on the growth profile of the PE multilayer; the data are represented in Figure 18b. The results indicate that while PLA1 exhibited a distinct growth profile characterized by either converging or diverging patterns, PLA2, which has a higher GSM, did not demonstrate a clear growth trend. This lack of specificity in the growth profile for PLA2 suggests that the structural properties of the substrate may significantly influence the multilayer growth dynamics.
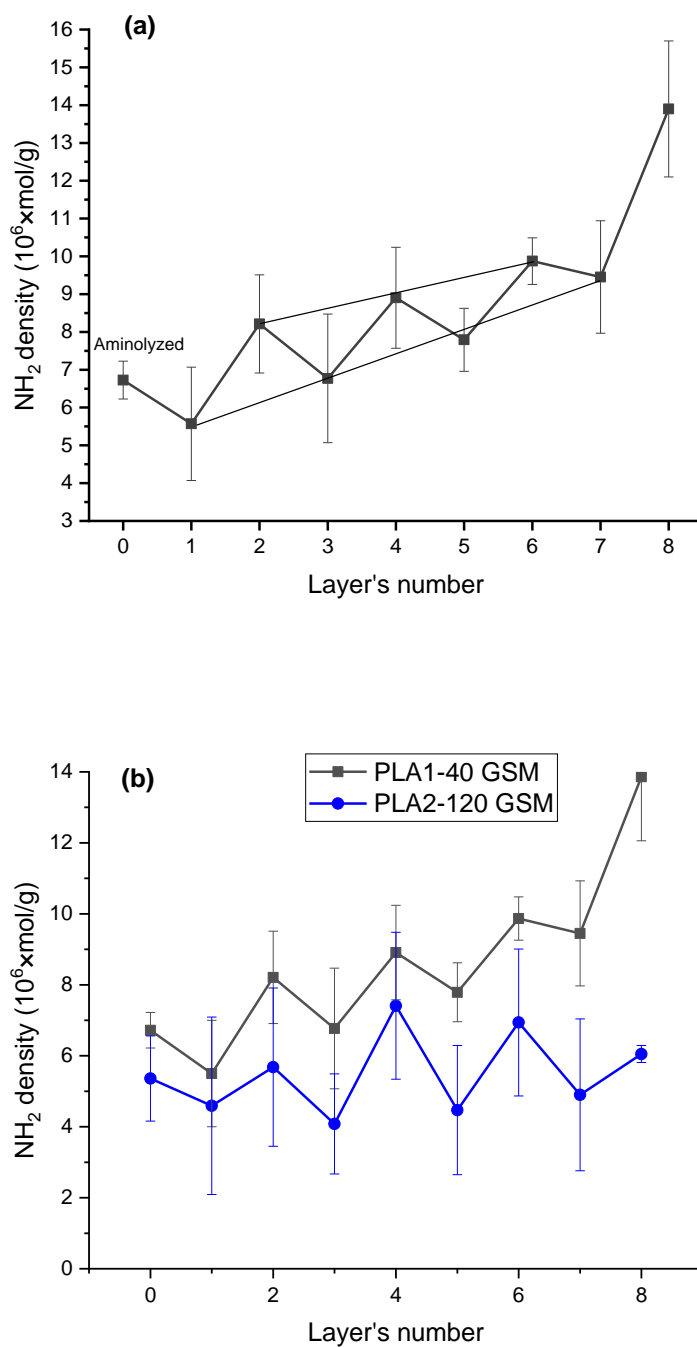
Figure 18. Amine density of the aminolyzed and multilayered-PLA nonwoven (a) PLa1 and (b) PLA1 and PLA2 as a function of layer number. The solid line in (a) is for the better visualization. Zero corresponds to functionalized PLA. Odd and even layers represent the amine density of the substrate after PAA and PAMAM layer deposition.

To scrutinize the influence of intermediate drying on the adsorption behavior of polyelectrolyte complexes (PEC), multilayered samples prepared by dry LBL were subjected to the ninhydrin assay. PLA1 with 40 GSM was selected to analyze the drying effect on the growth profile of PE since the samples prepared with hydrated LBL (without drying) showed distinct growth profile with converging behavior. The results of the ninhydrin assay, which quantifies amine density, are depicted in Figure 19. As shown in Figure 19, the application of intermediate drying in LBL caused a diverging growth profile of PE multilayers. In other words, intermediate drying resulted in increased PAMAM adsorption, which consequently led to greater PAMAM desorption during the subsequent PAA layer deposition. This is evidenced by the lower amine density at the odd layers of the dried samples compared to those multilayered with hydrated LBL. There are two possible hypotheses to explain this diverging behavior:

1. It has been demonstrated that the removal of previously adsorbed dendritic polycation (PAMAM) into the linear polyanion (PAA) polyelectrolyte solution during the deposition of the next layer leads to complex formation with PAA in the solution. This interaction results in increased coiling of PAA due to typical linear polyelectrolyte-dendrimer complexation [163]. Additionally, it has been observed that coiling of PAA induced by salt promotes greater deposition of PAA (aggregated complex) [82], [93]. Consequently, the presence of PAMAM in the solution alter the conformation of PAA, promoting its adsorption. In summary, the removal of PAMAM into the PAA solution not only promotes increased adsorption of PAA but also sets the stage for enhanced PAMAM adsorption in subsequent layers, driven by the interplay of electrostatic forces and the availability of ionized functional groups. This synergistic effect caused the diverging behavior in the dry LBL system.

2. Intermediate drying can lead to the neutralization and stabilization of the PAA layer on the substrate. In aqueous environments, polyelectrolytes tend to dissociate and ionize, whereas they remain non-

ionized in absence of the water molecules [165]. This stabilization may restrict the removal of PAA into the PAMAM solution, ultimately resulting in increased PAMAM deposition. As outlined in Section 5.2.2.3, the removal of previously adsorbed PAA into the PAMAM solution could reduce PAMAM adsorption due to competition between free PAMAM molecules and those already complexed with PAA. Nevertheless, the stable PAA layer promotes further PAMAM deposition leading to divergent behavior.

As hydrate LBL growth profile, where the eighth layer showed different behavior, here the diverging growth profile behavior was observed for layers one through seven, and the layer eight showed different behavior with unexpectedly lower amine density in comparison to layer 6. So, there is a chance that the ultimate amine density can be achieved by 6 cycles of dry LBL. At the end, it can be concluded that the growth profile of multilayer assemblies is highly tunable and can be effectively controlled by LBL operational factors, including intermediate drying.
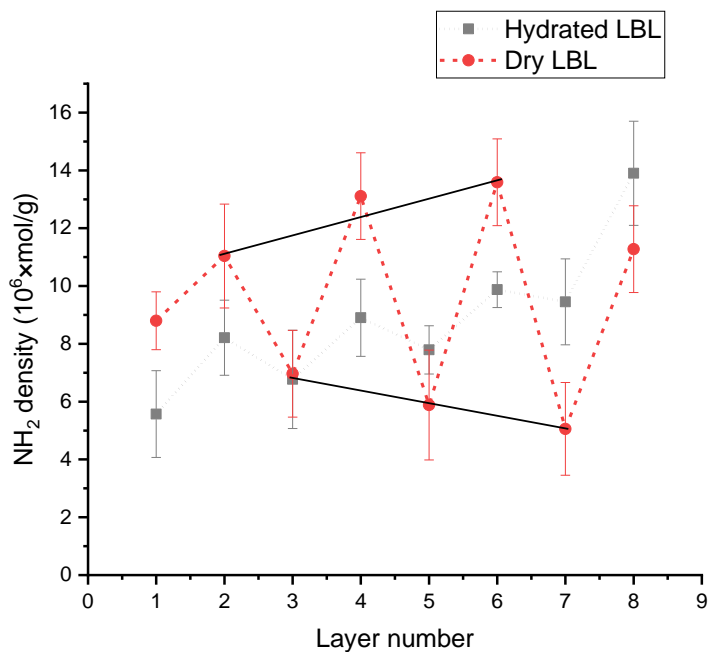

Figure 19. Amine density of multilayered substrate prepared by dry LBL. The hydrate LBL results are presented for better comparison. The solid line connecting the points is for better visualization.

5.2.2.5 Adsorption-desorption behavior; the effect of intermediate drying and the substrate GSM

Adsorption-desorption behavior refers to the partial removal (desorption) of the adsorbed layer from the substrate upon the deposition of the subsequent layer which influences the growth of multilayer film in LBL system [85], [87]. This section investigates the desorption dynamics of dendritic PAMAM polycation and linear PAA polyanion up to four layers, considering the effects of intermediate drying and the concentration ratio of the polyelectrolytes. To do this, the absorbance and turbidity of the PE solutions after each layer deposition (waste-PE) were measured; and the results were reported in Figures 20a, and 20b. The quantity of layer removed from the surface following each dipping process was estimated according to the fitted curve described in Section 2.2.1.5. The results of this analysis are presented in Table 13. The higher absorbance of the waste-PE rather than pure PE (or a negative percentage) indicates that desorption surpassed adsorption, and the lower absorbance of waste-PE (or a positive percentage) suggests that adsorption exceeded desorption.

In Figure 20a, the impact of intermediate air-drying on adsorption-desorption behavior was a concern. "Ln" and Ln-D refer to waste-PE after dipping the substrate prepared with hydrated LBL (without drying) and dry LBL (with intermediate drying) respectively, and "n" is the number of the layer. As shown in Figure 20a, the absorbance of the L1-D was significantly higher than pure PAA as well as L1; while the absorbance of L1 was lower than pure PAA. Indeed, this indicated desorption or removal of approximately 16.56×10^{-6} mol/g of residual and un-grafted PAMAM remained on the substrate upon aminolysis reaction into the PAA polyelectrolyte solution. In other words, a 3-times quick rinsing procedure after aminolysis seemed to be insufficient to remove the un-grafted-PAMAM from the PLA nonwoven structure. 10 minute pre-wetting of the substrate leads to better removal of the un-grafted-PAMAM from the surface and prevents PE contamination as much as before. Indeed, the quantity of removed PAMAM reduced about 98.25% unreacted to 0.29×10^{-6} mol/g. This finding underscores the critical role of the washing step following aminolysis. As the layering process progressed, as illustrated in Figure 20b, it became evident that lower

desorption in a step of LBL caused more desorption in the sequence layering. For instance, lower desorption of PAMAM in the layering first layer of hydrated LBL followed by more PAA desorption in the second layering in comparison to dry LBL. This trend continued until the deposition of layer 4. This trend culminated in lower and lower-layer desorption. As confirmed by the ninhydrin assay detailed in Section 2.2.2.4, regardless of the LBL approached dry or hydrated LBL, despite the partial removal of both PAMAM and PAA layer layers in the LBL system (Table 13), the remaining layers are sufficiently present to maintain an appropriate charge balance to facilitate the deposition of subsequent polyelectrolytes as additional layers. Also, from these data, it can be concluded that drying caused lower PAA removal as estimated in Table 13, which is in agreement with ninhydrin results obtained in the previous section. As it can be concluded complicated adsorption-desorption phenomenon was observed in dendritic PAMAM and linear PAA LBL process.
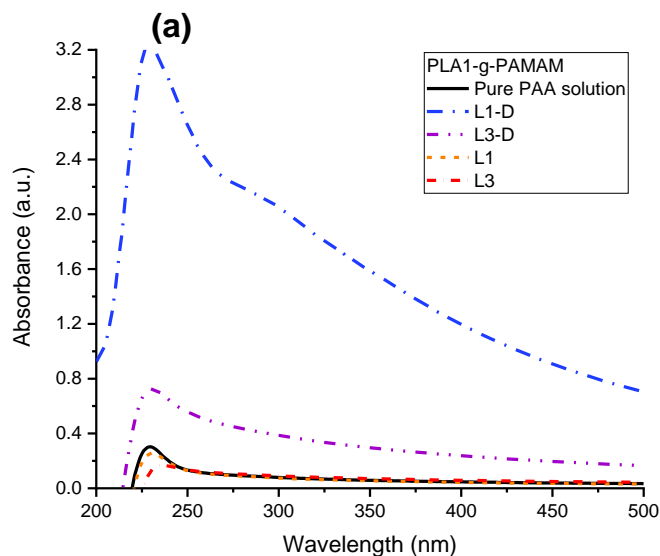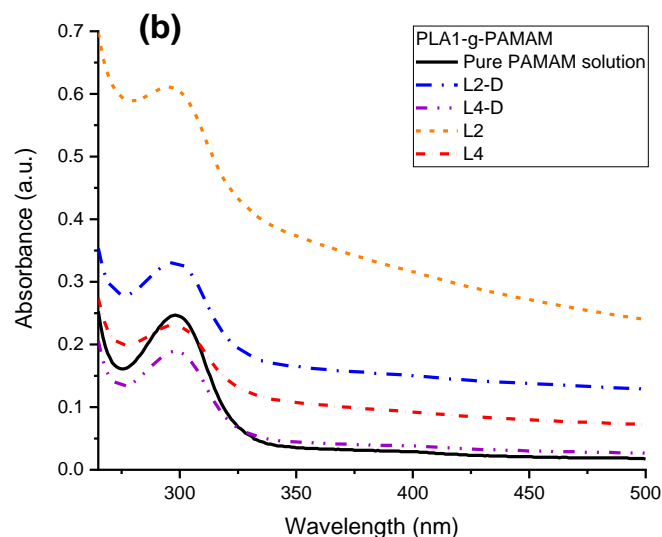
Figure 20. UV-visible spectra curve of waste-PE for the (a) deposition of PAA layer, and (b) deposition of the PAMAM layer on aminolyzed-PLA1 (40GSM)

Table 13. Calculated layer removal in mol/cm^2 upon the sequential layer deposition

Removed layer ($10^6 \times$mol/g)	Layer number	Hydrated LBL	Dry LBL
PAMAM	1	0.2907	16.6511
	3	0.1187	1.8789
PAA	2	0.0167	0.0098
	4	0.0091	0.0077

To investigate the effect of PE concentration ratio on adsorption-desorption behavior, aminolyzed-PLA2 was applied to LBL with three different concentration ratios including 7: 7 (a), 7:10 (b), and 4:10 (c) ($10^{-4} \times$g/mL), and the results of absorbance percentage are represented in Figure 21. According to Section 5.2.1.3, the maximum turbidity, indicating maximum complex formation in the liquid-liquid phase, followed this logical order: 7:7 (1668 NTU) > 7:10 (1271 NTU) > 4:10 (428 NTU) (PAA: PAMAM). Furthermore, as detailed in Section 5.2.2.1, which is related to the staining of the multilayered substrate (four layers) with varying concentration ratios of PEs, the color depth values were recorded in the following

order: 7:7 (2.86) > 7:10 (1.71) > 4:10 (0.88). Indeed, the concentration ratio leading to the maxim turbid colloidal formation in the liquid-liquid phase resulted in the higher multilayer film growth on the solid substrate. This indicates that the growth of the multilayer film on aminolyzed PLA was significantly dependent on the PE concentration ratio, aligning with the data obtained from the liquid-liquid phase.

In this regard, to study the adsorption-desorption behavior of multilayers, the absorbance of the waste-PE after each dipping process was recorded by UV-Vis spectrophotometer. The absorbance of the waste-PAA polyelectrolyte (odd layer) and the PAMAM polyelectrolyte (even layer) was recorded at 230 nm and 298 nm, respectively, and the percentage of absorbance is reported in Figure 21. The negative percentage of absorbance indicates that desorption surpassed adsorption, and the positive percentage of absorbance suggests that adsorption exceeded desorption. For clarity in interpretation, we assumed that the substrates had identical histories and equivalent amounts of amine density generated during the aminolysis reaction.

Considering the LBL assembly with varying PAA concentrations while maintaining a constant PAMAM concentration (conditions "a" and "b"), as shown in Figure 21, the deposition of the first PAA layer in both cases resulted in a positive percentage of absorbance, indicating that adsorption surpassed desorption. By continuing the LBL process, to deposit the second layer (PAMAM), the desorption of the previously adsorbed PAA corresponding to condition "a" was approximately 53% more than "b". Indeed, the increased adsorption in the first layer deposition led to greater desorption in the subsequent layer deposition. As the multilayer process continued to the third and fourth layers, the desorption of the PE layer onto the substrate under condition "a" exceeded adsorption, reaching about 7.4% adsorption, while condition "b" continued to show that desorption outpaced adsorption, resulting in a negative adsorption percentage.

When starting the LBL process with the same PAA concentration and varying PAMAM concentrations (conditions "b" and "c"), desorption consistently surpassed adsorption in layers 2, 3, and 4 (indicated by negative percentages of absorbance). However, the higher PAMAM concentration in condition "b" resulted in a greater adsorption percentage after fourth layer deposition compared to the lower PAMAM concentration in condition "c."

In conclusion, the multilayer growth on the solid phase was more sensitive to the PAMAM PE concentration than to the PAA concentration, as evidenced by the significant difference in absorbance percentages after four layers of deposition: 53.3% for conditions "a" and "b" versus 233% for conditions "b" and "c." Additionally, the adsorption-desorption behavior was heavily influenced by the growth of the first layer and the concentration ratio of the polyelectrolytes, and all these imply complicity of the adsorption-desorption phenomenon.
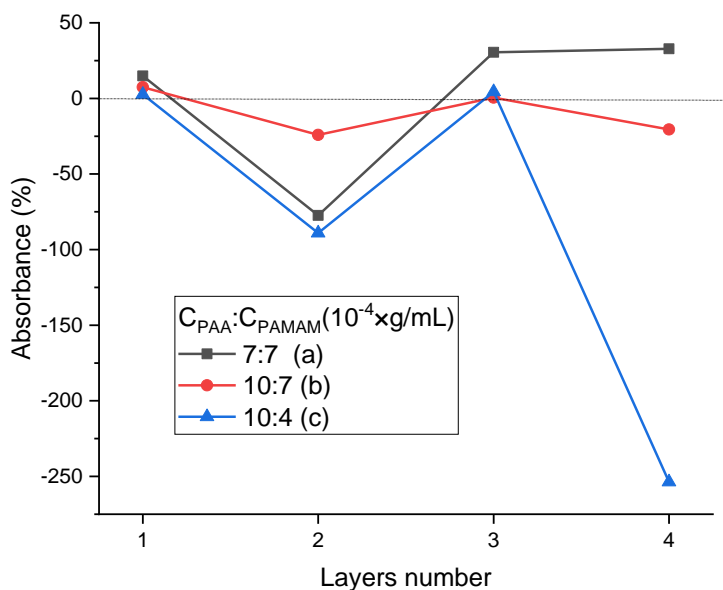
Figure 21. Adsorption percentage of PE calculated from the adsorbance data of waste-PE as a function of layer number

5.2.2.6 Adsorption Capacity of PE Multilayers

To investigate the influence of the number of layers and the intermediate drying process in layer-by-layer assembly (on PLA1 with lower GSM) on the host-guest properties of multilayer structures in relation to their interaction with guest molecules, a straightforward staining procedure utilizing the anionic model dye, Acid Red 1, was performed. The outcomes, represented by the color depth (Kubelka-Munk) (K/S value) of

the substrates and the absorbance of the dye solution after the staining process (waste-dye solution) to analysis the layer stability, are detailed in Figure 22 (a-b)."Wn" is referring to waste-dye solution in which "n" is corresponding to the layer number. For example, W4, is the waste-dye solution of the substrate with 4 multilayers.

As illustrated in Figure 22a, the color depth on the substrate exhibited a progressive increase from the aminolyzed (layer zero=aminolyzed PLA) to Layer 4, as indicated by the K/S values. This trend suggests a reduction in the adsorption of the waste dye solution following the staining process. Correspondingly, the adsorption data revealed a decrease in the dye content of the waste solution, consistent with these findings. As the layering process continued, interestingly, the K/S value of layered-PLA with 6 layers (PLA_6) reduced compared with PLA_4; while, the waste dye solution from the six-layer assembly exhibited lower dye adsorption (W6 < W4), indicating a reduced dye content in the dye solution. This observation can be interpreted as a result of partial turbid colloidal complex removal, which contributed to the decreased dye adsorption in the waste solution and the diminished color depth of the samples. Concerning Layer 8 (PLA_8), the dye adsorption observed in W_8 was higher than that in W4, yet the color depth was lower than that of PLA_4. This phenomenon can be elucidated by the following hypothesis: the increased availability of amine groups, as indicated by the ninhydrin results, does not necessarily correlate with a higher accessibility of these groups for reaction with dye molecules. It is plausible that a threshold effect exists, where the increase in amine density up to Layer 4 enhances dye adsorption. However, further increases to Layer 6 may induce instability in the layer structure, resulting in decreased color depth. As we progress to Layer 8, potential aggregation of the outermost layer could hinder the accessibility of the amine groups, despite the apparent stability of the layers, thereby reducing the interaction between the dye molecules and the amines.

Considering the intermediate drying in LBL deposition process, it can caused the different behavior of guest-host properties. The K/S value of the substrates increased progressively from the second to the eighth layers. This trend was consistent with the dye adsorption results observed in the waste dye solutions. However, the reduction in dye adsorption within the waste dye solutions may be attributed to the occurrence

of partial turbid colloidal complex removal during the staining process, which would typically lead to decreased dye adsorption and the color strength as well. This inconsistency largely rules out the possibility of layer removal, suggesting that the drying process employed in the LBL deposition technique was effective in stabilizing the layers, thereby maximizing dye uptake by the eight-layered substrate.
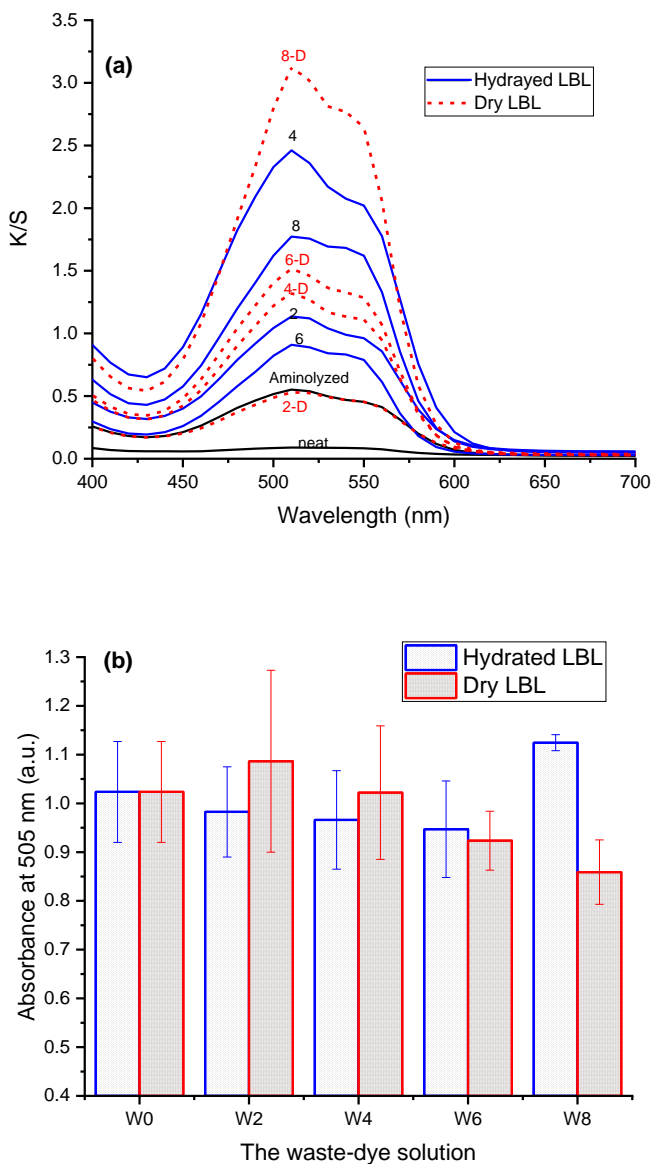

Figure 22. (a) Color depth value of layered substrate, (b) maximum absorbance of the waste-dye solution (W)." Wn" is responding to the layer number)

5.2.2.7 Construction of PAA/PAMAM multilayers on PLA nonwoven

Air permeability is defined as the volumetric flow rate of air per unit area at a specified pressure over a defined duration. This measurement serves as a reliable indicator of a substrate's porosity. The relationship between air permeability and substrate characteristics is significant; as basis weight, density, and thickness decrease, air permeability tends to increase. This is further influenced by the sizes of pores and fibers, where larger pore and fiber dimensions facilitate greater airflow [149], [166].

In the present study, air permeability was employed as a characterization technique to investigate the structure of the PEC multilayer assemblies deposited on the PLA substrate using LBL method, both with and without the intermediate drying step, as a function of the number of layers. To facilitate a more thorough analysis of the PEC multilayer structure, PLA1, which has a lower GSM, was chosen as the support layer. This selection is based on the observation that the neat PLA1 nonwoven exhibits significantly higher air permeability (15.5 ± 0.87 $cm^3.cm^{-2}.S^{-1}$) compared to the PLA2 nonwoven with a higher GSM (165 ± 47 $cm^3.cm^{-2}.S^{-1}$). Consequently, the changes in air permeability resulting from the PEC multilayer will be more readily detectable in the PLA1 substrate. The results of air permeability measurements for the neat, aminolyzed, and multilayered nonwoven, following each deposition of the PAA/PAMA complex, are illustrated in Figure 23. As illustrated in Figure 23, the air permeability of the substrate increased by approximately 12.3% following aminolysis. This observation is rational, as aminolysis induces surface erosion [63], resulting in a weight reduction of the substrate ($1.36 \pm 0.09\%$), which in turn contributes to the observed increase in air permeability.

The analysis of air permeability in relation to the number of layers provided valuable insights. The sharp slope of the graph and the notable decrease in air permeability suggested significant development of the PEC multilayer film up to certain layer counts (L4, L6-D), indicating a considerable increase in film density during the early stages of layering. However, as the LBL process continued to Layer 8, a more gradual growth pattern was observed. This indicates that the rate of film density increase began to slow down as more layers were added. In other words, the growth rate of the PE multilayers approached a plateau, leading

to a reduced impact of additional layers on both the air permeability and overall density of the multilayer film.

The application of intermediate drying in the LBL deposition process has demonstrated a notable effect on the structure and porosity of PEC multilayers. As shown in Figure 23, the multilayered substrates subjected to intermediate drying exhibited higher air permeability compared to those without this drying step. This increased air permeability in the PE multilayer assemblies can be attributed to their less compact structure, which facilitates greater airflow per unit area and per second. A potential explanation for this phenomenon is the distinct growth profile of the PE multilayers on samples layered with the dry and hydrated LBL method. As previously discussed, the growth profile of PEC multilayers exhibited converging behavior in the hydrated LBL process and diverging behavior in the dry LBL process. These differences in growth profiles led to a greater accumulation of amine content (PAMAM deposition) during the dry LBL method. Since PAMAM possesses an open structure, it is expected to enhance gas permeability [96]. Therefore, the increased accumulation of PAMAM at each even layer in the samples via the application of intermediate drying results in a more porous or less compact structure in the PEC multilayers, thereby contributing to the observed increase in air permeability.
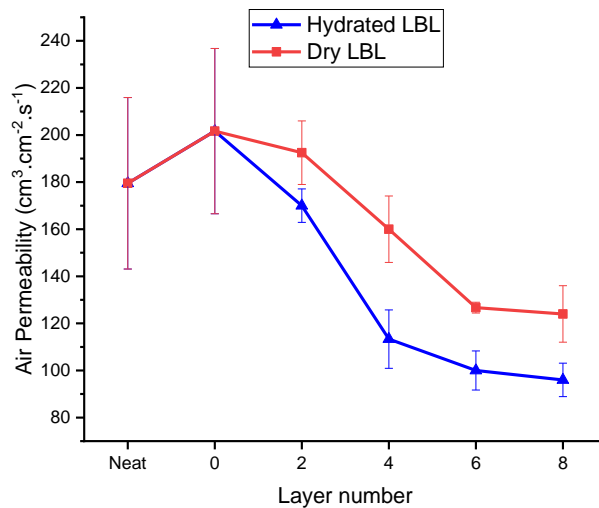

Figure 23. Air permeability of multilayered substrate as a function of layer number

5.2.2.8 Mechanical properties

The mechanical properties of modified PLA nonwoven fabrics were assessed in the machine direction (along the length of the fabric) using static tensile tests. The average results of these evaluations are presented in Table 14, providing a comprehensive overview of the material's performance characteristics. As previously discussed in section (5.1.6), the aminolysis reaction and surface erosion of the PLA nonwoven significantly contribute to a decrease in Young's modulus, tensile strength, and elongation at break. As previously reported by our research team [49], [154], aminolysis via amine-terminated PAMAM dendritic polymers can result in the shortening of molecular chains within the polymeric matrix. This alteration in chain length affects the overall mechanical integrity and performance of the material. J. H. Park et al. [167] prepared multilayers of poly (styrene sulfonate) (PSS) and poly(allylamine hydrochloride) (PAH) on electrospun nylon 6 fibers to enhance the mechanical properties of the substrate. The results indicated that tensile strength and Young's modulus of layered substrate were roughly increased by 134% and 157% in comparison to neat and unmodified substrate, respectively [167].

As can be seen from the Table 14, the application of a PE multilayer on aminolyzed PLA nonwoven resulted in substantial increases in stiffness and tensile strength, with improvements of approximately 989% and 88%, respectively. This improvement is likely due to the dense and rigid characteristics of the PE multilayer [167], which effectively mitigates the surface erosion caused by the aminolysis process. However, the PE multilayer assembled on aminolyzed PLA cost the ductility of the substrate since the layered PLA showed no elongation at break, indicating a loss of ductility and an increase in brittleness. Regarding the drying effect, there was a slight enhancement in stiffness and tensile strength compared to the hydrated LBL, suggesting greater growth of the PE multilayer, which aligns with previous findings.

Table 14. Tensile strength (σ_m), Young's modulus (E_t), and elongation at break ($\mathcal{E}_b$) of neat, aminolyzed, and multilayered PLA (with 8 layers)

Samples	σ_m	E_t	$\mathcal{E}_b$
Neat	2.97±0.95	1.26±0.29	26.03±6.66
Aminolyzed	0.85±0.07	0.18±0.03	7.29±2.84
Multilayered with hydrated LBL	1.60±0.20	0.84±0.06	---
Multilayered with dry LBL	1.96±0.28	0.88±0.03	---

5.2.2.9 Scanning electron microscopy analysis

To examine the alterations in surface morphology upon the LBL deposition process, scanning electron microscopy (SEM) analysis was utilized to analyze various PLA samples. These included neat PLA1, aminolyzed PLA1, and multilayered PLA1, with some samples undergoing intermediate drying. The analysis focused on samples with 4, 5, and 8 multilayers, as shown in Figure 24. The SEM results indicated that the initially smooth and uniform surface of the neat PLA became rougher following the aminolysis treatment, which alters the surface properties. As the LBL deposition continued, the roughness increased significantly due to the accumulation of multilayer assemblies made from PAA and PAMAM. Specifically, the substrates with 5 and 8 multilayer assemblies showed much rougher surfaces compared to those with only 4 layers. However, when comparing the samples that were layered with intermediate drying to those without it at the same number of layers, no major differences in surface appearance were found. The increased roughness in the multilayer assemblies with more layers is due to the buildup of aggregated PAA/PAMAM complexes. As the LBL process continued and more layers were added, these complex structures accumulated on the surface, resulting in a more varied and rough topography. This observation highlights the need to consider the number of layers, as well as the surface texture and roughness of the multilayer assemblies since these aspects can significantly influence various applications and interactions with other substances, like dye molecules. Understanding how surface roughness changes with the number of layers is crucial for effectively designing and improving multilayered-based materials and devices.
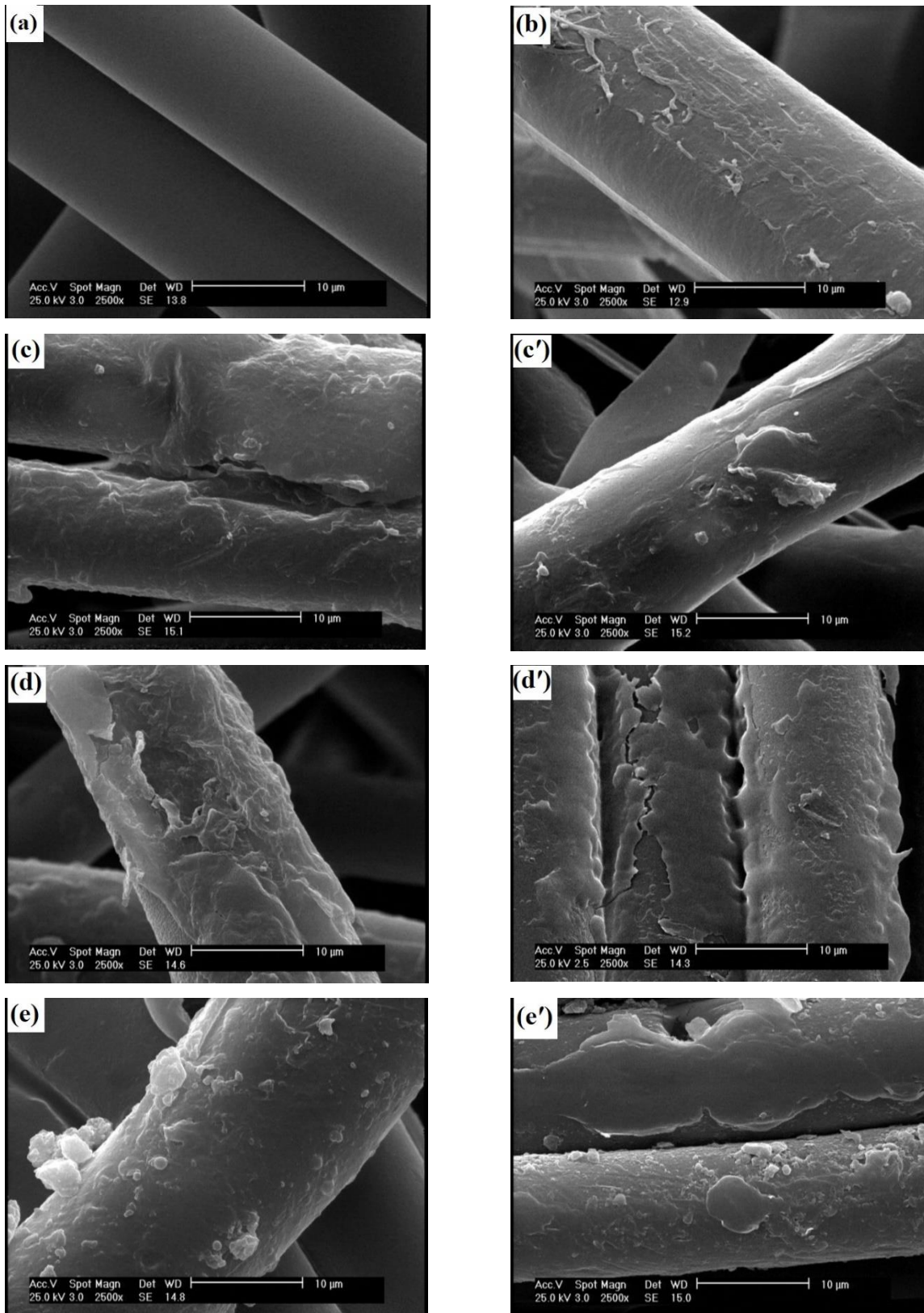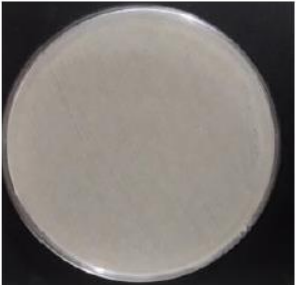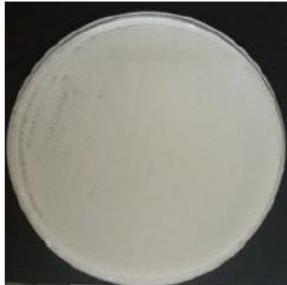
Figure 24. SEM images of (a) neat, (b) aminolyzed, and (c-e) Multilayered PLA; (c) PAMAM$_4$, (c′) PAMAM$_{4-D}$,
(d) PAA$_5$, (d′) PAA$_{5-D}$, (e) PAMAM$_8$, (e′) PAMAM$_{8-D}$

5.2.2.10Antibacterial properties

Cationic polymers, such as amine-terminated PAMAM, exhibit antibacterial properties due to the presence of numerous primary amines within their structure [1], [118]. The antibacterial effectiveness of these positively charged polymers is largely ascribed to their interactions with negatively charged bacterial cell membranes. Such interactions facilitate the formation of nanopores in the bacterial membrane, leading to cellular damage, the leakage of intracellular contents, and ultimately, the death of bacterial cells [7], [120]. In this study, we evaluated the antibacterial activity of modified PLA nonwoven fabrics, which were prepared through aminolysis followed by layer-by-layer LBL deposition. The evaluation was conducted against common bacterial strains, specifically Escherichia coli (E. coli), a Gram-negative bacterium, and Staphylococcus aureus (Staph), a Gram-positive bacterium. The assessment utilized the colony-forming unit (CFU) method in conjunction with ImageJ analysis. The samples analyzed included neat PLA, aminolyzed PLA, multilayered-PLA4 (with PAMAM as the top layer), and multilayered-PLA5 (with PAA as the top layer). The results presented in Table 15 provide compelling evidence that PAMAM showed significant bacteriostatic activity. This is particularly notable as there was a marked reduction in the bacterial populations of both Escherichia coli (E. coli) (99.99%) and Staphylococcus species (Staph) following the aminolysis process. The data indicates that the impact of PAMAM is especially pronounced on the Gram-positive strain, suggesting a potentially greater efficacy in targeting these types of bacteria. In addition to the initial findings, the application of PAMAM onto aminolyzed PLA through the LBL assembly technique resulted in the formation of multilayer structures containing more amine density. These structures included up to four and five layers, with two of those layers specifically composed of PAMAM. Remarkably, these multilayer configurations demonstrated bactericidal activity against both E. coli and Staph. The experimental results revealed that no bacterial growth was observed in the samples labeled as multilayered-PLA4 and PLA5, regardless of the composition of the top layer. This finding underscores the potential of PAMAM-modified PLA as an effective antibacterial material, especially PE multilayer

assembly containing PAMAM, which could have significant implications for biomedical applications and the development of surfaces that resist bacterial colonization.

Table 15. Antibacterial results of neat, aminolyzed, and multilayered PLA with 4 and 5 layers

Samples	E.coli	Staph.	(Cuf/ml)	
			E. coli	Staph
Neat PLA			1.5×10^8	1.5×10^8
Aminolysed-PLA			5.3×10^3	2.7×10^3
Multilayered-PLA with 4 layers, PAMAM as the top layer			0	0
Multilayered-PLA with 5 layers, PAA as the top layer			0	0

6 Conclusions

This study provides insights into (1) the aminolysis of polylactide nonwoven using amine-terminated PAMAM dendritic polymer for pre-treatment; (2) characterization and optimization of polyelectrolyte complex (PEC) formation in liquid-liquid phase; (3) monitoring multilayer assemblies on pre-treated PLA in liquid-solid phase; and (4) structural confirmation and property analysis of PE multilayer, utilizing PAMAM and poly(acrylic acid) as polyionic components.

(1) Aminolysis reaction results showed that elevated temperatures (60°C) significantly accelerated the process, as evidenced by weight reduction, color depth, ninhydrin, and Instron analysis. Maximum weight loss was 1.36±0.09% for PLA1 after 1 hour and 1.00±0.13% for PLA after 1.5 hours, with the highest color depths of 1.6 and 1.5 for PLA1 and PLA2, respectively, indicating optimal conditions.

Ninhydrin assay results indicated that a maximum of 6.72±1.00 and 5.36±1.20 micro mole amine groups were presented per gram of PLA1 and PLA2, respectively.

Water contact angle results revealed approximately 23% increase in hydrophilicity of aminolyzed-PLAs at the optimum condition.

FTIR-ATR analysis identified new peaks associated with N-H bending (~1650 cm^{-1}) and amide group stretching (3100-3650 cm^{-1}), indicating successful modification of the PLA structure.

(2) To characterize PEs in liquid-liquid phase, acid-based titration and dynamic light scattering showed that PAMAM at pH 8.93 (DoI=55.37%) and PAA at pH 4.27 (DoI=50.44%) are partially charged and exhibit compact and globular conformations, respectively. These conditions resulted in the highest concentration of aggregated PECs, measured at 1668 NTU via turbidity measurement. Stable colloidal PECs formed at PAMAM concentrations $\geq 4\times10^{-4}$ g/mL, with no PEC formation or stability at $\leq 1\times10^{-4}$ g/mL. A PAMAM: PAA ratio of 7:7 (10^{-4} g/mL) yielded the highest PEC formation, achieving a turbidity of approximately 1668 NTU.

UV-visible spectroscopy showed a reduction in the peak at 298 nm, indicating that tertiary amines of PAMAM are involved in complex formation. This suggests that the PAA chain can penetrate the PAMAM structure, demonstrating a host-guest behavior in the complex.

(3) Results obtained in In liquid-solid phases, the optimal PEC concentration ratio (7:7 (10^{-4} g/mL) also promoted significant growth of PE multilayers on PLA as confirmed by color depth analysis. FTIR-ATR analysis confirmed the deposition of the first PAA layer with a new broad peak around 1535 cm^{-1} associated with the symmetric vibration of ionized –COO^{-} groups of PAA.

Monitoring PE multilayer deposition revealed complex adsorption-desorption behavior influenced by intermediate drying and PEs concentration ratio.

To study of growth profile of PE multilayers, it was concluded that dried LBL contributed to the stabilization of the PAA layer, leading to a divergent growth profile characterized by an increased density of amine groups on the even layers. In contrast, hydrated LBL led to the converging growth profile characterized by diminished increase in NH$_2$ density as layering process continued.

(4) To study the PE multilayer properties, air permeability analysis showed increased film density with up to 4 layers (hydrated LBL) and 6 layers (dried LBL). By the 8th layer, the growth rate slowed, indicating reduced effects on air permeability and density. Dried LBL resulted in higher air permeability due to a less compact structure.

A higher density of available amine groups did not enhance interaction with other molecules, such as an anionic model dye, indication a threshold in the number of layers for optimal functionality. Mechanical and antibacterial analyses showed that PE multilayers significantly improved the substrate's mechanical performance and provided bactericidal activity, as evidenced by the absence of bacterial growth (both gram-positive and gram-negative) on the multilayered substrate.

In conclusion, understanding the growth profile of PE multilayers and controlling their density to optimize surface properties with accessible functional groups is essential for designing nonwoven substrates with advanced multilayer assemblies. This is particularly important for applications such as drug delivery and biomedical applications where microbial contamination is critical concern.

Supplementary data section

Dynamic light scattering results of PAMAM and PAA polyelectrolyte solution at different pH media, related to section 5.2.1, are reported as below:

PAMAM at ~pH 8
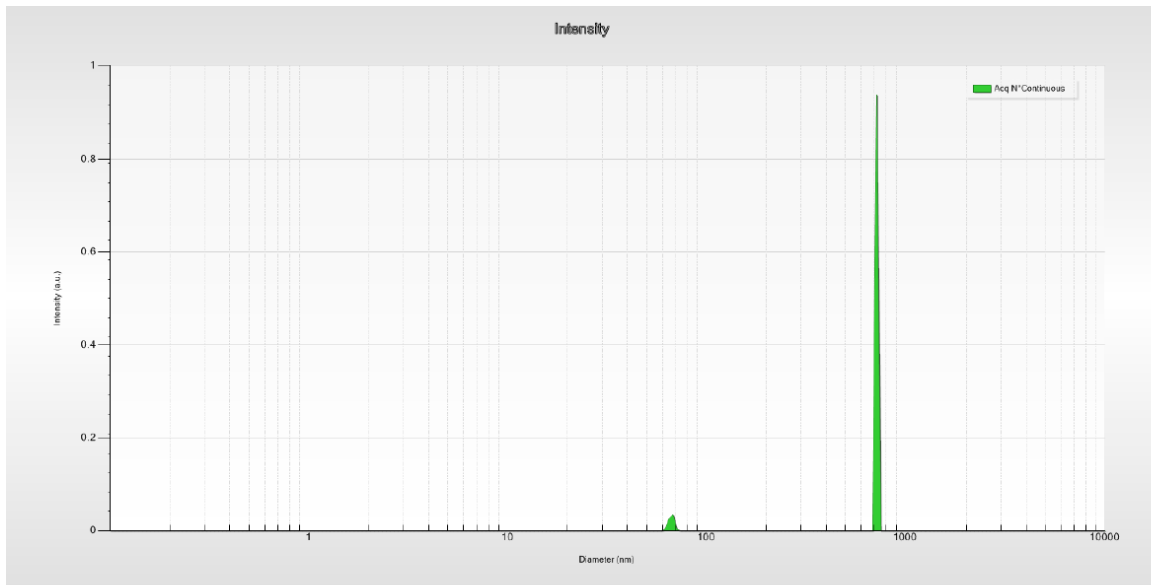
Distribution statistics

Di 10%: 716.84 nm	Di 50%: 716.84 nm	Di 90%: 716.84 nm

Mean Intensity: 675.55 nm
Solution index: 21

Peak : 1 | Mode: 750.76 nm Mean: 750.76 nm Dev.: 0 % Intensity.: 83.1 %

Peak : 2 | Mode: 67.81 nm Mean: 66.57 nm Dev.: 4.73 % Intensity.: 16.9 %

PAMAM at ~pH 4
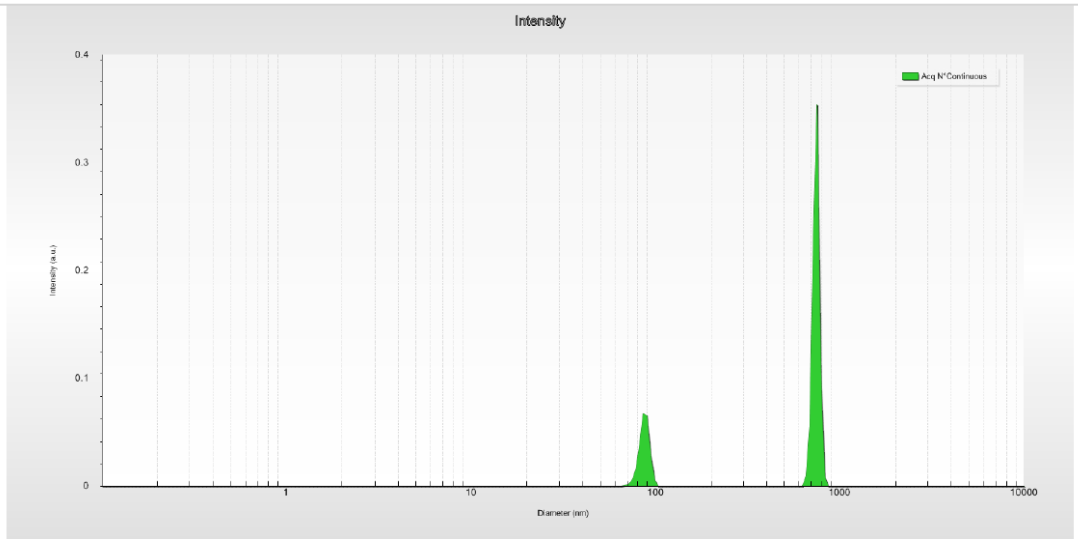
Distribution statistics

Di 10%: 85.45 nm	**Di 50%:** 716.84 nm	**Di 90%:** 786.29 nm
Mean Intensity: 588.2 nm		
Solution index: 9		

Peak : 1	**Mode:** 750.76 nm	**Mean:** 740.89 nm	**Dev.:** 5.57 %	**Intensity.:** 76.73 %
Peak : 2	**Mode:** 85.45 nm	**Mean:** 86.47 nm	**Dev.:** 7.32 %	**Intensity.:** 23.27 %

PAA ~pH 10
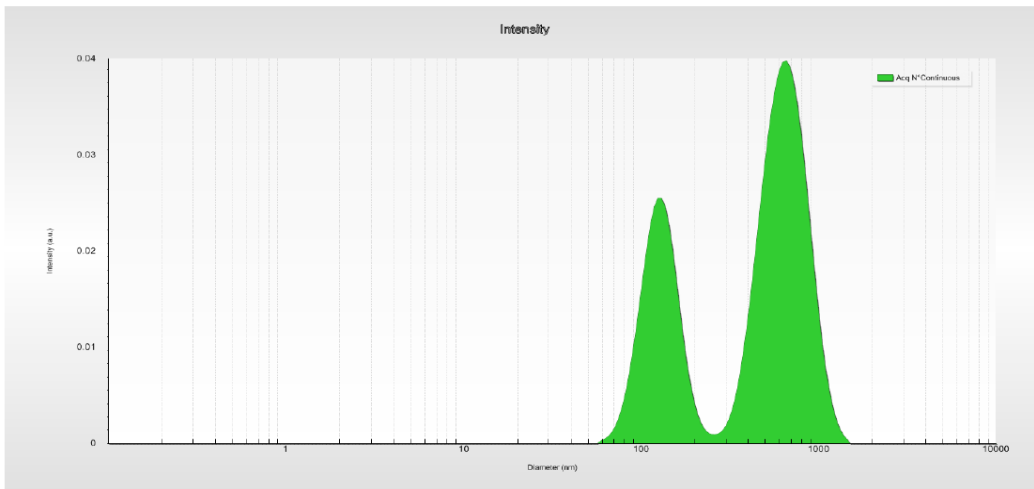
Distribution statistics

Di 10%: 112.77 nm	**Di 50%:** 518.63 nm	**Di 90%:** 862.47 nm
Mean Intensity: 479.86 nm		
Solution index: 4		

Peak : 1	**Mode:** 653.52 nm	**Mean:** 658.05 nm	**Dev.:** 29.77 %	**Intensity.:** 66.31 %
Peak : 2	**Mode:** 123.7 nm	**Mean:** 129.56 nm	**Dev.:** 25.26 %	**Intensity.:** 33.69 %

PAA ~pH 4
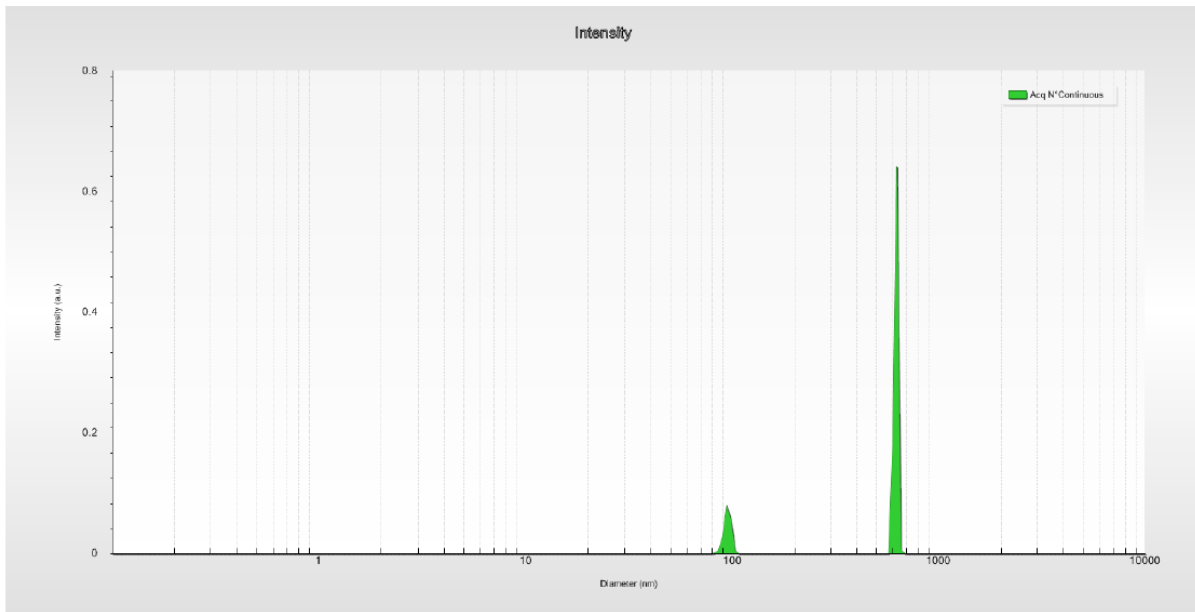
Distribution statistics

Di 10%: 93.73 nm   **Di 50%:** 623.99 nm   **Di 90%:** 623.99 nm
Mean Intensity: 527.35 nm
Solution index: 11

Peak : 1 | **Mode:** 623.99 nm **Mean:** 618.61 nm **Dev.:** 4.25 %   **Intensity.:** 82.66 %

Peak : 2 | **Mode:** 93.73 nm   **Mean:** 94.43 nm   **Dev.:** 5.44 %   **Intensity.:** 17.34 %

Supplementary data related to section 5.2.1.3, presenting the participation of formed PEC at the concentration ratio of 1:7 (10^{-4} g/mL), by decreasing the pH of PAMAM PE solution from 8 to 3
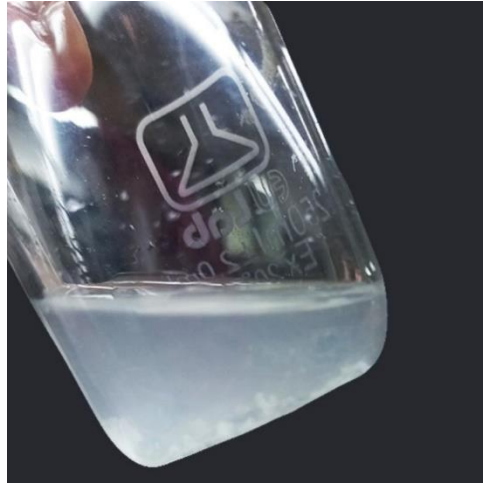
Image 1. Precipitation of turbid colloidal PECs at pH=3 of PAMAM and pH=4 of PAA

References

[1]   S. A. Delyanee M, Akbari S, "Amine-terminated dendritic polymers as promising nanoplatform for diagnostic and therapeutic agents' modification: A review," *Eur. J. Med. Chem.*, vol. 221, p. 113572, 2021, doi: 10.1016/j.ejmech.2021.113572.

[2]   J. Borges *et al.*, "Recent Developments in Layer-by-Layer Assembly for Drug Delivery and Tissue Engineering Applications," *Adv. Healthc. Mater.*, vol. 13, no. 2302713, pp. 1–28, 2024.

[3]   D. Stawski, "Application of the Layer-by-layer Method for Textiles," in *Textiles, Uses and Production Methods*, 1 st ed., EI Nemr, A., ED., 2012, pp. 507–518.

[4]   M. H. Iqbal, H. Kerdjoudj, and F. Boulmedais, "Protein-based layer-by-layer films for biomedical applications," *Chem. Sci.*, vol. 15, pp. 9408–9437, 2024, doi: 10.1039/d3sc06549a.

[5]   S. Akbari and R. M. Kozłowski, "A review of application of amine-terminated dendritic materials in textile engineering," *Journal of the Textile Institute*, vol. 110, no. 3. Taylor and Francis Ltd., pp. 460–467, Mar. 04, 2019, doi: 10.1080/00405000.2018.1512361.

[6]   M. Malkoch and S. García-Gallego, "Introduction to dendrimers and other dendritic polymers," in *Dendrimer Chemistry: Synthetic Approaches Towards Complex Architectures*, vol. 2020-Janua, no. 29, Royal Society of Chemistry, 2020, pp. 1–20.

[7]   S. Alfei and A. M. Schito, "Positively Charged Polymers as Promising Devices against Multidrug Resistant Gram-Negative Bacteria: A Review," *Polymers (Basel).*, vol. 12, no. 5, p. 1195, 2020, doi: 10.3390/polym12051195.

[8]   W. Tang, D. Huang, X. Qiang, and W. Liu, "Hydrophilic and Fire-Resistant Phytic Acid/Chitosan/Polydopamine-Coated Expanded Polystyrene Particles by Using Coating Method," *Coatings*, vol. 14, no. 5, p. 574, 2024, doi: 10.3390/coatings14050574.

[9]   N. Dole, K. Ahmadi, D. Solanki, V. Swaminathan, V. Keswani, and M. Keswani, "Corona Treatment of Polymer Surfaces to Enhance Adhesion," in *Polymer Surface Modification to*

Enhance Adhesion, Wiley, 2024, pp. 45–76.

[10]   P. Slepička, N. Slepičková Kasálková, Z. Kolská, and V. Švorčík, "Surface Modification of Polymer Substrates for Biomedical Applications," in *Surface Modification of Polymers: Methods and Applications*, Wiley, 2019, pp. 399–426.

[11]   J. Karger-Kocsis and T. Bárány, *Polypropylene handbook*. Switzerland: Springer Nature, 2019.

[12]   M. S. Singhvi, S. S. Zinjarde, and D. V. Gokhale, "Polylactic acid: synthesis and biomedical applications," *J. Appl. Microbiol.*, vol. 127, no. 6, pp. 1612–1626, Dec. 2019, doi: 10.1111/JAM.14290.

[13]   Y. Uyama, K. Kato, and Y. Ikada, "Surface modification of polymers by grafting," *Grafting/Characterization Tech. Model.*, vol. 137, pp. 1–39, 1998, doi: 10.1007/3-540-69685-7_1.

[14]   A. Bhattacharya, A. Bhattacharya, and B. N. Misra, "Grafting:a versatile means to modify polymers: techniques, factors and applications," *Prog. Polym. sciecece*, vol. 29, no. 8, pp. 767–814, 2004, doi: 10.1016/j.progpolymsci.2004.05.002.

[15]   J. Parameswaranpillai, S. Thomas, and Y. Grohens, "Polymer blends: state of the art, new challenges, and opportunities," in *Characterization of polymer blends*, 2014, pp. 1–6.

[16]   I. Khan, M. M. Chohan, and M. A. J. Mazumder, "Polymer Blends," in *Functional Polymers. Polymers and Polymeric Composites: A Reference Series*, 2018, pp. 1–38.

[17]   S. Jeong, "Investigation of intrinsic characteristics of polymer blends via molecular simulation: a review," *Korea-Australia Rheol. J.*, vol. 35, no. 4, pp. 249–266, 2023.

[18]   P. Purohit, A. Bhatt, R. K. Mittal, M. H. Abdellattif, and T. A. Farghaly, "Polymer Grafting and its chemical reactions," *Front. Bioeng. Biotechnol.*, vol. 10, p. 1044927, 2023, doi: 10.3389/fbioe.2022.1044927.

[19]   D. Abliza, Y. Duana, L. Steuernagel, L. Xiea, D. Lia, and G. Ziegmann, "Curing Methods for Advanced Polymer Composites - A Review," *Polym. Polym. Compos.*, vol. 21, no. 6, pp. 341–348,

2013.

[20]   M. Lang, S. Hirner, F. Wiesbrock, and P. Funchs, "A Review on Modeling Cure Kinetics and Mechanisms of Photopolymerization," *Polymers (Basel).*, vol. 14, no. 10, p. 2047, 2022, doi: 10.3390/polym14102074.

[21]   B. Jiang, X. Shi, T. Zhang, and Y. Huang, "Recent advances in UV/thermal curing silicone polymers," *Chem. Eng. J.*, vol. 435, p. 134843, 2022, doi: 10.1016/j.cej.2022.134843.

[22]   S. K. Nemani *et al.*, "Surface Modification of Polymers: Methods and Applications," *Adv. Mater. Interfaces*, vol. 5, no. 24, p. 1801247, 2018, doi: 10.1002/admi.201801247.

[23]   C. J. Can-Herrera LA, Oliva AI, "Enhancement of chemical, physical, and surface properties of electrospun PCL/PLA blends by means of air plasma treatment.," *Polym. Eng. Sci.*, vol. 62, no. 5, pp. 1608–1618, 2022, doi: 10.1002/pen.25949.

[24]   H. Y. Ye G, Gu T, Chen B, Bi H, "Mechanical, thermal properties and shape memory behaviors of PLA/PCL/PLA-g-GMA blends.," *Polym. Eng. Sci.*, vol. 63, no. 7, pp. 2084–2092, 2023, doi: 10.1002/pen.26347.

[25]   S. F. M. YousefniaPasha H, Mohtasebi SS, Tabatabaeekoloor R, Taherimehr M, Javadi A, "Preparation and characterization of the plasticized polylactic acid films produced by the solvent-casting method for food packaging applications," *J. Food Process. Preserv.*, vol. 45, no. 12, p. 16089, 2021, doi: 10.1111/jfpp.16089.

[26]   D. Briassoulis, I.-G. Athanasoulia, and P. Tserotas, "PHB/PLA plasticized by olive oil and carvacrol solvent-cast films with optimised ductility and physical ageing stability," *Polym. Degrad. Stab.*, vol. 200, p. 109958, Jun. 2022, doi: 10.1016/J.POLYMDEGRADSTAB.2022.109958.

[27]   A. S. Narmon, A. Dewaele, K. Bruyninckx, B. F. Sels, P. Van Puyvelde, and M. Dusselier, "Boosting PLA melt strength by controlling the chirality of co-monomer incorporation," *Chem.*

Sci., vol. 12, no. 15, pp. 5672–5681, Apr. 2021, doi: 10.1039/D1SC00040C.

[28]   Y. Ding, B. Lu, P. Wang, G. Wang, and J. Ji, "PLA-PBAT-PLA tri-block copolymers: Effective compatibilizers for promotion of the mechanical and rheological properties of PLA/PBAT blends," *Polym. Degrad. Stab.*, vol. 147, pp. 41–48, Jan. 2018, doi: 10.1016/J.POLYMDEGRADSTAB.2017.11.012.

[29]   K. Sriwongsa, K. Hemvichian, W. Kangsumrith, P. Suwanmala, and T. Pongprayoon, "Radiation-Induced Crosslinking of Polylactic Acid: Effects of Air and Vacuum," 2011.

[30]   M. Bednarek, K. Borska, and P. Kubisa, "New Polylactide-Based Materials by Chemical Crosslinking of PLA," *Polym. Rev.*, vol. 61, no. 3, pp. 493–519, 2021, doi: 10.1080/15583724.2020.1855194.

[31]   P. K. Raj A, Samuel C, Malladi N, "Enhanced (thermo) mechanical properties in biobased poly (l-lactide)/poly (amide-12) blends using high shear extrusion processing without compatibilizers," *Polym. Eng. Sci.*, vol. 60, no. 8, pp. 1902–1916, 2020, doi: 10.1002/pen.25426.

[32]   J. Pinson and D. eds. Thiry, *Surface modification of polymers: methods and applications*. John Wiley & Sons., 2020.

[33]   G. A. El-Awadi, "Review of effective techniques for surface engineering material modification for a variety of applications," *AIMS Mater. Sci.*, vol. 10, no. 4, pp. 625–692, 2023, doi: 10.3934/matersci.2023037.

[34]   F. Ferrero and Periolatto. M, "Modification of surface energy and wetting of textile fibers," in *Wetting and Wettability*, 2015, pp. 139–168.

[35]   N. Encinas, M. Pantoja, J. Abenojar, and M. A. Martínez, "Control of wettability of polymers by surface roughness modification," in *Journal of Adhesion Science and Technology*, Aug. 2010, vol. 24, no. 11–12, pp. 1869–1883, doi: 10.1163/016942410X511042.

[36]   Y. V. Kamalov A, Ivanov A, Smirnova N, Sokolova M, Kolbe K, Pavlov A, Malafeev K,

"Nonlinear plasma surface modification of polylactide to promote interaction with fibroblasts," *Polym. Eng. Sci.*, vol. 63, no. 1, pp. 3565–3576, 2023, doi: 10.1002/pen.26466.

[37]   J. Q. Kim, J. H. Lee, J. Park, H. Park, S.-M. Lim, and C.-G. Lee, "New Surface Modification Method To Develop a PET-Based Membrane with Enhanced Ion Permeability and Organic Fouling Resistance for Efficient Production of Marine Microalgae," *Appl. Mater. Interfaces*, vol. 12, pp. 25253–25265, 2020, doi: 10.1021/acsami.0c00546.

[38]   S. Pinto, T. Miranda, M. Kašparová, and J. Wiener, "Modification of Polyester Properties through Functionalization with PVA," *Mater. Sci. Forum*, vol. 1092, pp. 57–73, 2023, doi: 10.4028/p-olfttp.

[39]   G. F. de Lima, A. G. de Souza, C. R. Bauli, R. F. da S. Barbosa, D. B. Rocha, and D. dos S. Rosa, "Surface modification effects on the thermal stability of cellulose nanostructures obtained from lignocellulosic residues," *J. Therm. Anal. Calorim.*, vol. 141, no. 4, pp. 1263–1277, 2020, doi: 10.1007/s10973-019-09109-4.

[40]   F. J. LM Gonçalves J, J. Castanheira E, PC Alves S, Baleizão C, "Grafting with RAFT—gRAFT strategies to prepare hybrid nanocarriers with core-shell architecture," *Polymers (Basel).*, vol. 12, no. 10, p. 2175, 2020.

[41]   E. Y. Choi and S. H. Moon, "Characterization of acrylic acid-grafted PP membranes prepared by plasma-induced graft polymerization," *J. Appl. Polym. Sci.*, vol. 105, no. 4, pp. 2314–2320, 2007.

[42]   P. Wei *et al.*, "Preparation of PP non-woven fabric with good heavy metal adsorption performance via plasma modification and graft polymerization," *Appl. Surf. Sci.*, vol. 539, p. 148195, 2021.

[43]   Y. Wang, J. H. Kim, K. H. Choo, Y. S. Lee, and C. H. Lee, "Hydrophilic modification of polypropylene microfiltration membranes by ozone-induced graft polymerization.," *J. Memb. Sci.*, vol. 169, no. 2, pp. 269–276, 2000.

[44]   D. Y. Lee, Y. S. Lee, and J. P. Jeun, "Study on aminated PP-g-GMA synthesized by radiation-

induced graft polymerization for silver adsorption," *J. Nanosci. Nanotechnol.*, vol. 20, no. 9, pp. 5411–5417, 2020.

[45] L. Pryhazhayeva, A. Shunkevich, A. Polikarpov, and L. Krul, "Synthesis and long-term stability of acrylic acid and N, N-methylene-bis-acrylamide radiation grafted polypropylene fibers," *J. Appl. Polym. Sci.*, vol. 138, no. 32, p. 50805, 2021.

[46] K. Mehta, V. Kumar, B. Rai, M. Talwar, and G. Kumar, "Silver nanoparticles-immobilized-radiation grafted polypropylene fabric as breathable, antibacterial wound dressing," *Radiat. Phys. Chem.*, vol. 204, p. 110683, 2023.

[47] J. Wei *et al.*, "Dense Polyacrylic Acid-Immobilized Polypropylene Non-woven Fabrics Prepared Via UV-Induced Photograft Technique for the Recovery of Rare Earth Ions from Aqueous Solution," *J. Polym. Environ.*, vol. 29, no. 8, pp. 2492–2503, 2021.

[48] N. Dehbashi Nia, S. W. Lee, S. Bae, T. H. Kim, and Y. Hwang, "Surface modification of polypropylene non-woven filter by O2 plasma/acrylic acid enhancing Prussian blue immobilization for aqueous cesium adsorption," *Appl. Surf. Sci.*, vol. 590, p. 153101, 2022.

[49] S. Shakoorjavan, M. Eskafi, D. Stawski, and S. Akbari, "New effective ways of polypropylene and polylactide nonwovens functionalization," *J. Text. Inst.*, pp. 1–13, 2024, doi: 10.1080/00405000.2024.2379221.

[50] Y. Liu *et al.*, "Modified ammonium persulfate oxidations for efficient preparation of carboxylated cellulose nanocrystals," *Carbohydr. Polym.*, vol. 229, p. 115572, 2020.

[51] A. Afzal, P. Drzewicz, J. W. Martin, and M. G. El-Din, "Decomposition of cyclohexanoic acid by the UV/H2O2 process under various conditions," *Sci. Total Environ.*, vol. 426, pp. 387–392, 2012.

[52] H. D. Lee C, Graves DB, Lieberman MA, "Global Model of Plasma Chemistry in a High Density Oxygen Discharge," *J. Electrochem. Soc.*, vol. 141, no. 6, p. 1546, 1994.

[53] P. J. Hawkins and D. S. Tarbell, "Studies on Model Compounds for Coenzyme A. A Kinetic Study

of Aminolysis and Hydrolysis of Ethyl Thioacetate and β-Acetaminoethyl Thioacetate in Aqueous

Solution," *J. Am. Chem. Soc.*, vol. 57, no. 12, pp. 2982–2985, 1953, doi: 10.1021/ja01108a057.

[54]   N. Rabiei and M. H. Kish, "Aminolysis of polyesters for cracking and structure clarifying: A

review. Polymers for Advanced Technologies," *Polym. Adv. Technol.*, vol. 33, no. 12, pp. 3903–

3919, 2022, doi: 10.1002/pat.5837.

[55]   M. Somani, S. Mukhopadhyay, and B. Gupta, "Amination of Polyurethane for Designing

Infection-Resistant Surfaces," *Ind. Eng. Chem. Res.*, vol. 62, no. 37, pp. 14937–14946, 2023, doi:

10.1021/acs.iecr.3c02181.

[56]   X. Zhong, Z. Lu, P. Valtchev, H. Wei, H. Zreiqat, and F. Dehghani, "Surface modification of

poly(propylene carbonate) by aminolysis and layer-by-layer assembly for enhanced

cytocompatibility," *Colloids Surfaces B Biointerfaces*, vol. 93, pp. 75–84, 2012, doi:

10.1016/j.colsurfb.2011.12.016.

[57]   Y. Zhu, Z. Mao, and C. Gao, "Aminolysis-based surface modification of polyesters for biomedical

applications," *RSC Adv.*, vol. 3, no. 8, pp. 2509–2519, 2013.

[58]   S. Shakoorjavan, M. Eskafi, D. Stawski, and S. Akbari, "New effective ways of polypropylene and

polylactide nonwovens functionalization," *J. Text. Inst.*, vol. Accepted, 2024.

[59]   J. F. Bunnett and G. T. Davis, "The mechanism of aminolysis of esters1, 2," *J. Am. Chem. Soc.*,

vol. 82, no. 3, pp. 665–674, 1960, doi: 10.1021/ja01488a043.

[60]   G. C. Zhu Y, Mao Z, Shi H, "In-depth study on aminolysis of poly (ε-caprolactone): Back to the

fundamentals," *Sci. China Chem.*, vol. 55, pp. 2419–2427, 2012.

[61]   I. Gancarz, J. Bryjak, and K. Zynek, "Chemical modification of poly(ethylene terephthalate) and

immobilization of the selected enzymes on the modified film," *Appl. Surf. Sci.*, vol. 255, no. 19,

pp. 8293–8298, 2009, doi: 10.1016/j.apsusc.2009.05.126.

[62]   Y. Zhu, C. Gao, X. Liu, and J. Shen, "Surface modification of polycaprolactone membrane via

aminolysis and biomacromolecule immobilization for promoting cytocompatibility of human endothelial cells," *Biomacromolecules*, vol. 3, no. 6, pp. 1312–1319, Nov. 2002, doi: 10.1021/bm020074y.

[63]   G. Mallamaci *et al.*, "Surface modification of polyester films with polyfunctional amines: Effect on bacterial biofilm formation," *Surfaces and Interfaces*, vol. 39, p. 102924, 2023, doi: 10.1016/j.surfin.2023.102924.

[64]   L. Bech, T. Meylheuc, B. Lepoittevin, and P. Roger, "Chemical surface modification of poly(ethylene terephthalate) fibers by aminolysis and grafting of carbohydrates," *J. Polym. Sci. Part A Polym. Chem.*, vol. 45, pp. 2172–2183, 2007, doi: 10.1002/pola.21983.

[65]   J. Burnett, A. King, I. Martin, L. T.-T. Letters, and U. 2002, "The effect of size on the rate of an aminolysis reaction using a series of amine terminated PAMAM dendrimers," *Tetrahedron Lett.*, vol. 43, no. 13, pp. 2431–2433, 2002, doi: 10.1016/S0040-4039(02)00113-2.

[66]   T. G. Bee and T. J. McCarthy, "Surface modification of poly(chlorotrifluoroethylene): introduction of reactive carboxylic acid functionality," *Macromolecules*, vol. 25, no. 8, pp. 2093–2098, 1992, doi: 10.1021/ma00034a006.

[67]   W. Chen and T. J. McCarthy, "Layer-by-layer deposition: A tool for polymer surface modification," *Macromolecules*, vol. 30, no. 1, pp. 78–86, 1997, doi: 10.1021/ma961096d.

[68]   H. F. Mark, "Encyclopedia of polymer science and technology," *15 volum set*, vol. 14. Wiley, pp. 519–520, 2014.

[69]   R. k. Iler, "Multilayers of colloidal particles," *J. Colloid Interface Sci.*, vol. 21, pp. 569–594, 1966.

[70]   G. Decher, J. D. Hong, and J. Schimmit, "Buildup of ultrathin multilayer films by a self-assembly process: III. Consecutively alternating adsorption of anionic and cationic polyelectrolytes on charged surfaces," *Thin Solid Films*, vol. 210–211, pp. 831–835, 1992.

[71]   A. K. Oliveira Jr ON, Caseli L, "The past and the future of Langmuir and Langmuir–Blodgett

films.," *Chem. Rev.*, vol. 122, no. 6, p. 6459−6513, 2022, doi: 10.1021/acs.chemrev.1c00754.

[72]   J. Borges and J. F. Mano, "Molecular Interactions Driving the Layer-by-Layer Assembly of Multilayers," *Chem. Rev.*, vol. 114, no. 18, pp. 8883–8942, 2014, doi: 10.1021/cr400531v.

[73]   M. Cai, J. Yang, X. Lu, and X. Lu, "Layer-by-Layer Self-Assembly Strategies of Atomically Thin Two-Dimensional Nanomaterials: Principles, Methods, and Functional Applications," *Appl. Nano Mater.*, 2024, doi: 10.1021/acsanm.3c06286.

[74]   H. Yao and N. Hu, "pH-Controllable On−Off Bioelectrocatalysis of Bienzyme Layer-by-Layer Films Assembled by Concanavalin A and Glucoenzymes with an Electroactive Mediator," *J. Phys. Chem. B*, vol. 114, no. 30, pp. 9926–9933, 2010, doi: 10.1021/jp104360q.

[75]   Y. Shimazaki, M. M. Yamamoto, S. Ito, and M. Yamamoto, "Preparation of the Layer-by-Layer Deposited Ultrathin Film Based on the Charge-Transfer Interaction," *Langmuir*, vol. 13, no. 6, pp. 1385–1387, 1997, doi: 10.1021/la9609579.

[76]   M. Dolmat, V. Kozlovskaya, D. Inman, C. Thomas, and E. Kharlampieva, "Hydrogen-bonded polymer multilayer coatings via dynamic layer-by-layer assembly," *J. Polym. Sci.*, vol. 61, no. 11, pp. 1052–1064, 2022, doi: 10.1002/pol.20220473.

[77]   Q. An, T. Huang, and F. Shi, "Covalent layer-by-layer films: chemistry, design, and multidisciplinary applications," *Chem. Soc. Rev.*, vol. 47, no. 13, pp. 5061–5098, 2018, doi: 10.1039/C7CS00406K.

[78]   T. A. Yuan W, Weng GM, Lipton J, Li CM, Van Tassel PR, "Weak polyelectrolyte-based multilayers via layer-by-layer assembly: Approaches, properties, and applications," *Adv. Colloid Interface Sci.*, vol. 282, no. 102200, 2020, doi: 10.1016/j.cis.2020.102200.

[79]   L. M. Petrila, F. Bucatariu, M. Mihai, and C. Teodosiu, "Polyelectrolyte Multilayers: An Overview on Fabrication, Properties, and Biomedical and Environmental Applications," *Materials (Basel).*, vol. 14, no. 15, p. 4152, 2021.

[80]   M. C. Stuart, R. de Vries, and H. Lyklema, "Chapter 2-Polyelectrolytes," in *Fundamentals of interface and colloid science*, 2005, pp. 2.1-2.84.

[81]   D. Scheepers, J. de Keizer, Z. Borneman, and K. Nijmeijer, "The pH as a tool to tailor the performance of symmetric and asymmetric layer-by-layer nanofiltration membranes," *J. Memb. Sci.*, vol. 670, p. 121320, 2023.

[82]   J. Zhang, L., Zheng, M., Liu, X. and Sun, "Layer-by-layer assembly of salt-containing polyelectrolyte complexes for the fabrication of dewetting-induced porous coatings," *Langmuir*, vol. 27, no. 4, pp. 1346–1352, 2011.

[83]   M. Yu *et al.*, "Theoretical and experimental research of polyelectrolyte multilayer membrane prepared by layer by layer self-assembly," *Desalination*, vol. 580, p. 117561, 2024.

[84]   A. J. Khopade and F. Caruso, "Electrostatically Assembled Polyelectrolyte/Dendrimer Multilayer Films as Ultrathin Nanoreservoirs," *Nano Lett.*, vol. 2, no. 4, pp. 415–418, Apr. 2002, doi: 10.1021/NL015696O.

[85]   Y. Zhu, C. Gao, T. He, X. Liu, and J. Shen, "Layer-by-Layer Assembly To Modify Poly(L-lactic acid) Surface toward Improving Its Cytocompatibility to Human Endothelial Cells," *Biomacromolecules*, vol. 4, pp. 446–452, 2003, doi: 10.1021/bm025723k.

[86]   K. T. Lvov Y, Ariga K, Onda M, Ichinose I, "A careful examination of the adsorption step in the alternate layer-by-layer assembly of linear polyanion and polycation," *Colloids Surfaces A Physicochem. Eng. Asp.*, vol. 146, no. 1–3, pp. 337–346, 1999.

[87]   S. Tomita, K. Sato, and J. I. Anzai, "Layer-by-layer assembled thin films composed of carboxyl-terminated poly (amidoamine) dendrimer as a pH-sensitive nano-device," *J. Colloid Interface Sci.*, vol. 326, no. 1, pp. 35–40, 2008.

[88]   V. S. Meka, M. K. Sing, M. R. Pichika, S. R. Nali, V. R. Kolapalli, and P. Kesharwani, "A comprehensive review on polyelectrolyte complexes," *Drug Discov. Today*, vol. 22, no. 11, pp.

1697–1706, 2017.

[89]   Y. Ghimire and A. Bhattarai, "A Review on Polyelectrolytes (PES) and Polyelectrolyte Complexes (PECs)," *Int. J. Eng. Res. Technol.*, vol. 9, no. 8, pp. 876–889, 2020.

[90]   T. Swift, L. Swanson, M. Geoghegan, and S. Rimmer, "The pH-responsive behaviour of poly(acrylic acid) in aqueous solution is dependent on molar mass†," *Soft Matter*, vol. 12, no. 9, pp. 2542–2549, 2016.

[91]   W. Chen, D. A. Tomalia, and J. L. Thomas, "Unusual pH-Dependent Polarity Changes in PAMAM Dendrimers: Evidence for pH-Responsive Conformational Changes," *Macromolecules*, vol. 33, pp. 9169–9172, 2000.

[92]   L. A, U. S, L. J, F.-R. N, S. S, and B. J., "Size and pH effect on electrical and conformational behavior of poly(acrylic acid): Simulation and experiment," *Eur. Polym. J.*, vol. 42, no. 5, pp. 1135–1144, 2006.

[93]   G. Yao, J. Zhao, S. B. Ramisetti, and D. Wen, "Atomistic molecular dynamic simulation of dilute polyacrylic acid solution: effects of simulation size sensitivity and ionic strength," *Ind. Eng. Chem. Res.*, vol. 57, no. 50, pp. 17129–17141, 2018.

[94]   D. Cakara, J. Kleimann, and M. Borkovec, "Microscopic Protonation Equilibria of Poly(amidoamine) Dendrimers from Macroscopic Titrations," *Macromolecules*, vol. 36, pp. 4201–4207, 2003, doi: 10.1021/ma0300241.

[95]   Y. Liu, V. S. Bryantsev, M. S. Diallo, and W. A. Goddard, "PAMAM Dendrimers Undergo pH Responsive Conformational Changes without Swelling," *J. Am. Chem. Soc.*, vol. 131, pp. 2798–2799, 2009.

[96]   B. Y. Kim and M. L. Bruening, "pH-dependent growth and morphology of multilayer dendrimer/poly(acrylic acid) films," *Langmuir*, vol. 19, no. 1, pp. 94–99, Jan. 2003, doi: 10.1021/LA026353O.

[97]   A. J. Khopade and F. Caruso, "Investigation of the Factors Influencing the Formation of Dendrimer/Polyanion Multilayer Films," *Langmuir*, vol. 18, no. 20, pp. 7669–7676, 2002.

[98]   A. Vidyasagar, C. Sung, R. Gamble, and J. L. Lutkenhaus, "Thermal Transitions in Dry and Hydrated Layer-by-Layer Assemblies Exhibiting Linear and Exponential Growth," *ACS Nano*, vol. 6, no. 7, pp. 6174–6184, 2012, doi: 10.1021/nn301526b.

[99]   T. Y. Honda K, Yoshida K, Sato K, Ida H, "In situ visualization of LbL-assembled film nanoscale morphology using scanning ion conductance microscopy," *Electrochim. Acta.*, vol. 469, p. 143152, 2023, doi: 10.1016/j.electacta.2023.143152.

[100]   P. M. Popkov A, Su Z, Sigurdardóttir SB, Luo J, Malankowska M, "Engineering polyelectrolyte multilayer coatings as a strategy to optimize enzyme immobilization on a membrane support," *Biochem. Eng. J.*, vol. 193, p. 108838, 2023, doi: 10.1016/j.bej.2023.108838.

[101]   K. S. Tedeschi C, Caruso F, Möhwald H, "Adsorption and Desorption Behavior of an Anionic Pyrene Chromophore in Sequentially Deposited Polyelectrolyte-Dye Thin Films," *J. Am. Chem. Soc.*, vol. 122, no. 24, pp. 5841–5848, 2000.

[102]   J. M. Fréchet, C. J. Hawker, I. Gitsov, and J. W. Leon, "Dendrimers and hyperbranched polymers: two families of three-dimensional macromolecules with similar but clearly distinct properties," *ournal Macromol. Sci. Part A Pure Appl. Chem.*, vol. 33, no. 10, pp. 1399–1425, 1996.

[103]   T. DA *et al.*, "A new class of polymers: starburst-dendritic macromolecules.," *Polym. J.*, vol. 17, no. 1, pp. 117–132, 1985.

[104]   P. Patel, V. Patel, and P. M. Patel, "Synthetic strategy of dendrimers: A review," *J. Indian Chem. Soc.*, vol. 99, no. 7, p. 100514, 2022, doi: 10.1016/j.jics.2022.100514.

[105]   S. E. Stiriba, H. Frey, and R. Haag, "Dendritic polymers in biomedical applications: from potential to clinical use in diagnostics and therapy," *Angew. Chemie Int. Ed.*, vol. 41, no. 8, pp. 1329–1334, 2002, doi: 10.1002/1521-3773(20020415)41:8<1329::AID-ANIE1329>3.0.CO;2-P.

[106] P. Razmshoar, S. Shakoorjavan, and S. Akbari, "Surface-engineered dendrimers in targeting and delivery of drugs," in *Dendrimer-Based Nanotherapeutics*, P. Kesharwani, Ed. Elsevier Inc., 2021, pp. 203–223.

[107] D. S. Bradshaw and D. L. Andrews, "Mechanisms of light energy harvesting in dendrimers and hyperbranched polymers," *Polymers (Basel).*, vol. 3, no. 4, pp. 2053–2077, 2011, doi: 10.3390/polym3042053.

[108] M. R. Thalji, A. A. Ibrahim, and G. A. Ali, "Cutting-edge development in dendritic polymeric materials for biomedical and energy applications," *Eur. Polym. J.*, vol. 160, p. 110770, 2021, doi: 10.1016/j.eurpolymj.2021.110770.

[109] C. Gao and D. Yan, "Hyperbranched polymers: from synthesis to applications," *Prog. Polym. Sci.*, vol. 29, no. 3, pp. 183–275, 2004, doi: 10.1016/j.progpolymsci.2003.12.002.

[110] S. Sadjadi and S. Sadjadi, "Dendritic polymers for environmental remediation," in *New Polymer Nanocomposites for Environmental Remediation*, Elsevier, 2018, pp. 279–335.

[111] S. Khaliliazar, S. Akbari, and M. H. Kish, "Modification of poly (l-lactic acid) electrospun fibers and films with poly (propylene imine) dendrimer," *Appl. Surf. Sci.*, vol. 363, pp. 593–603, 2016, doi: 10.1016/j.apsusc.2015.12.070.

[112] A. Ganjalinia, S. Akbari, and A. Solouk, "PLLA scaffolds surface-engineered via poly (propylene imine) dendrimers for improvement on its biocompatibility/controlled pH biodegradability," *Appl. Surf. Sci.*, vol. 394, pp. 446–456, 2017, doi: 10.1016/j.apsusc.2016.10.110.

[113] P. A. Fard, S. Shakoorjavan, and S. Akbari, "The relationship between odour intensity and antibacterial durability of encapsulated thyme essential oil by PPI dendrimer on cotton fabrics," *J. Text. Inst.*, vol. 109, no. 6, pp. 832–841, Sep. 2018, doi: 10.1080/00405000.2017.1376820.

[114] A. Tayebi, A. Kargari, and S. Akbari, "Enhancing the performance of a modified poly(ether-b-amide) blend membrane by PAMAM dendritic polymer for separation of CO2/CH4," *Polym.*

Test., vol. 128, p. 108225, 2023, doi: 10.1016/j.polymertesting.2023.108225.

[115] J. Burnett, A. King, L. T.-R. and F. Polymers, and U. 2006, "Probing the onset of dense shell packing by measuring the aminolysis rates for a series amine terminated dendrimers," *React. Funct. Polym.*, vol. 66, no. 1, pp. 187–194, 2006, doi: 10.1016/j.reactfunctpolym.2005.07.022.

[116] A. S. Razmshoar P, Bahrami SH, "Functional hydrophilic highly biodegradable PCL nanofibers through direct aminolysis of PAMAM dendrimer," *Int. J. Polym. Mater. Polym. Biomater.*, vol. 69, no. 16, pp. 1069–1080, 2020, doi: 10.1080/00914037.2019.1655751.

[117] A. E, S. R, A. S, and A. AG., "Electrospun PLLA/PEI nanofibers for controlled drug release behaviors and antibacterial efficiency," *J. Macromol. Sci.*, vol. 61, no. 3, pp. 186–202, 2024, doi: 10.1080/10601325.2024.2322427.

[118] A. S. Razmshoar P, Shakoorjavan S, "Surface-engineered dendrimers in targeting and delivery of drugs," in *Dendrimer-Based Nanotherapeutics*, 2021, pp. 203–223.

[119] K. Sato and J. I. Anzai, "Dendrimers in Layer-by-Layer Assemblies: Synthesis and Applications," *Mol. 2013, Vol. 18, Pages 8440-8460*, vol. 18, no. 7, pp. 8440–8460, 2013, doi: 10.3390/MOLECULES18078440.

[120] P. A. Fard, S. Shakoorjavan, and S. Akbari, "The relationship between odour intensity and antibacterial durability of encapsulated thyme essential oil by PPI dendrimer on cotton fabrics," *J. Text. Inst.*, vol. 109, no. 6, pp. 832–841, 2018, doi: 10.1080/00405000.2017.1376820.

[121] C. F. Sousa, E. Fernandez-Megia, J. Borges, and J. F. Mano, "Supramolecular dendrimer-containing layer-by-layer nanoassemblies for bioapplications: current status and future prospects," *Polym. Chem.*, vol. 12, no. 41, pp. 5902–5930, 2021, doi: 10.1039/D1PY00988E.

[122] M. Xu *et al.*, "Eco-friendly fabrication ofporphyrin@hyperbranched polyamide-amine@phytic acid/PVDF membrane forsuperior oil-water separation and dyedegradation," *Appl. Surf. Sci.*, vol. 608, p. 155075, 2023, doi: 10.1016/j.apsusc.2022.155075.

[123]   X. Xu *et al.*, "Multifunctional drug carriers comprised of mesoporous silica nanoparticles and polyamidoamine dendrimers based on layer-by-layer assembly," *Mater. Des.*, vol. 88, pp. 1127–1133, 2015, doi: 10.1016/j.matdes.2015.09.069.

[124]   A. Ahmad, F. Banat, H. Alsafar, and S. W. Hasan, "An overview of biodegradable poly (lactic acid) production from fermentative lactic acid for biomedical and bioplastic applications," *Biomass Convers. Biorefinery*, 2022, doi: 10.1007/s13399-022-02581-3.

[125]   X. Li, Y. Lin, M. Liu, L. Meng, and C. Li, "A review of research and application of polylactic acid composites," *J. Appl. Polym. Sci.*, vol. 140, no. 7, p. 53477, 2023, doi: 10.1002/app.53477.

[126]   E. F. Ramezani Dana H, "Synthesis, properties, and applications of polylactic acid-based polymers," *Polym. Eng. Sci.*, vol. 63, no. 1, pp. 22–43, 2023, doi: 10.1002/pen.26193.

[127]   N. G. Khouri, J. O. Bahú, C. Blanco-Llamero, P. Severino, V. O. Concha, and E. B. Souto, "Polylactic acid (PLA): Properties, synthesis, and biomedical applications – A review of the literature," *J. Mol. Struct.*, p. 138243, 2024.

[128]   I. C. Odera RS, "Novel advancements in additive manufacturing of PLA: A review," *Polym. Eng. Sci.*, vol. 63, no. 10, pp. 3189–3208, 2023, doi: 10.1002/pen.26450.

[129]   G. R. Maurya AK, de Souza FM, Dawsey T, "Biodegradable polymers and composites: Recent development and challenges," *Polym. Compos.*, 2023, doi: doi.org/10.1002/pc.28023.

[130]   S. Liu *et al.*, "Current applications of poly (lactic acid) composites in tissue engineering and drug delivery," *Compos. Part B Eng.*, vol. 199, p. 108238, 2020, doi: 10.1016/j.compositesb.2020.108238.

[131]   M. A. Nonato RC, Mei LH, Bonse BC, Leal CV, Levy CE, Oliveira FA, Delarmelina C, Duarte MC, "Nanocomposites of PLA/ZnO nanofibers for medical applications: Antimicrobial effect, thermal, and mechanical behavior under cyclic stress," *Polym. Eng. Sci.*, vol. 62, no. 4, pp. 1147–55, 2022, doi: 10.1002/pen.25913.

[132] C. S. Naskar A, Sanyal I, Nahar N, Ghosh DD, "Bionanocomposites films applied as active and smart food packaging: A review," *Polym. Eng. Sci.*, vol. 63, no. 9, pp. 2675–2699, 2023, doi: 10.1002/pen.26415.

[133] R. B. Attari K, Molla-Abbasi P, "Fabrication of a packaging film based on PLA blends: The evolution of physical, mechanical, and rheological properties," *Polym. Eng. Sci.*, 2024, doi: 10.1002/pen.26612.

[134] N. A. A. B. Taib *et al.*, "A review on poly lactic acid (PLA) as a biodegradable polymer," *Polym. Bull.*, vol. 80, no. 2, pp. 1179–1213, 2023, doi: 10.1007/S00289-022-04160-Y.

[135] A. A. Rajeshkumar G, Seshadri SA, Devnani GL, Sanjay MR, Siengchin S, Maran JP, Al-Dhabi NA, Karuppiah P, Mariadhas VA, Sivarajasekar N, "Environment friendly, renewable and sustainable poly lactic acid (PLA) based natural fiber reinforced composites – A comprehensive review," *J. Clean. Prod.*, vol. 310, p. 127483, 2021, doi: 10.1016/J.JCLEPRO.2021.127483.

[136] R. M. Rasal, A. V. Janorkar, and D. E. Hirt, "Poly(lactic acid) modifications," *Prog. Polym. Sci.*, vol. 35, no. 3, pp. 338–356, Mar. 2010, doi: 10.1016/J.PROGPOLYMSCI.2009.12.003.

[137] J. A. Juarez-Moreno *et al.*, "Surface Modification of Polylactic Acid Films with Acrylic Acid Plasma to Modify the Fibroblast Viability," *SSRN*, 2024.

[138] G. S. Mann, L. P. Singh, P. Kumar, S. Singh, and C. Parkash, "On briefing the surface modifications of polylactic acid: A scope for betterment of biomedical structures," *J. Thermoplast. Compos. Mater.*, vol. 34, no. 7, p. 1005, 2021.

[139] C. Y. Tham, Z. A. A. Hamid, Z. Ahmad, and I. Hanafi, "Surface modification of poly (lactic acid)(PLA) via alkaline hydrolysis degradation," *Adv. Mater. Res.*, vol. 970, pp. 324–327, 2014, doi: 10.4028/www.scientific.net/AMR.970.324.

[140] S. Alippilakkotte and L. Sreejith, "Alippilakkotte, Shebi, and Lisa Sreejith. "Benign route for the modification and characterization of poly (lactic acid)(PLA) scaffolds for medicinal application,"

J. Appl. Polym. Sci., vol. 135, no. 13, p. 46065, 2017.

[141] A. V. Janorkar, A. T. Metters, and D. E. Hirt, "Modification of poly(lactic acid) films: Enhanced wettability from surface-confined photografting and increased degradation rate due to an artifact of the photografting process," *Macromolecules*, vol. 37, no. 24, pp. 9151–9159, Nov. 2004, doi: 10.1021/MA049056U.

[142] M. Källrot, U. Edlund, and A. C. Albertsson, "Surface functionalization of degradable polymers by covalent grafting," *Biomaterials*, vol. 27, no. 9, pp. 1788–1796, 2006.

[143] H. G. Geus, "Developments in manufacturing techniques for technical nonwovens," in *Advances in technical nonwovens*, Woodhead Publishing, 2016, pp. 133–153.

[144] D. Venkataraman, E. Shabani, and J. H. Park, "Advancement of nonwoven fabrics in personal protective equipment.," *Materials (Basel).*, vol. 16, no. 11, p. 3964, 2023, doi: 10.3390/ma16113964.

[145] A. Wilson, "The formation of dry, wet, spunlaid and other types of nonwovens," in *Applications of nonwovens in technical textiles*, 2010, pp. 3–17.

[146] G. S. Bhat, S. R. Malkan, and S. Islam, "Spunbond and meltblown web formation," in *Handbook of Nonwovens*, Woodhead Publishing, 2020, pp. 217–278.

[147] V. M. Kister G, Cassanas G, "Effects of morphology, conformation and configuration on the IR and Raman spectra of various poly (lactic acid) s," *Polymer (Guildf).*, vol. 39, no. 2, pp. 267–273, 1998, doi: 10.1016/S0032-3861(97)00229-2.

[148] S. H. Amirshahi and M. T. Pailthorpe, "Applying the Kubelka-Munk equation to explain the color of blends prepared from precolored fibers," *Text. Res. J.*, vol. 64, no. 6, pp. 357–364, 1994.

[149] M. Sabry, G. Baioumy, and A. M. Taha, "Influence of Multilayer Fabric Construction on Thermal Conductivity of Protective Fabrics," *Int. Des. J.*, vol. 14, no. 3, pp. 21–27, 2024.

[150] R. Ahmed, R. R. Rafia, and M. A. Hossain, "Kinetics and thermodynamics of acid red 1

adsorption on used black tea leaves from aqueous solution," *Int. J. Sci.*, vol. 10, no. 6, pp. 7–15, 2021, doi: 10.18483/ijSci.2469.

[151]   M. Friedman, "Applications of the ninhydrin reaction for analysis of amino acids, peptides, and proteins to agricultural and biomedical sciences," *J. Agric. Food Chem.*, vol. 52, no. 3, pp. 358–406, 2004, doi: 0.1021/jf030490p.

[152]   J. Araki, S. Yoda, and R. Kudo, "Rapid and facile quantification of surface amino groups on chitinnanowhiskers and nanofibers via spectrophotometry," *Polym. J.*, vol. 56, pp. 705–710, 2024.

[153]   S. D. Bottom CB, Hanna SB, "Mechanism of the ninhydrin reaction," *Biochem. Educ.*, vol. 6, no. 1, pp. 4–5, 1978.

[154]   S. T. Shakoorjavan S, Dobrzyńska-Mizera M, Akbari S, "Thermal and mechanical properties of aminolyzed-poly (lactic acid) with amine-terminated dendritic polymer: Surface and bulk functionalization," *Polym. Eng. Sci.*, pp. 1–10, 2024.

[155]   N. Miura, P. L. Dubin, C. N. Moorefield, and G. R. Newkome, "Complex Formation by Electrostatic Interaction between Carboxyl-Terminated Dendrimers and Oppositely Charged Polyelectrolytes†," *Langmuir*, vol. 15, no. 12, pp. 4245–4250, 1999.

[156]   N. Y, S. L, and C. RM., "Determination of the Intrinsic Proton Binding Constants for Poly(amidoamine) Dendrimers via Potentiometric pH Titration," *Macromolecules*, vol. 36, no. 15, pp. 5725–5731, 2003.

[157]   L. JR, J. PS, and J. KA., "Characterization of Polyamidoamino (PAMAM) Dendrimers Using In-Line Reversed Phase LC Electrospray Ionization Mass," *Anal. methods*, vol. 8, no. 2, pp. 263–269, 2016.

[158]   P. Wolski and T. Panczyk, "Conformational Properties of PAMAM Dendrimers Adsorbed on the Gold Surface Studied by Molecular Dynamics Simulation," *J. Phys. Chem.*, vol. 123, pp. 22603–22613, 2019.

[159] J. Choi and M. F. Rubner, "Influence of the Degree of Ionization on Weak Polyelectrolyte Multilayer Assembly," *Macromolecules*, vol. 38, pp. 116–124, 2005, doi: 10.1021/ma048596o.

[160] L. Webster and M. B. Huglin, "Complex formation between polyelectrolytes in dilute aqueous solution," *Polymer (Guildf).*, vol. 38, no. 6, pp. 1373–1380, 1997.

[161] A. V. Shovsky, I. Varga, R. Makuska, and P. M. Claesson, "Formation and Stability of Soluble Stochiometric Polyelectrolyte Complexes: Effects of Charge Density and Polyelectrolyte Concentration," *J. Dispers. Sci. Technol.*, vol. 30, pp. 980–988, 2009, doi: 10.1080/01932690802646512.

[162] S. Pande and R. M. Crooks, "Analysis of poly (amidoamine) dendrimer structure by UV–Vis spectroscopy," *Langmuir*, vol. 27, no. 15, pp. 9609–9613, 2011.

[163] P. Welch and M. Muthukumar, "Dendrimer-Polyelectrolyte Complexation: A Model Guest-Host System," *Macromolecules*, vol. 33, pp. 6159–6167, 2000.

[164] D. Stawski and J. Szumilewicz, "Formation of Interpolymer Complexes on Polypropylene Textiles via Layer-by-Layer Modification as Revealed by FTIR Method," *Walailak J. Sci. Technol.*, vol. 9, no. 2, pp. 165–171, 2012.

[165] C. G. Lopez, A. Matsumoto, and A. Q. Shen, "Dilute polyelectrolyte solutions: recent progress and open questions," *Soft Matter*, vol. 20, pp. 2635–2687, 2024, doi: 10.1039/D3SM00468F.

[166] T. Yang *et al.*, "Determination of the permeability coefficient and airflow resistivity of nonwoven materials," *Text. Res. J.*, vol. 92, no. 1–2, pp. 126–142, 2022, doi: 10.1177/00405175211029212.

[167] J. H. Park, B. S. Kim, Y. C. Yoo, M. S. Khil, and H. Y. Kim, "Enhanced mechanical properties of multilayer nano-coated electrospun nylon 6 fibers via a layer-by-layer self-assembly," *J. Appl. Polym. Sci.*, vol. 107, no. 4, pp. 2211–2216, 2008, doi: 10.1002/app.27322.